Inorganic Scintillators in High Energy Physics Experiments

Ren-Yuan Zhu

California Institute of Technology

June 22, 2023

Presented in the 2023 HEPCAT Summer School, UC San Diego

Outline

- Physics motivation and crystal calorimeters in HEP.
- Crystal characterization:
  - Transmittance and light attenuation length;
  - Radio-, X- and photo- luminescence;
  - Temporal response and rising/decay time; and
  - Light yield, light output and decay kinetics.
- Crystal radiation damage:
  - Scintillation mechanism, afterglow and radiation induced absorption;
  - Dose rate dependence and color center kinetics; and
  - Radiation damage mechanism.
- Applications for future HEP experiments.

References for further readings

Why Inorganic Scintillators?

arXiv: 2203.06731 and arXiv: 2203.06788

- **Precision e/γ enhance physics discovery potential.**
- **Performance of total absorption ECAL is well understood for e/γ and jets:**
  - **The best possible energy resolution;**
  - **Good position resolution;**
  - **Good identification and reconstruction efficiency;**
  - **Excellent jet mass resolution with dual readout: C/S light or S/L gate.**
- **On-going Development in Caltech Crystal Lab:**
  - **Rad-hard LYSO:Ce crystals and LuAG:Ce ceramics (RADiCAL) for HL-LHC and FCC-hh;**
  - **Ultrafast BaF_2:Y and Lu_2O_3:Yb for TOF and ultrafast calorimetry;**
  - **Cost-effective crystals/glasses for the proposed Higgs factory (Calvision) and HHCAL.**

Precision e/γ Physics in HEP

Charmonium system observed by CB through Inclusive photons

CB NaI(Tl)

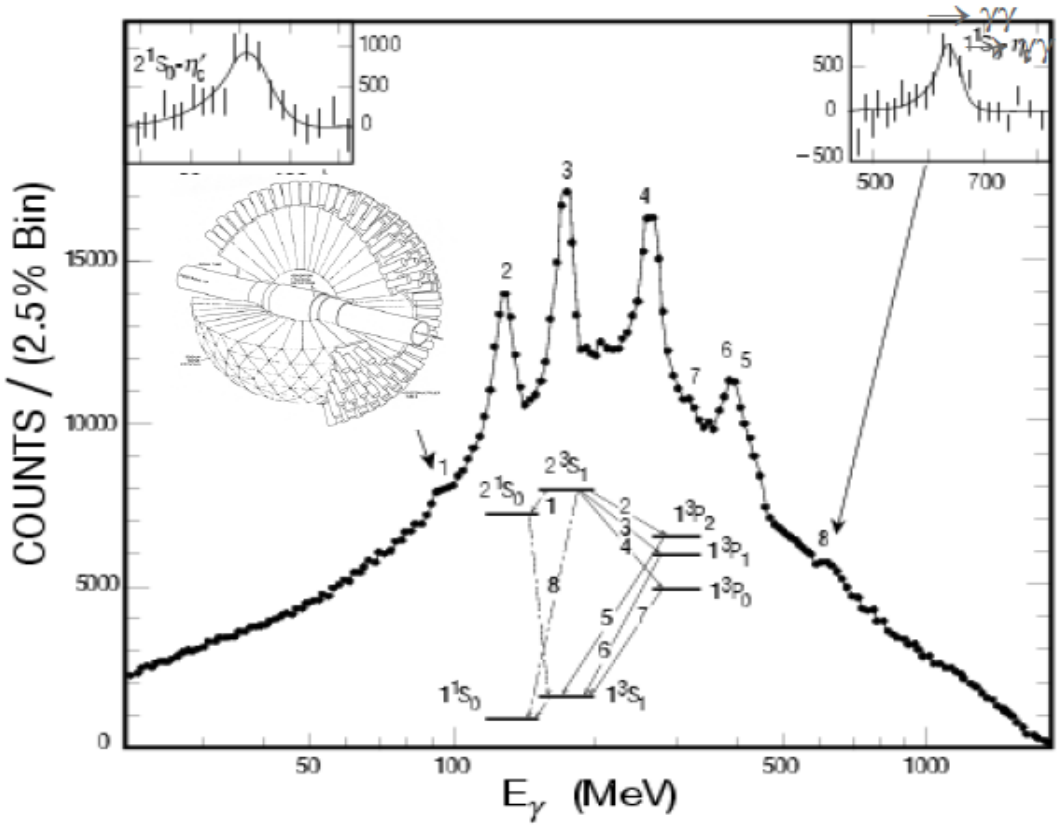

Higgs -> γγ by CMS through reconstructing photon pairs

CMS PWO

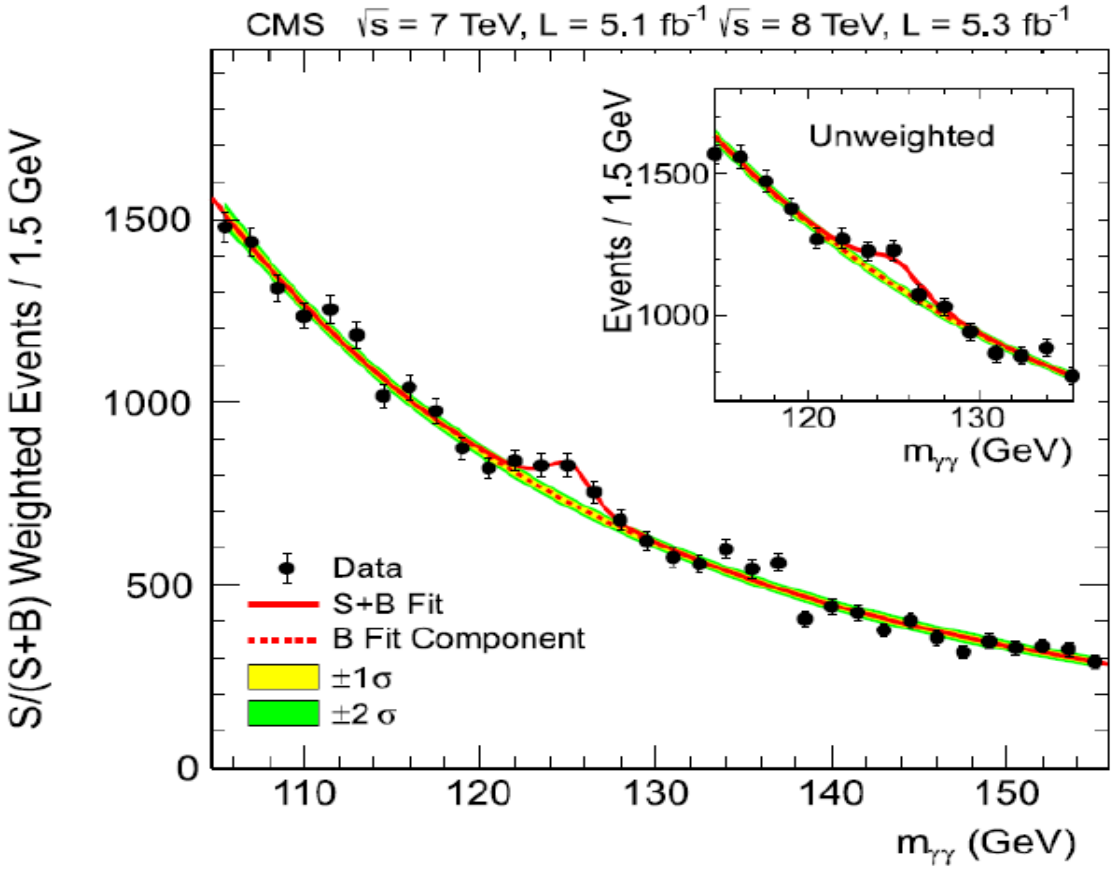

HEP Crystal Calorimeters

CsI:Tl, BGO, CsI and PWO with volume from 1 to 11 m^3

Date	75-85	80-00	80-00	80-00	90-10	94-10	94-10	95-Now	10-Now
Experiment	C. Ball	L3	CLEO II	C. Barrel	KTeV	BaBar	BELLE	CMS	BES III
Accelerator	SPEAR	LEP	CESR	LEAR	Tevatron	PEP	KEKB	LHC	BEPC
Laboratory	SLAC	CERN	Cornell	CERN	FNAL	SLAC	KEK	CERN	IHEP
Crystal Type	NaI:Tl	BGO	CsI:Tl	CsI:Tl	CsI	CsI:Tl	CsI:Tl	PWO	CsI:Tl
B-Field（T）	-	0.5	1.5	1.5	-	1.5	1.0	4.0	1.0
r_{inner} (m)	0.254	0.55	1.0	0.27	-	1.0	1.25	1.29	0.94
Crystal number	672	11,400	7,800	1,400	3,300	6,580	8,800	75,848	6,240
Crystal Depth（X_0）	16	22	16	16	27	16 to 17.5	16.2	25	15
Crystal Volume（m^3）	1	1.5	7	1	2	5.9	9.5	11	5.3
Light Output（p.e./MeV）	350	1,400	5,000	2,000	40	5,000	5,000	2	5,000
Photo-detector	PMT	Si PD	Si PD	WS+Si PD	PMT	Si PD	Si PD	Si APD	Si PD
Gain of Photo-detector	Large	1	1	1	4,000	1	1	50	1
σ_N/Channel（MeV）	0.05	0.8	0.5	0.2	Small	0.15	0.2	40	0.2
Dynamic Range	10^4	10^5	10^4	10^4	10^4	10^4	10^4	10^5	10^4

L3 BGO, BaBar CsI, CMS PWO ECAL

11.4k BGO

75.8k PWO

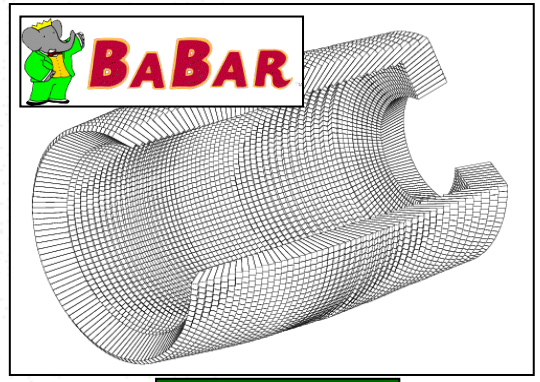

6.6k CsI:Tl

Inorganic Scintillators for Imaging

TNS 65 (2018) 2097; NIM A 940 (2019) 223; TNS 67 (2020) 1086

- **Pixelized detector is standard in medical industry. Laser slicing & micropore provide excellent coverage and position resolution.**
- **Ultrafast scintillators are needed for GHz Hard X-Ray Imaging at Future FEL facilities.**

Performance	Type I imager	Type II imager
X-ray energy	**up to 30 keV**	**42-126 keV**
Frame-rate/inter-frame time	**0.5 GHz / 2 ns**	**3 GHz / 300 ps**
Number of frames per burst	≥ 10	10 - 30
X-ray detection efficiency	above 50%	above 80%
Pixel size/pitch	**≤ 300 µm**	**< 300 µm**
Dynamic range	10^3 X-ray Photons/pixel/frame	≥ 10^4 X-ray Photons/pixel/frame
Pixel format	64 × 64[a] (scalable to 1 Mpix)	1 Mpix

- **Detection efficiency for hard X-ray requires bulk detector; 2 ns and 300 ps inter-frame time requires ultrafast sensor.**

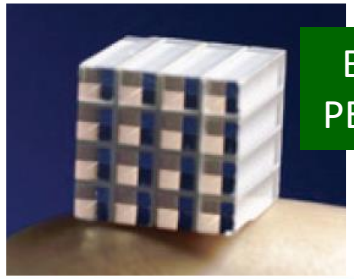

BGO pixels for PET: 1x1x10 mm

CsI:Tl pixel panel for CT
30 x 40 cm panel
0.3x0.3x10 mm

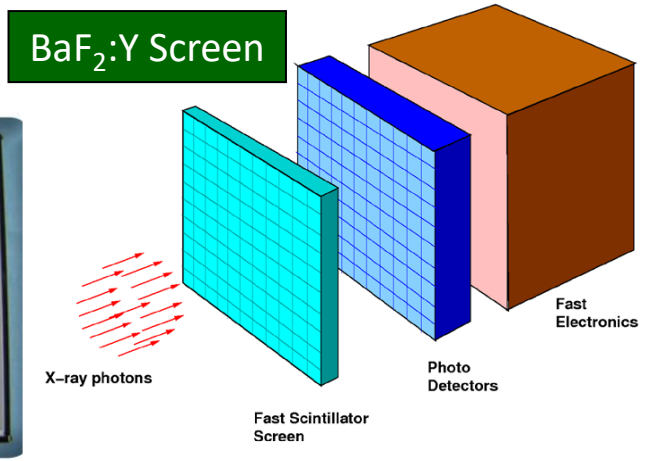

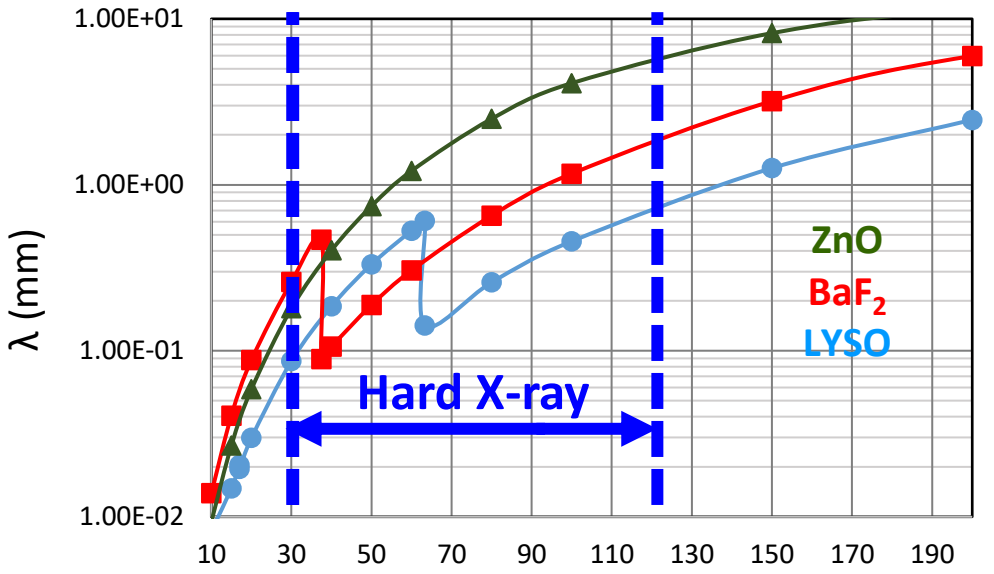

History of Inorganic Crystals

M.J. Weber, J. Lumin. 100 (2002) 35

21 Century: $LaBr_3$

Nineties: PWO, LSO

Seventies: BGO

Fifties: NaI and CsI

Trigger

Fast UV response

HPGe

Ge:Li

Invention of the photomultiplier tube

Cs_2LiYCl_6:Ce	2003
LuI_3:Ce	2003
K_2LaI_5:Ce	2002
$LaBr_3$:Ce	2001
$LaCl_3$:C	2000
Lu_2O_3:Eu, Tb	2000
$Lu_2Si_2O_7$:Ce	2000
$RbGd_2Br_7$:Ce	1997
$^6Li_6Gd(BO_3)_3$:Ce	1996

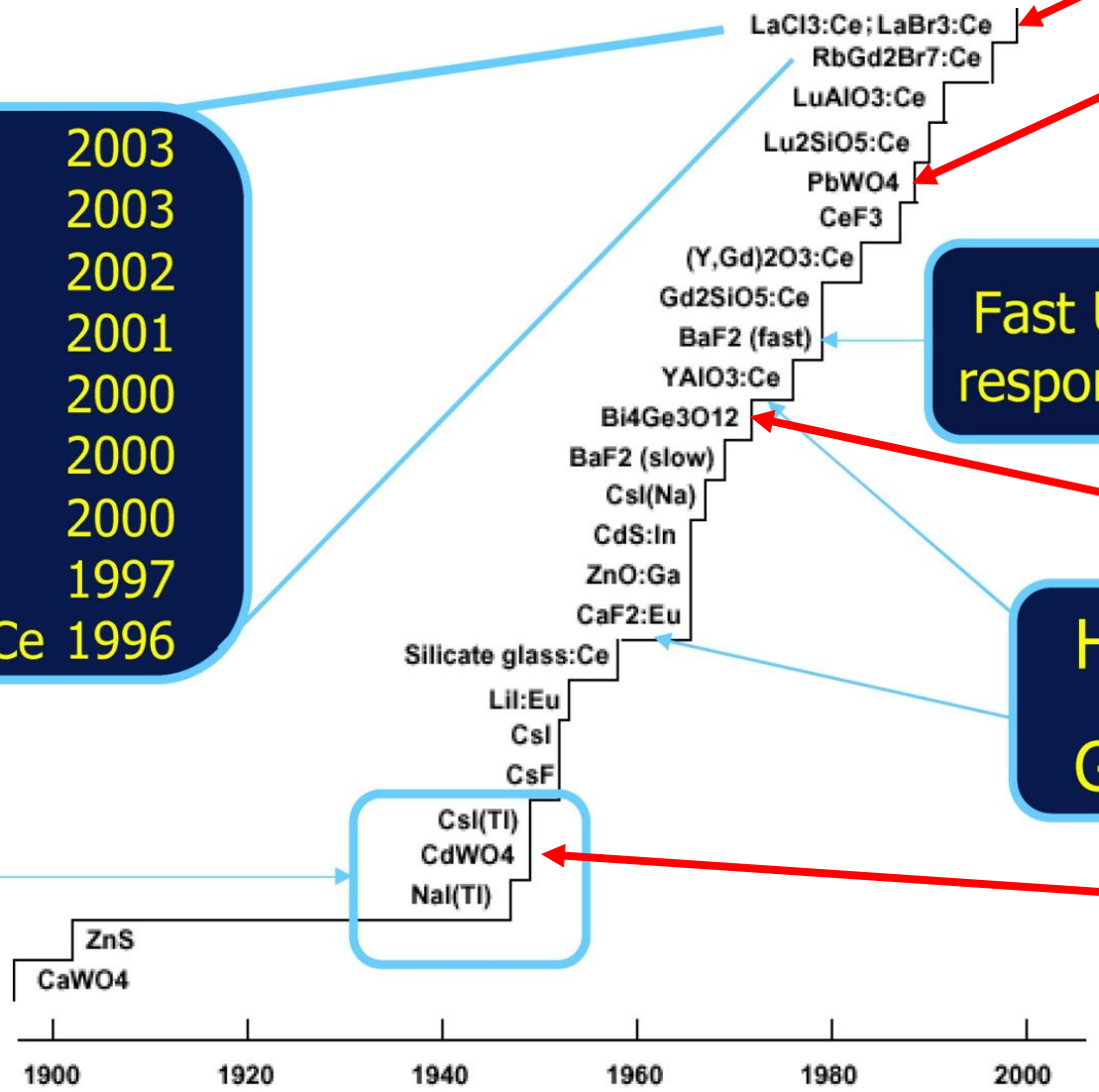

TU Delft

Crystals Used in HEP Calorimeters

Crystal	NaI:Tl	CsI:Tl	CsI	BaF_2	BGO	LYSO:Ce	PWO	PbF_2
Density (g/cm^3)	3.67	4.51	4.51	4.89	7.13	7.40	8.3	7.77
Melting Point (°C)	651	621	621	1280	1050	2050	1123	824
Radiation Length (cm)	2.59	1.86	1.86	2.03	1.12	1.14	0.89	0.93
Molière Radius (cm)	4.13	3.57	3.57	3.10	2.23	2.07	2.00	2.21
Interaction Length (cm)	42.9	39.3	39.3	30.7	22.8	20.9	20.7	21.0
Refractive Index[a]	1.85	1.79	1.95	1.50	2.15	1.82	2.20	1.82
Hygroscopicity	Yes	Slight	Slight	No	No	No	No	No
Luminescence[b] (nm) (at peak)	410	550	420 310	300 220	480	402	425 420	-
Decay Time[b] (ns)	245	1220	30 6	650 0.9	300	40	30 10	-
Light Yield[b,c] (photons/MeV)	38,000	63,000	1,400 420	13,680 1,560	8,000	32,000	114 40	-
d(LY)/dT[b] (%/ °C)	-0.2	0.4	-1.4	-1.9 0.1	-0.9	-0.2	-2.5	-
Experiment	Crystal Ball	BaBar BELLE BES III	KTeV Mu2e S. BELLE	TAPS Mu2e-II	L3 BELLE	COMET CMS BTL PIONEER	CMS ALICE PANDA EIC	A4 G-2

a. at emission peak; b. up/low row: slow/fast component; c. with QE of readout device taken out.

Crystal Samples for Calorimetry

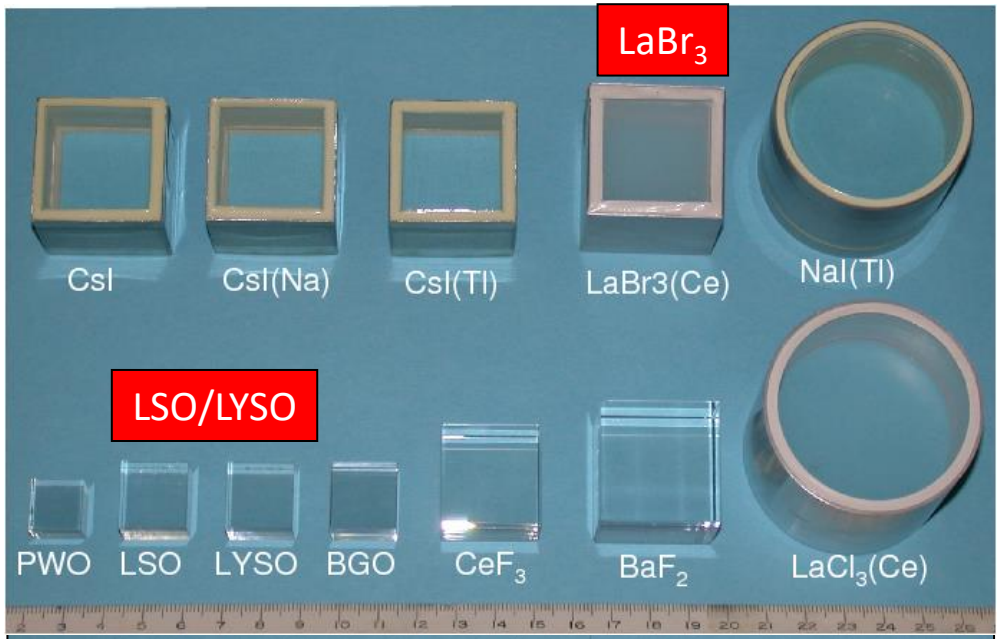

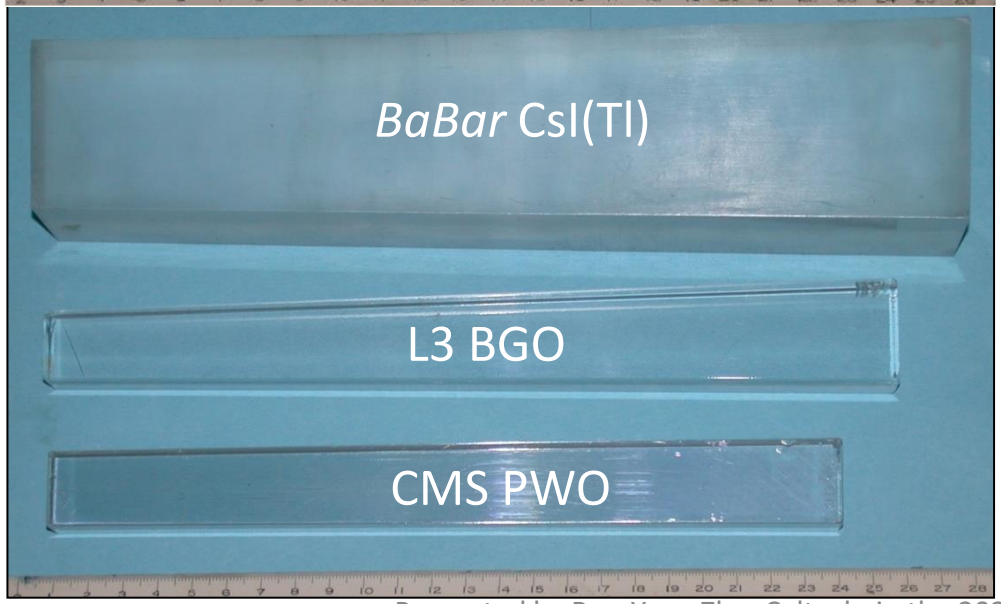

1.5 X_0 Samples:

Hygroscopic: Sealed

Surfaces: Polished

ECAL Crystals:

BaBar CsI(Tl): 16 X_0

L3 BGO: 22 X_0

CMS PWO(Y): 25 X_0

Crystal Growth Techniques

Micro-Pulling Down

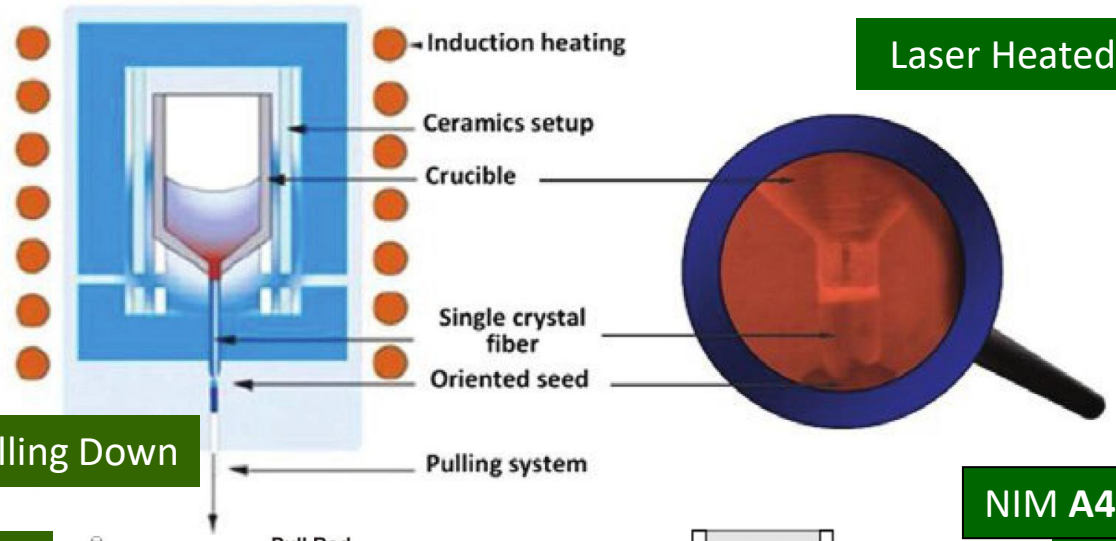

Laser Heated Pedestal Growth

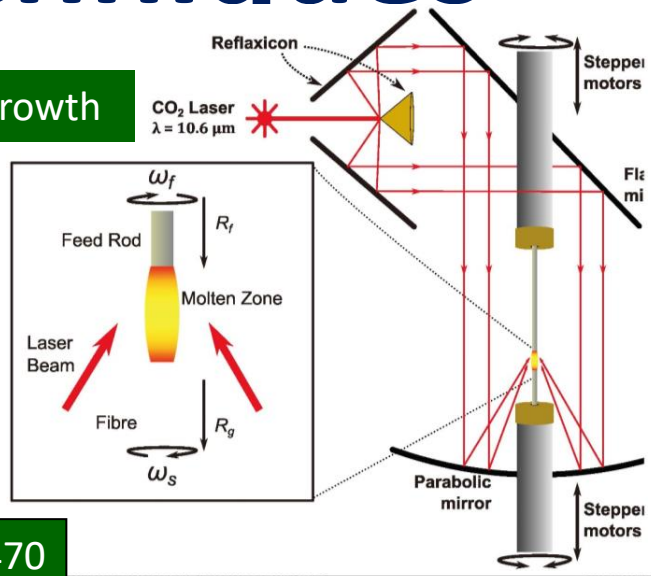

Czochralski

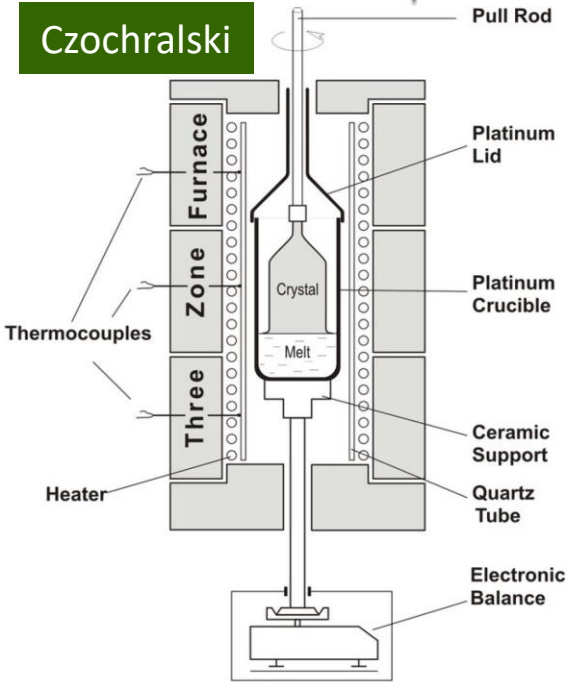

NIM **A480** (2002) 470

Bridgman

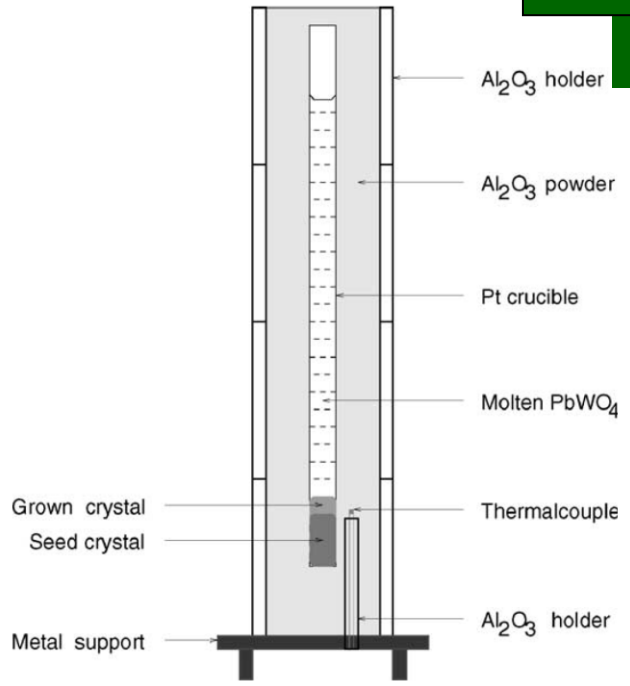

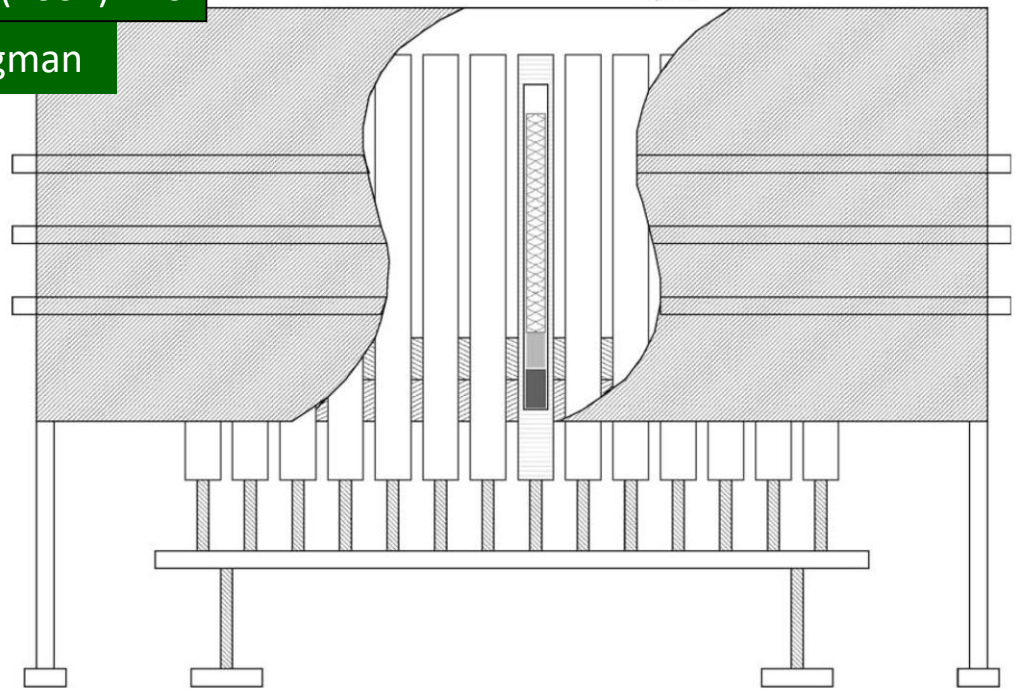

Light Yield/Output and Response Uniformity

Crystal light yield (LY) in photons/MeV energy deposition: βE_g is the energy required for an e-h pair, S is energy transferred to the luminescence center and Q is its quantum efficiency.

Particle Databook

$$LY = 10^6 \; S \cdot Q/(\beta \cdot E_g)$$

Measured light output (LO) in photoelectrons/MeV depends on crystal LY, light collection efficiency (LC) and the quantum efficiency of the photodetector used for the measurement.

$$N_{\mathrm{p.e.}}/\mathrm{MeV} = LY \cdot LC \cdot QE$$

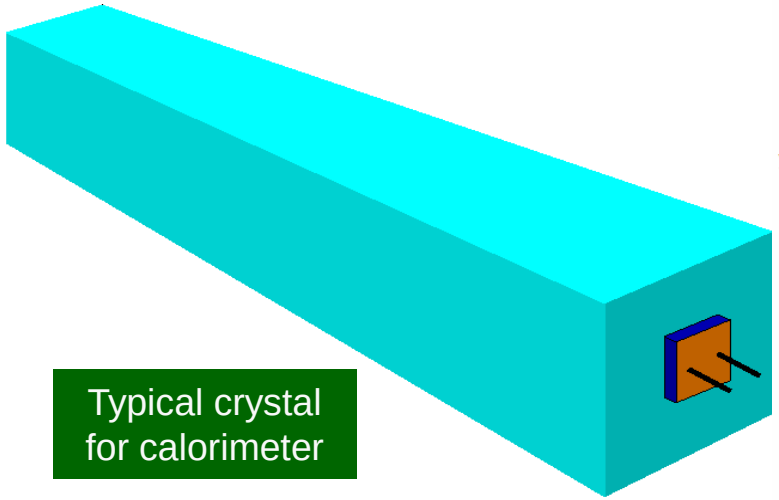

Typical crystal for calorimeter

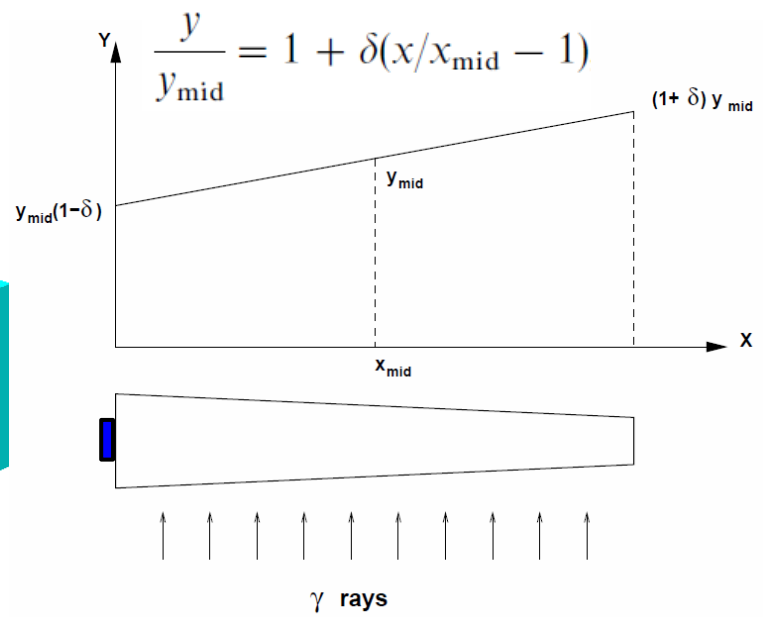

CMS Specification

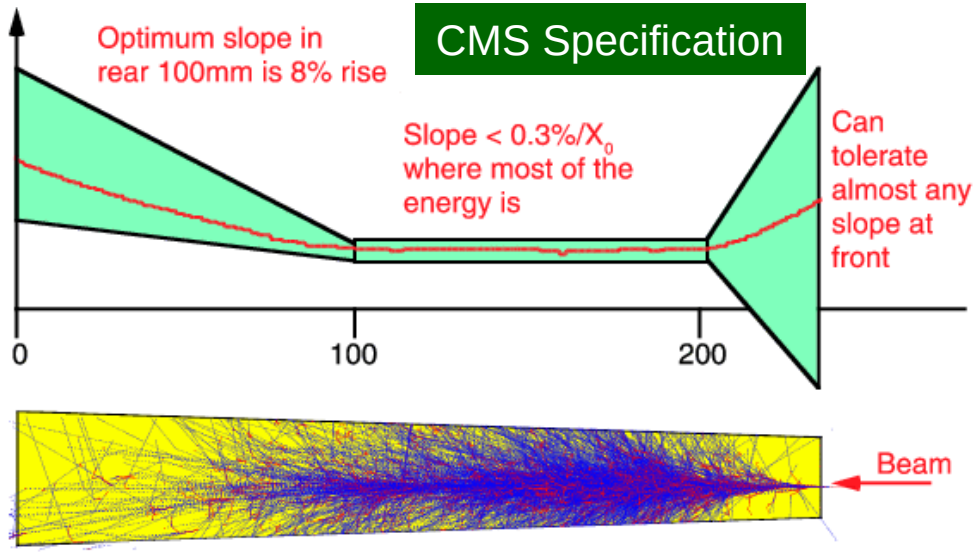

Excitation, Emission, Transmittance

IEEE TNS **59** (2012) 2229

Black Dots: Theoretical limit of transmittance: NIM A333 (1993) 422

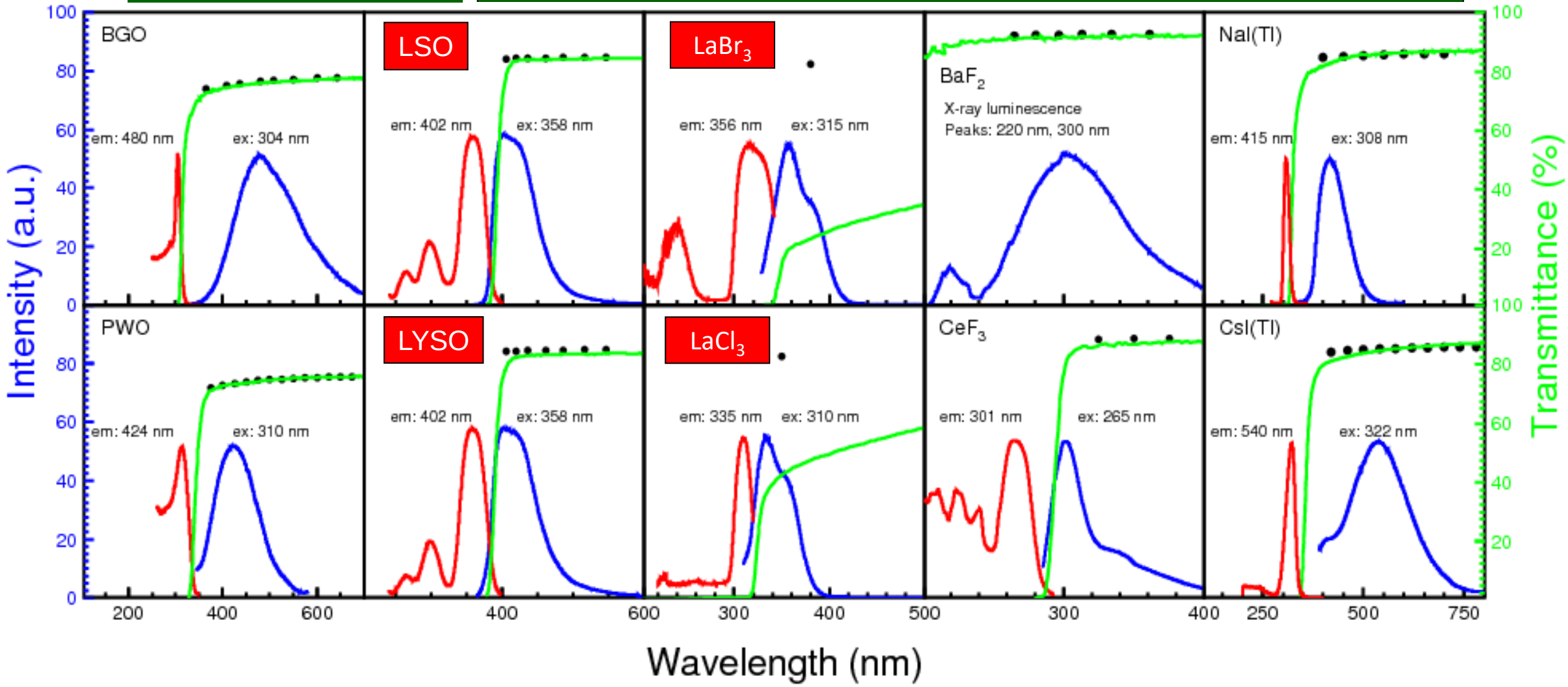

Self-absorption observed in LSO/LYSO, $LaBr_3$, La Cl_3 and CeF_3

Transmittance and Absorption

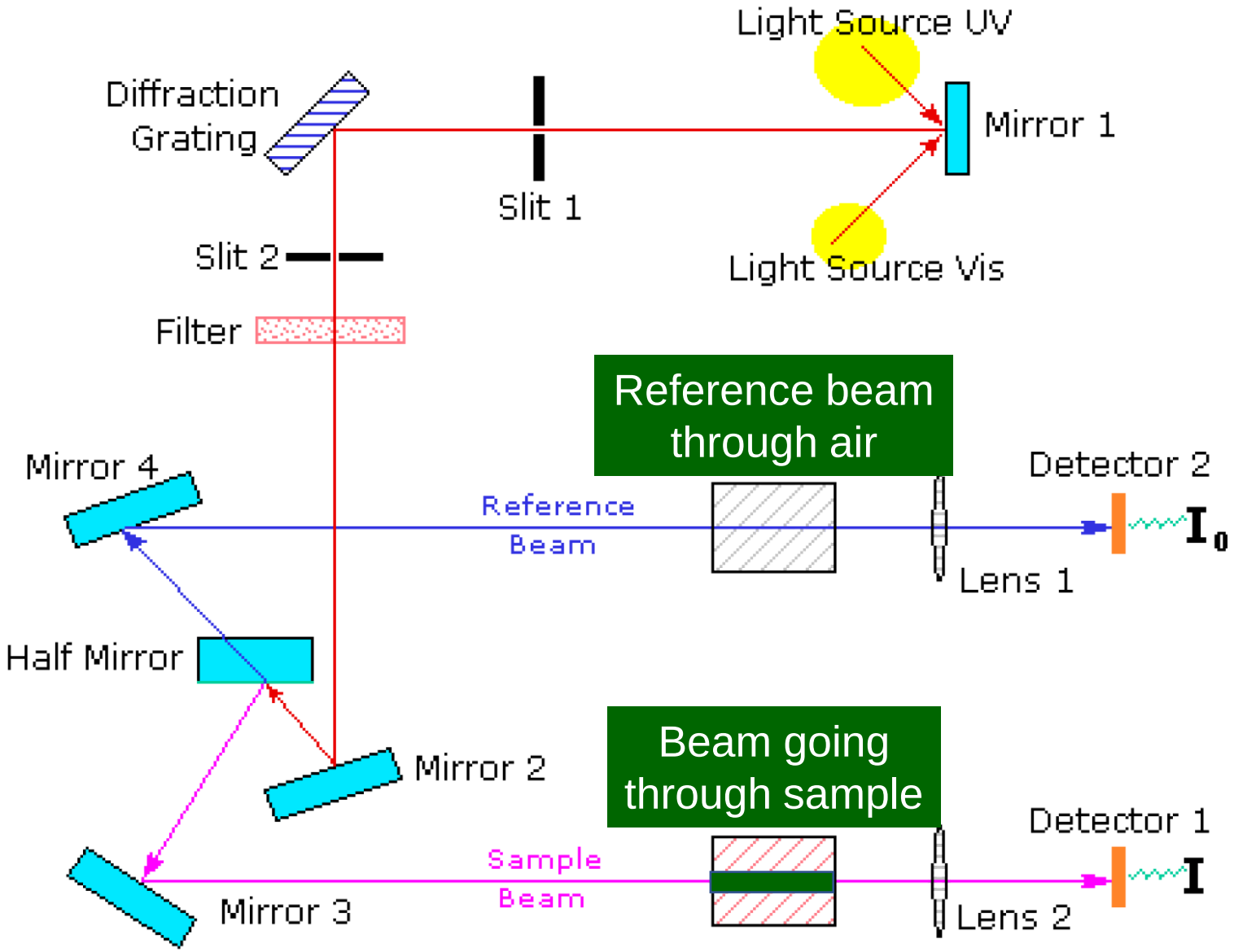

HITACHI U3210 UV/VIS and PerkinElmer Lambda 950 UV/VIS/NIR spectrophotometer with large sample compartment to measure transmittance and absorption

Typical Precision:
0.2 to 0.3%

Watch out:
Birefringence, sample surface and scattering centers

Light Attenuation Length is

Light attenuation length (LAL), or inverse of its light absorption coefficient, extracted from transmittance

$$LAL\,(\lambda) = \frac{l}{\ln\left\{\left[T\,(\lambda)\,(1-T_s\,(\lambda))^2\right] / \left[\sqrt{4T_s^4\,(\lambda)+T^2\,(\lambda)\left(1-T_s^2\,(\lambda)\right)^2}-2T_s^2\,(\lambda)\right]\right\}} \quad (2)$$

where T(λ) is the longitudinal transmittance measured along crystal length l, and $T_s\,(\lambda)$ is the theoretical transmittance assuming multiple bouncings between two crystal ends and without internal absorption:

$$T_s\,(\lambda) = (1-R\,(\lambda))^2 + R^2\,(\lambda)\,(1-R\,(\lambda))^2 + \cdots = (1-R\,(\lambda))\,/\,(1+R\,(\lambda)) \quad (3)$$

and

NIM **A333** (1993) 422

$$R\,(\lambda) = \frac{\left(n_{\text{crystal}}\,(\lambda) - n_{\text{air}}\,(\lambda)\right)^2}{\left(n_{\text{crystal}}\,(\lambda) + n_{\text{air}}\,(\lambda)\right)^2} \quad (4)$$

where $n_{\text{crystal}}\,(\lambda)$ and $n_{\text{air}}\,(\lambda)$ are the refractive indices for crystal and air, respectively.

PWO Birefringence

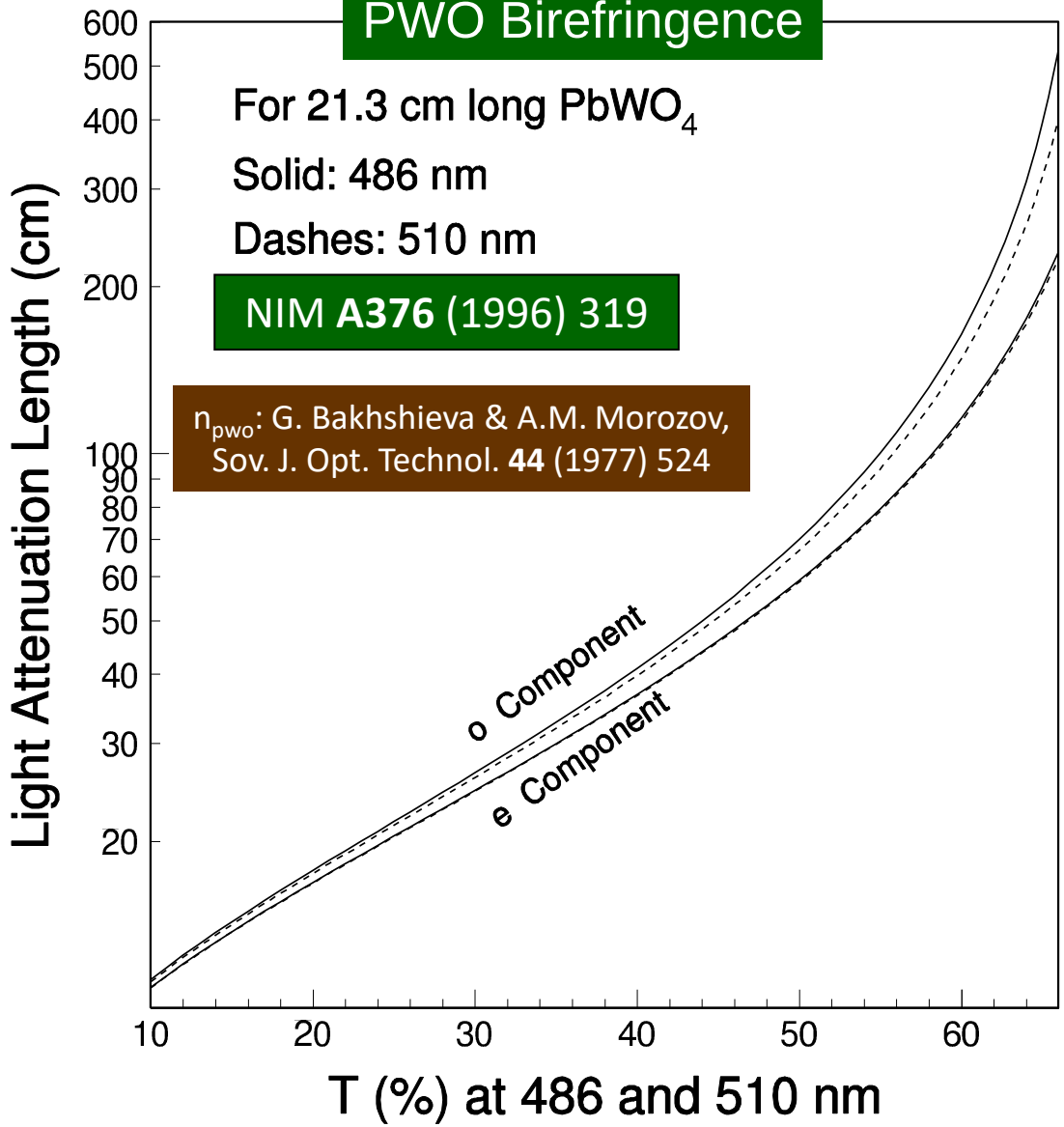

Birefringent PWO Crystals

Attention to be paid to the crystal orientation vs. optical axis

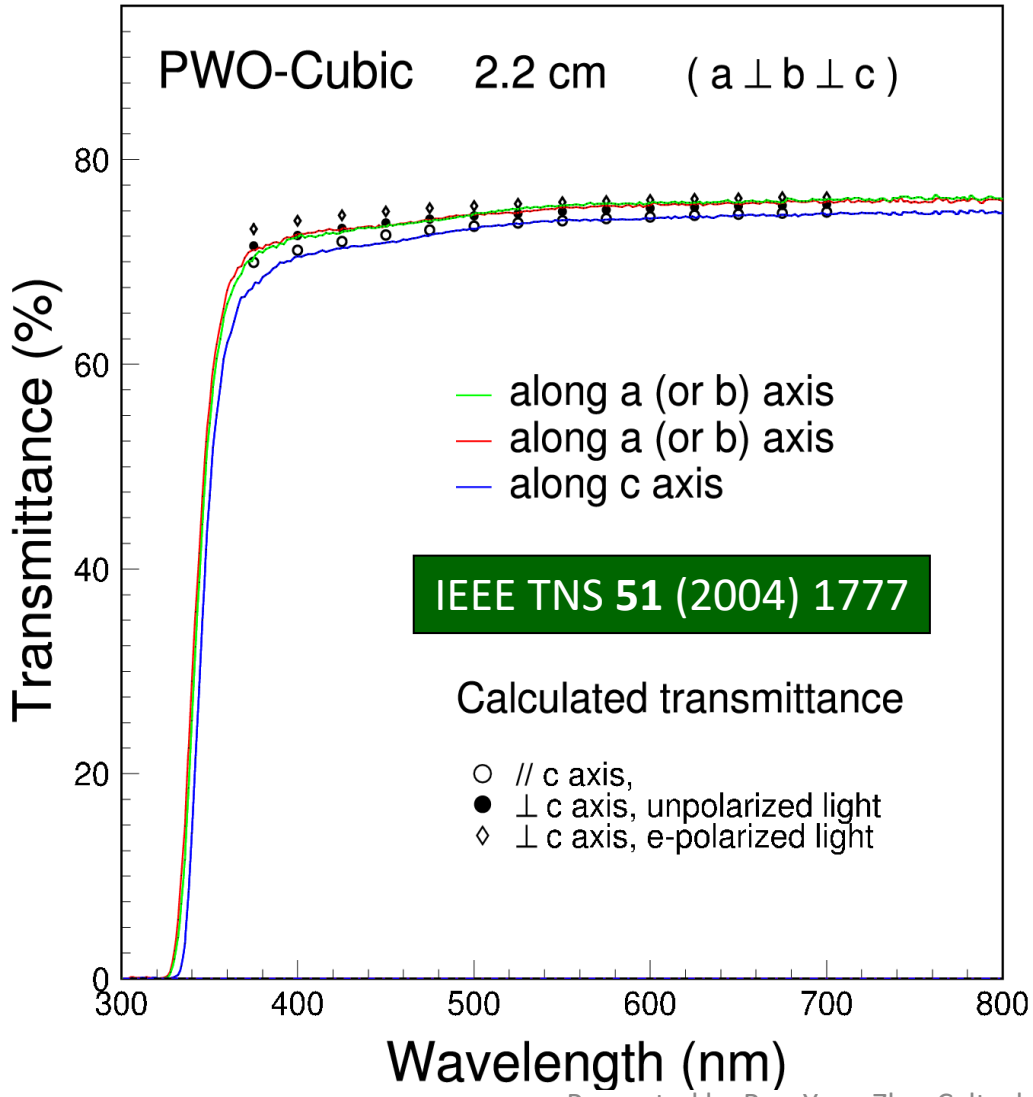

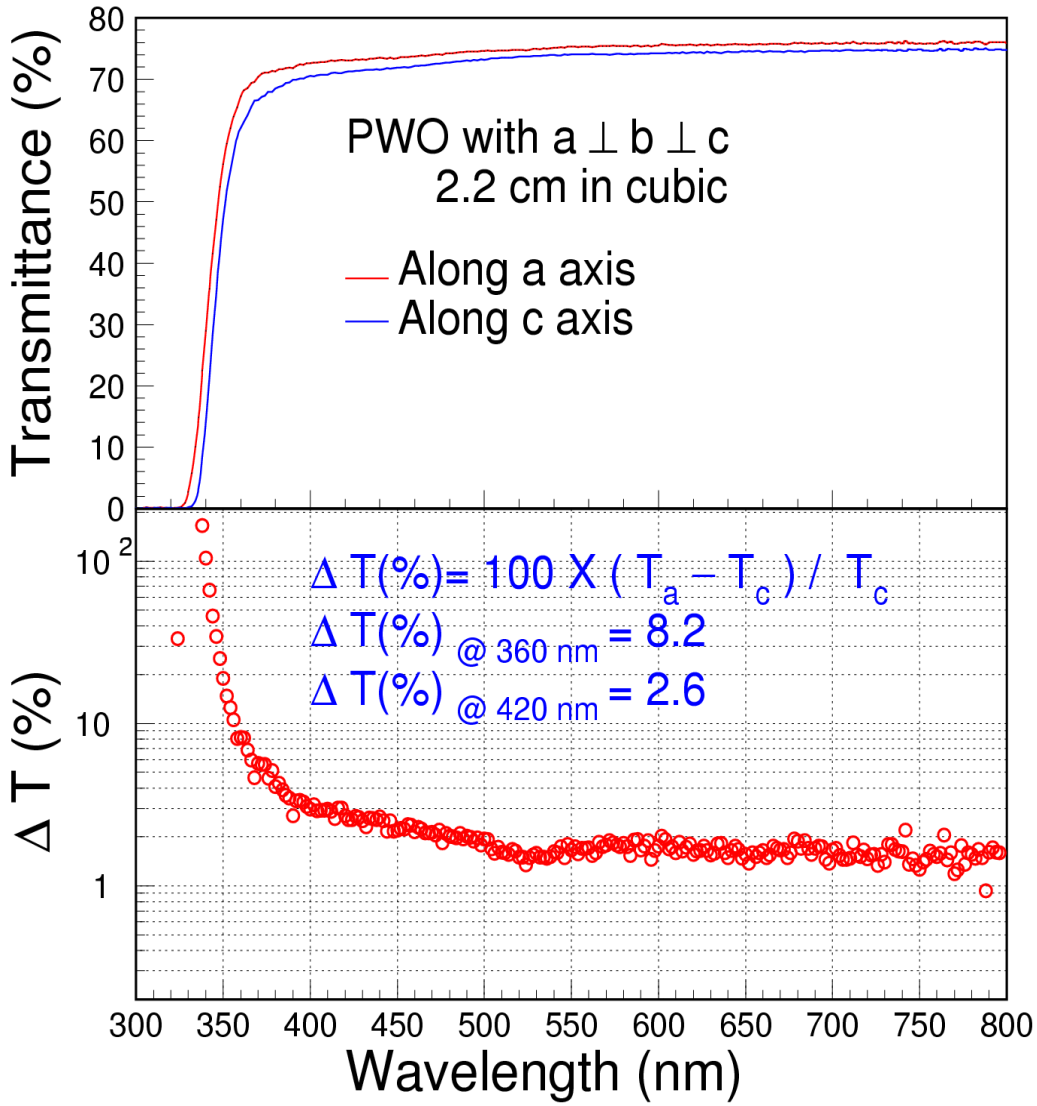

Radio/X-Luminescence

Corrections: Grating efficiency & PMT (Hamamatsu R758) QE

NIM **A376** (1996) 319

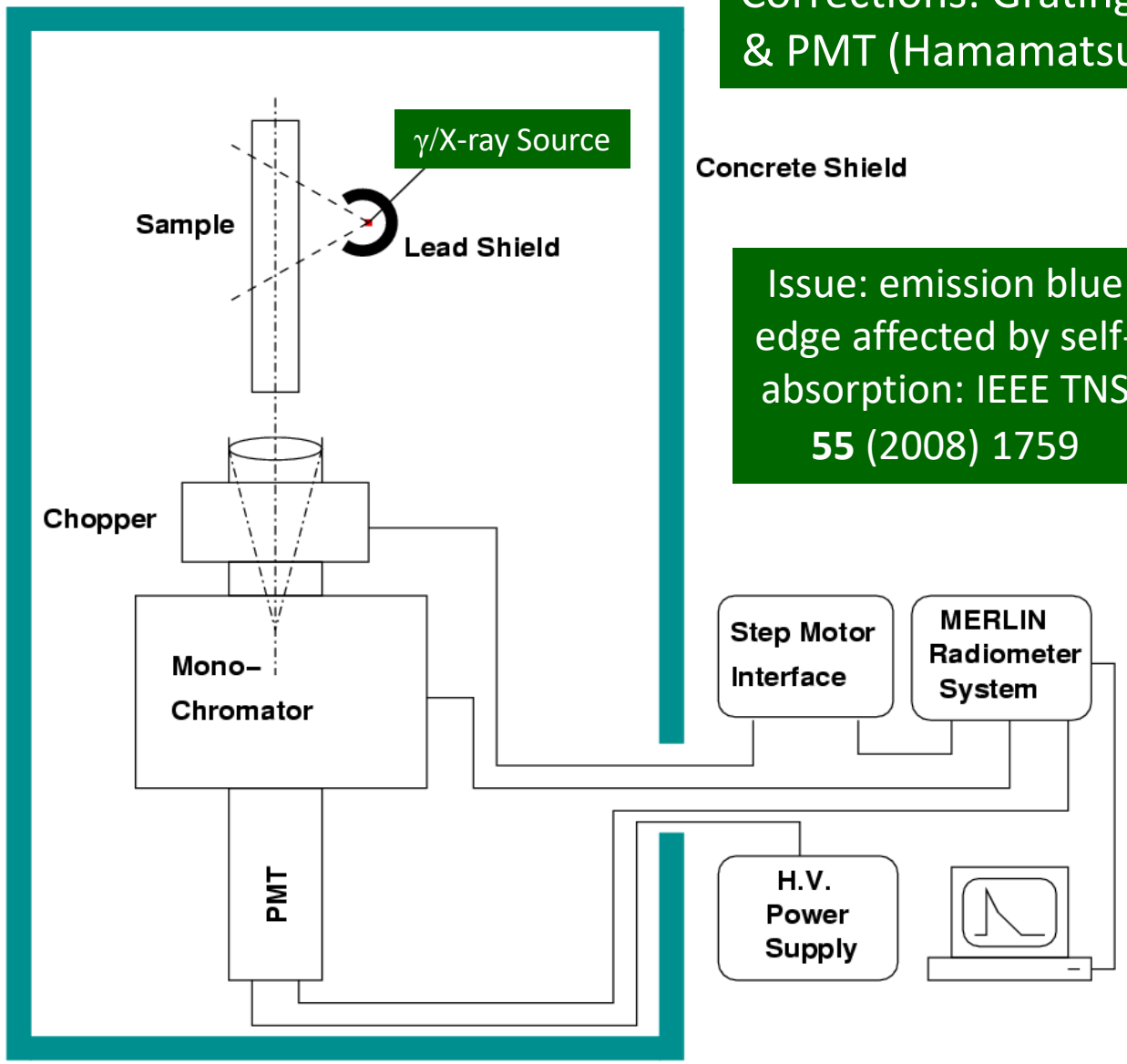

Issue: emission blue edge affected by self-absorption: IEEE TNS **55** (2008) 1759

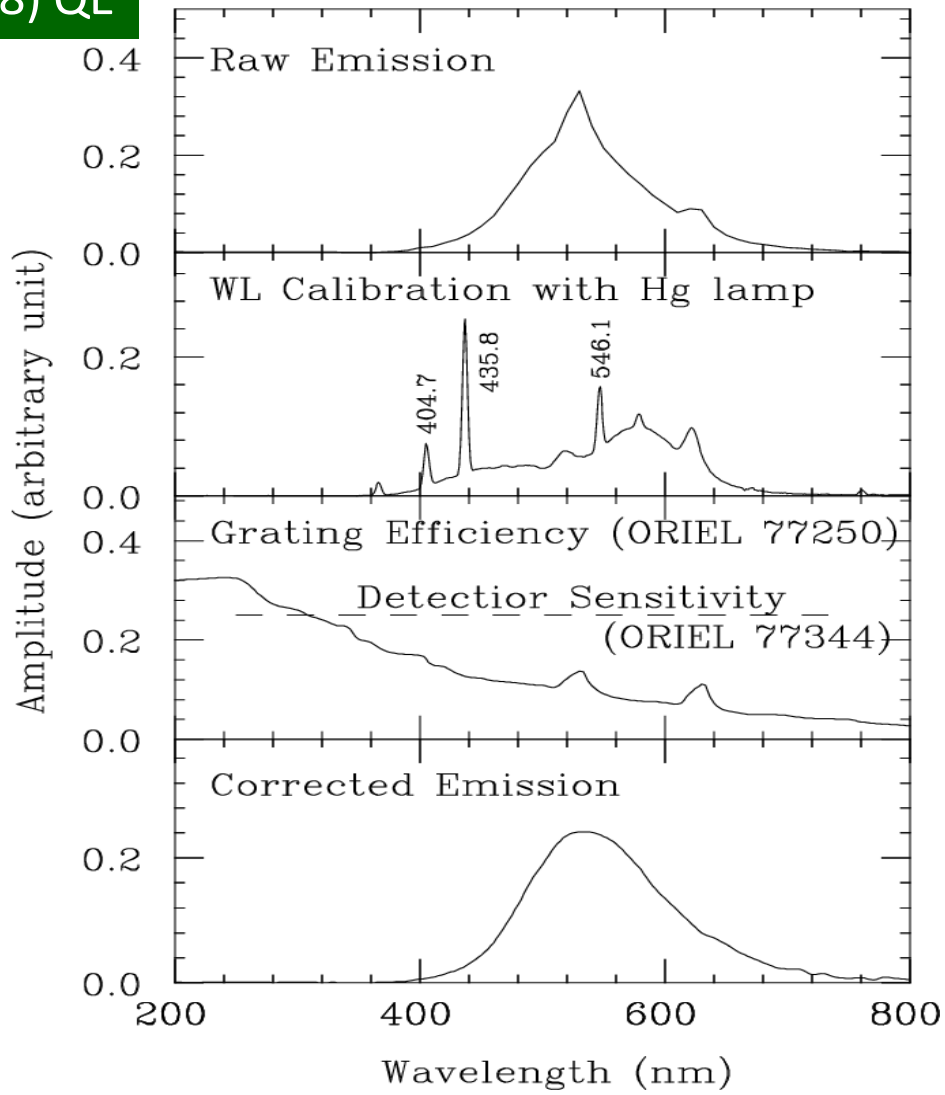

Photo-Luminescence

HITACHI F4500 Fluorescence Spectrophotometer

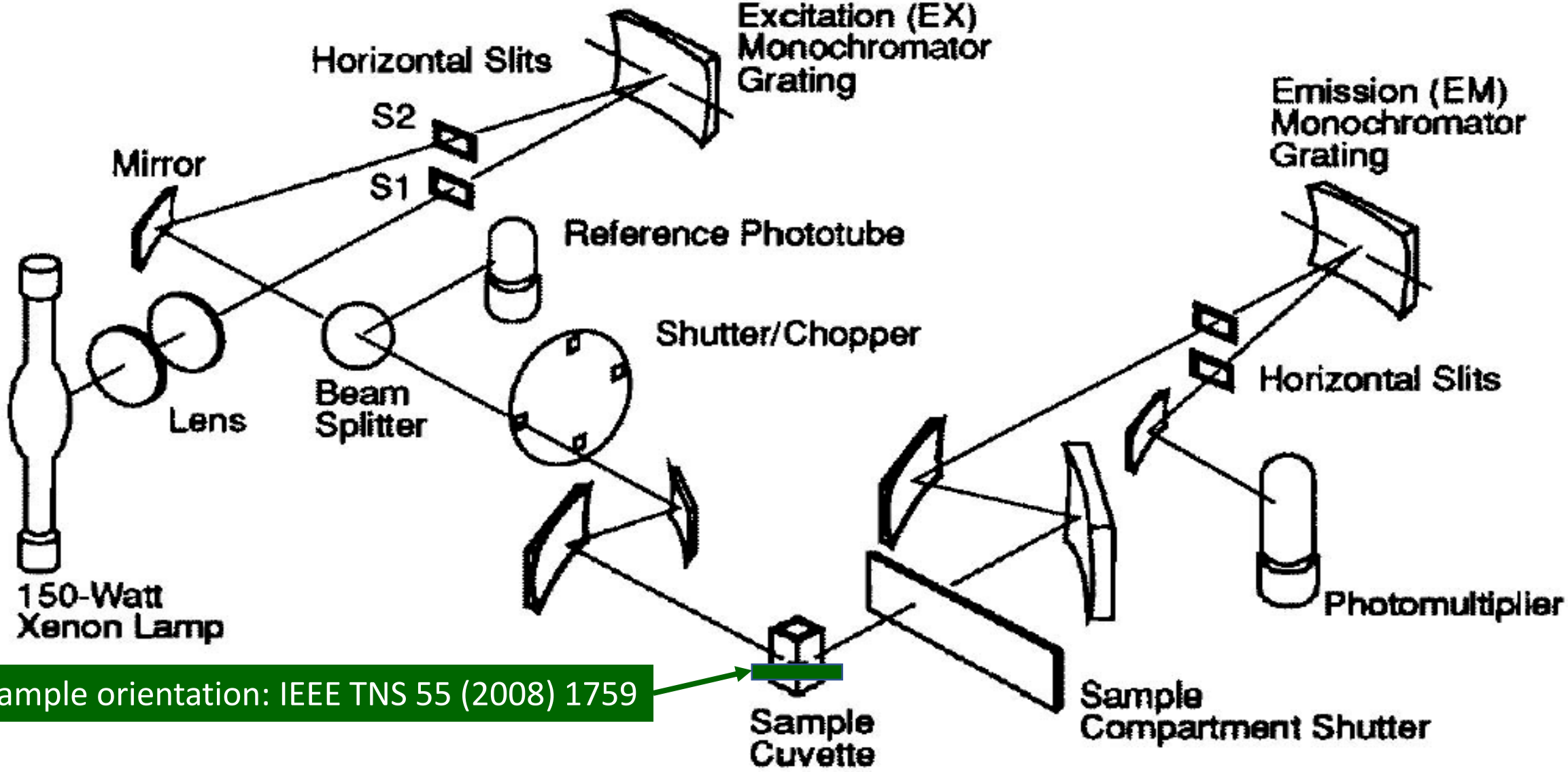

Sample orientation: IEEE TNS 55 (2008) 1759

2-D Contour: Emission & Excitation

IEEE TNS **55** (2008) 1759

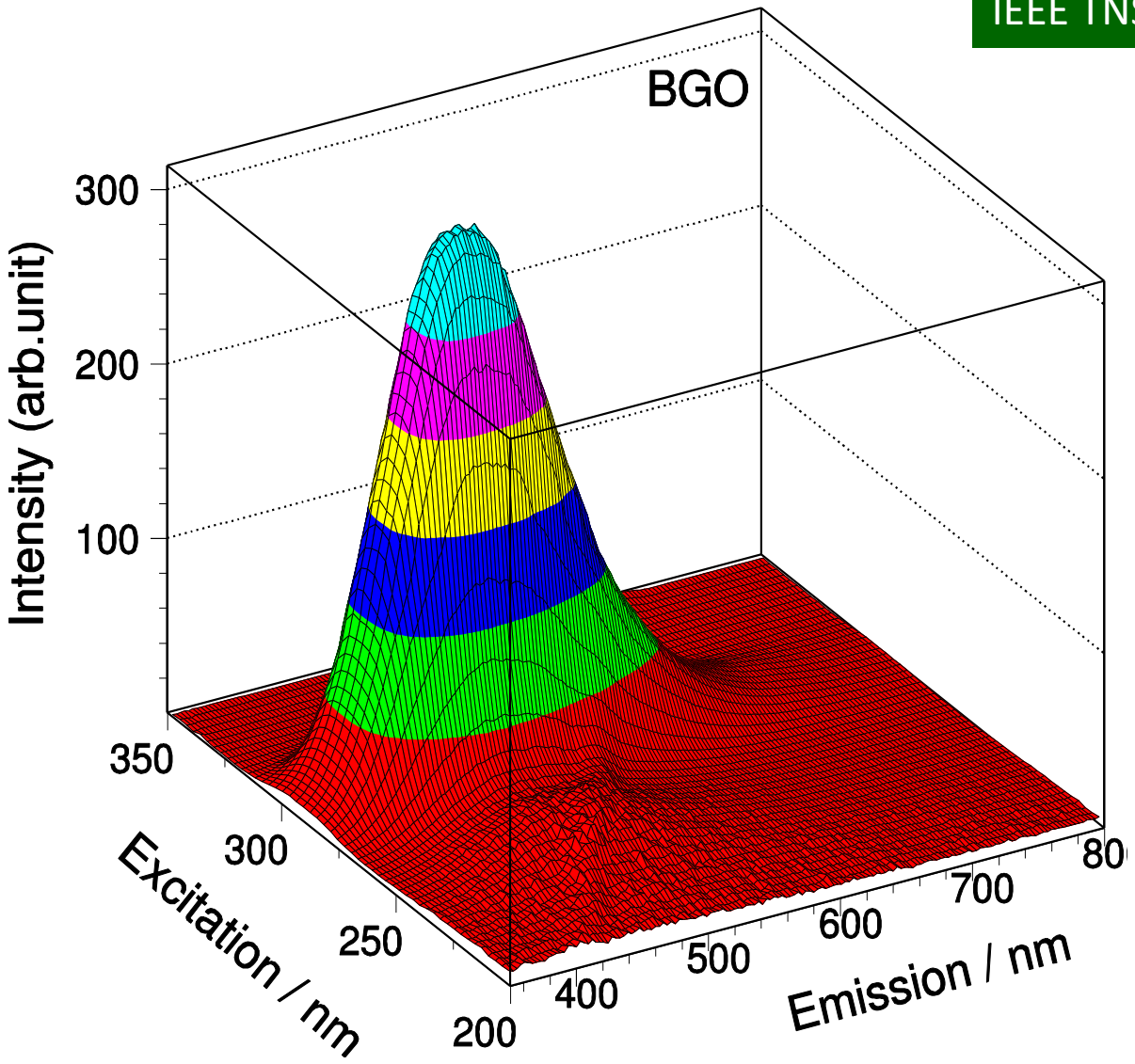

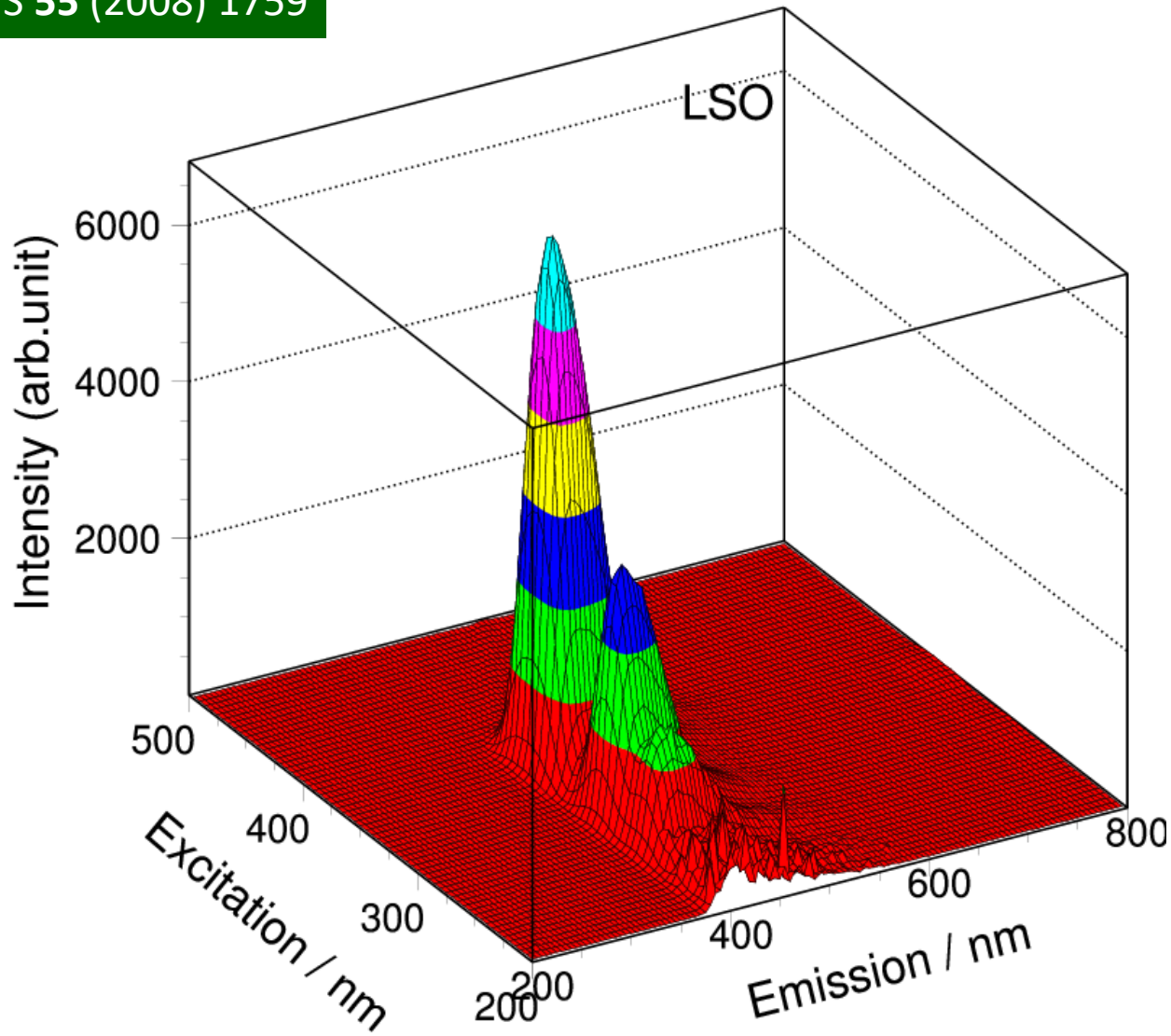

Pulse Shape and Decay Time

IEEE TNS **55** (2008) 2425 | Recorded with PMT and an Agilent 6052A (500 MHz) digital scope

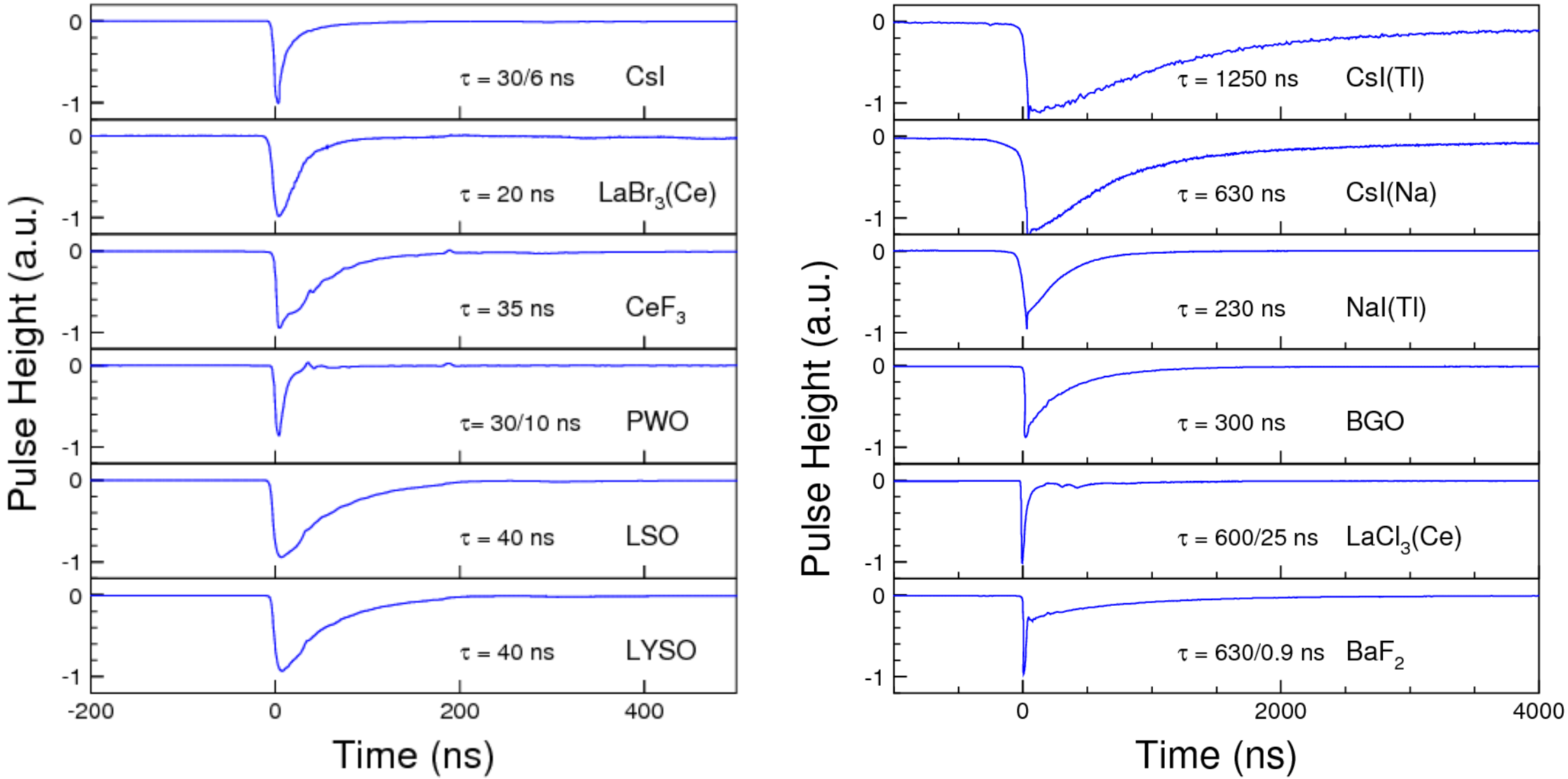

Temporal Response: 1.5 X_0 Samples

Agilent MSO9254A (2.5 GHz) DSO and Hamamatsu R2059 PMT (2500 V) with 0.14 and 1.3 ns rise time

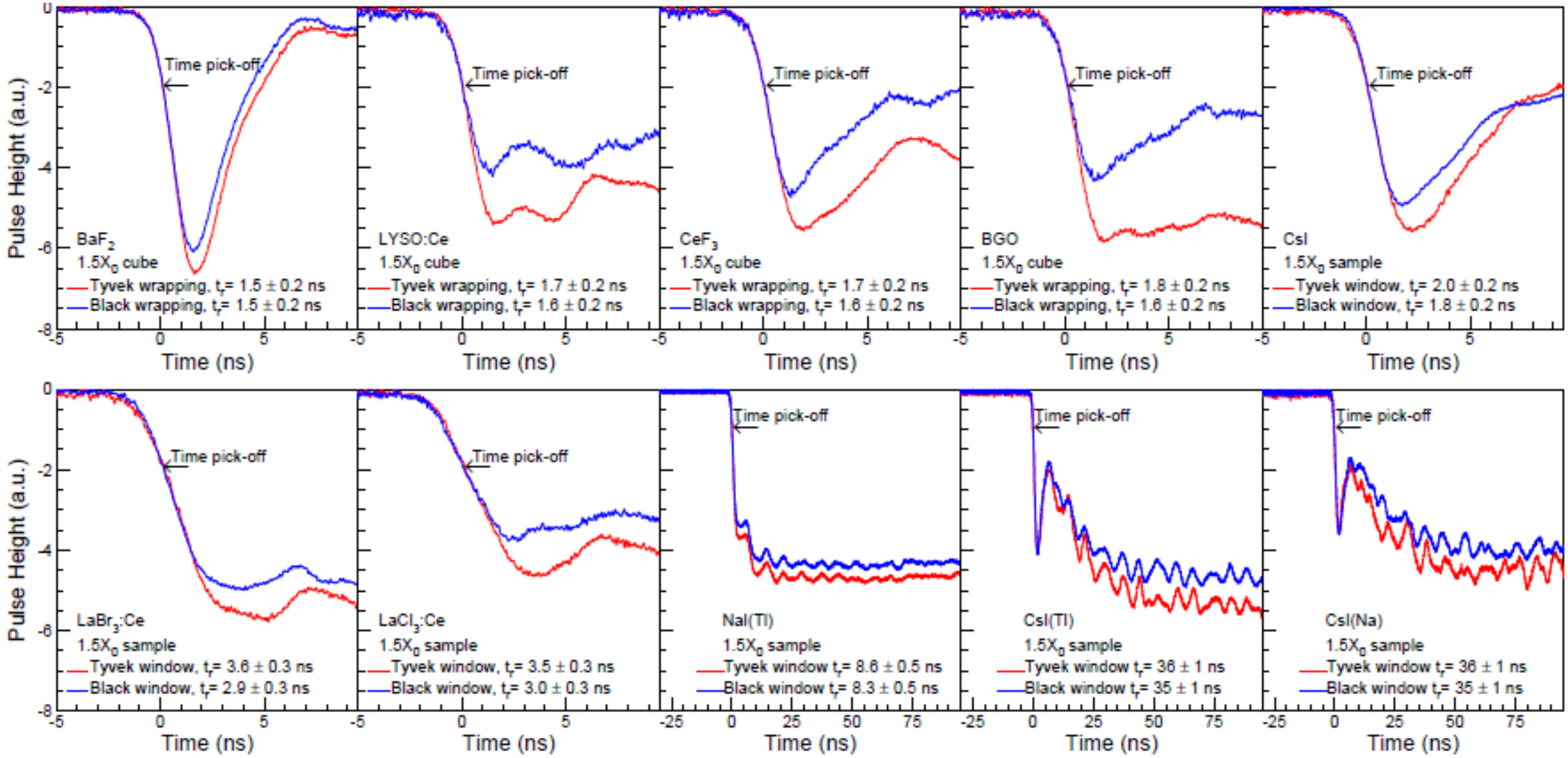

Scintillation Rising Time

S. Derenzo et al., IEEE TNS 47 (2000) 860-864

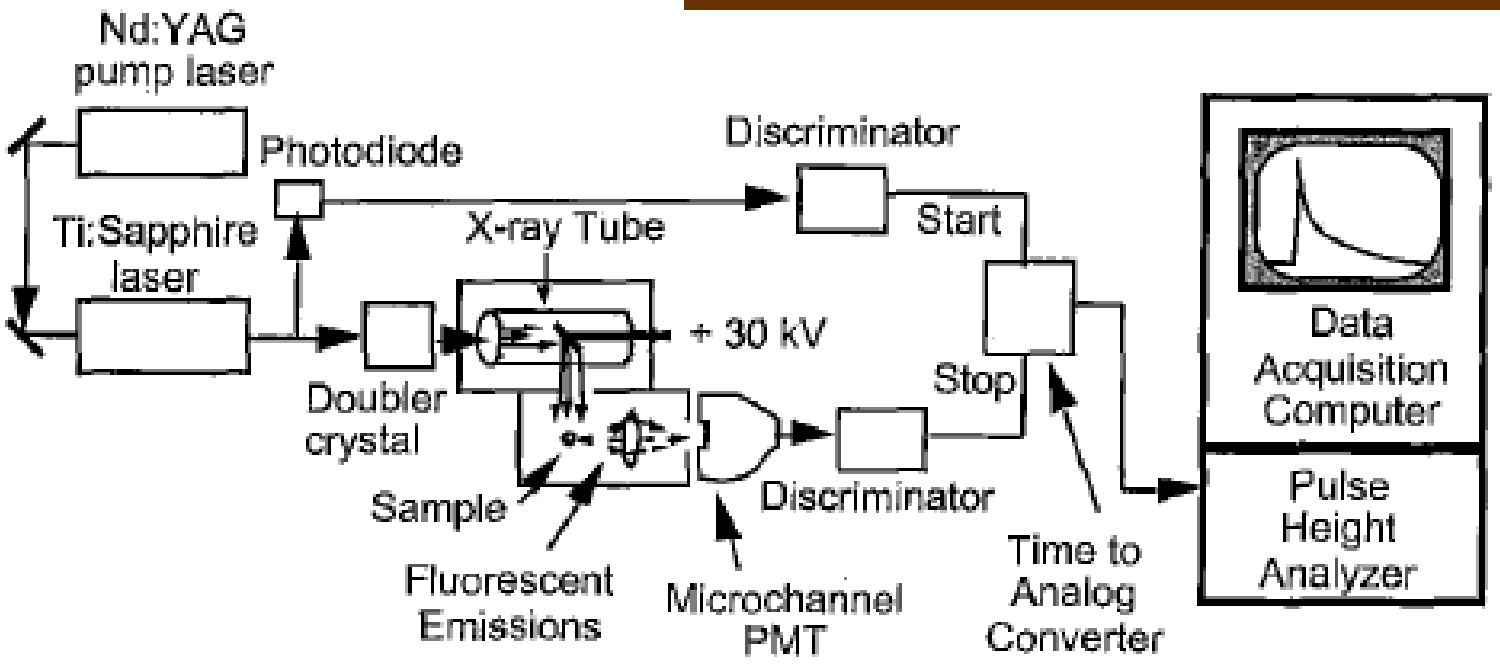

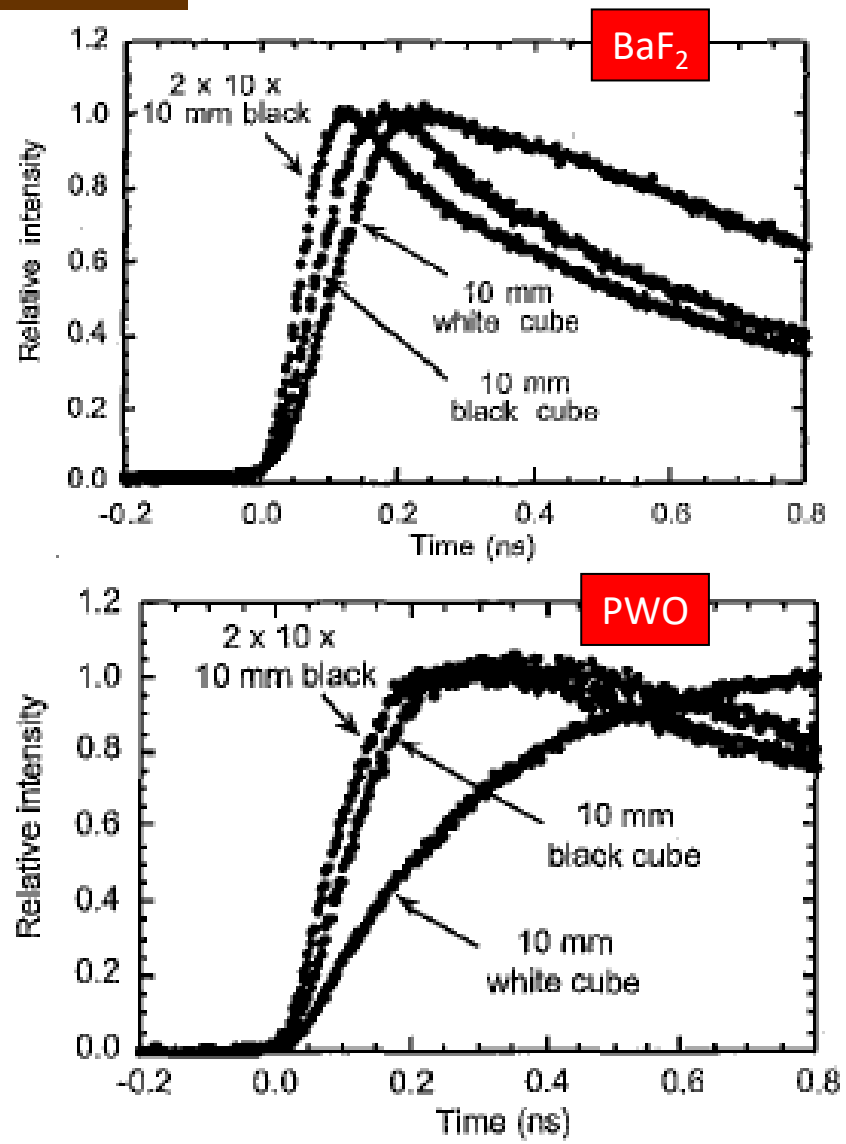

Excitation: 60 ps x-ray, Detector: MCP with 45 ps response

< 30 ps: BaF_2, ZnO:Ga; 30 ps: BGO, CeF_3, CsI, LSO; 60 ps: PWO

Effects of light propagation noticed: difference between small and large size samples and different wrappings.

Instrumental Response Function

Decay time by MCP: BaF_2 0.5 ns; Lu_2O_3:Yb 1.1 ns
Taking out IRF: BaF_2 <0.1 ns; Lu_2O_3:Yb 0.63 ns

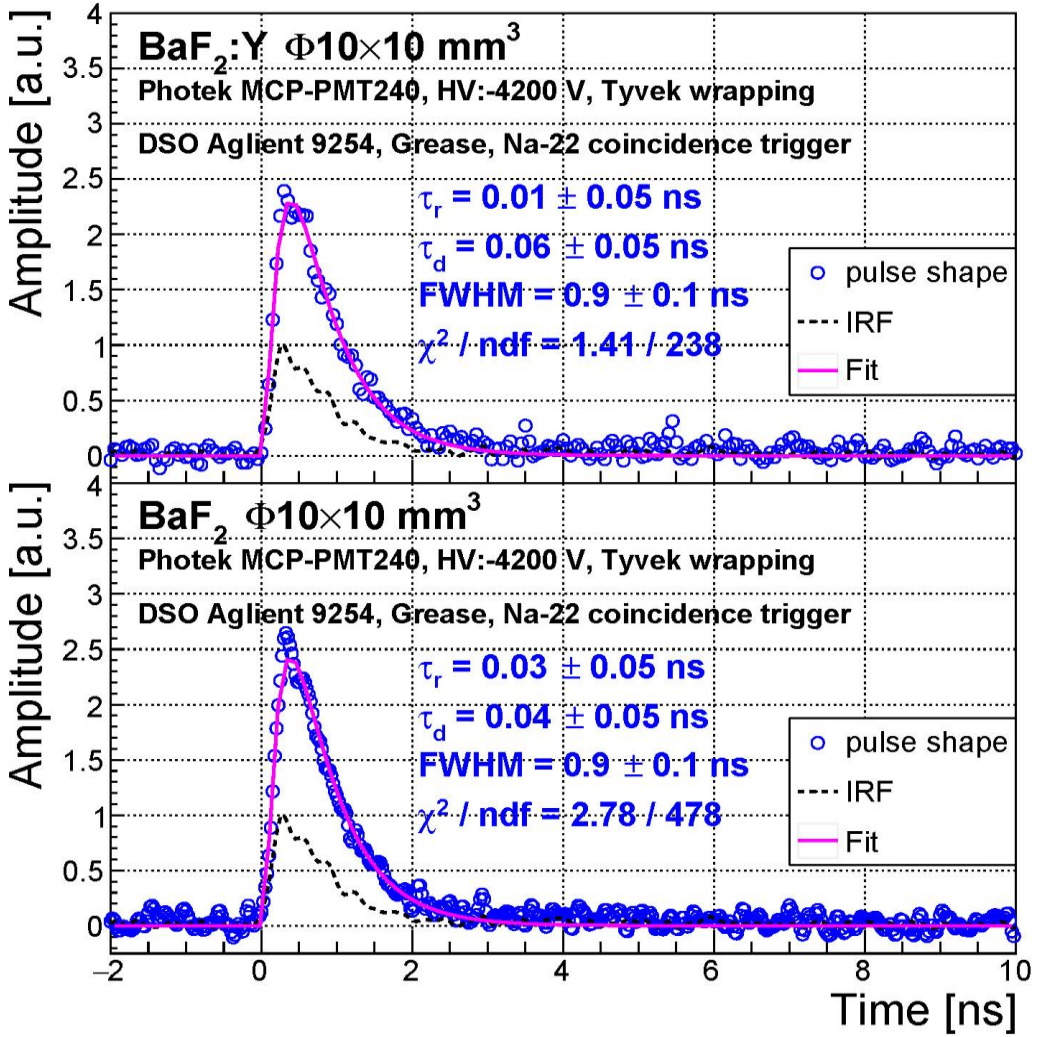

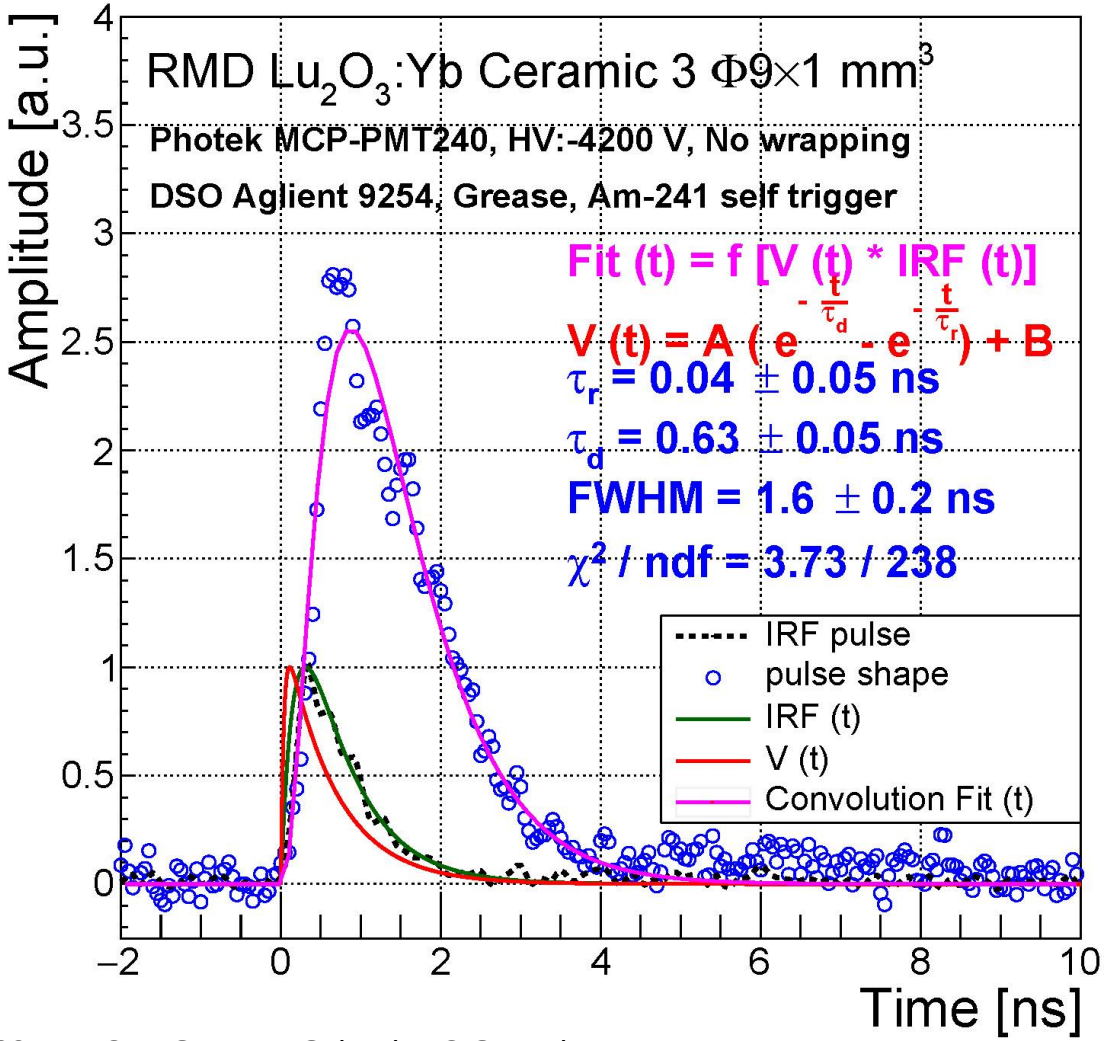

Pulse Height Spectrum

FWHM: 3 to 80 % by a Hamamatsu R1306 PMT (bi-alkali cathode)

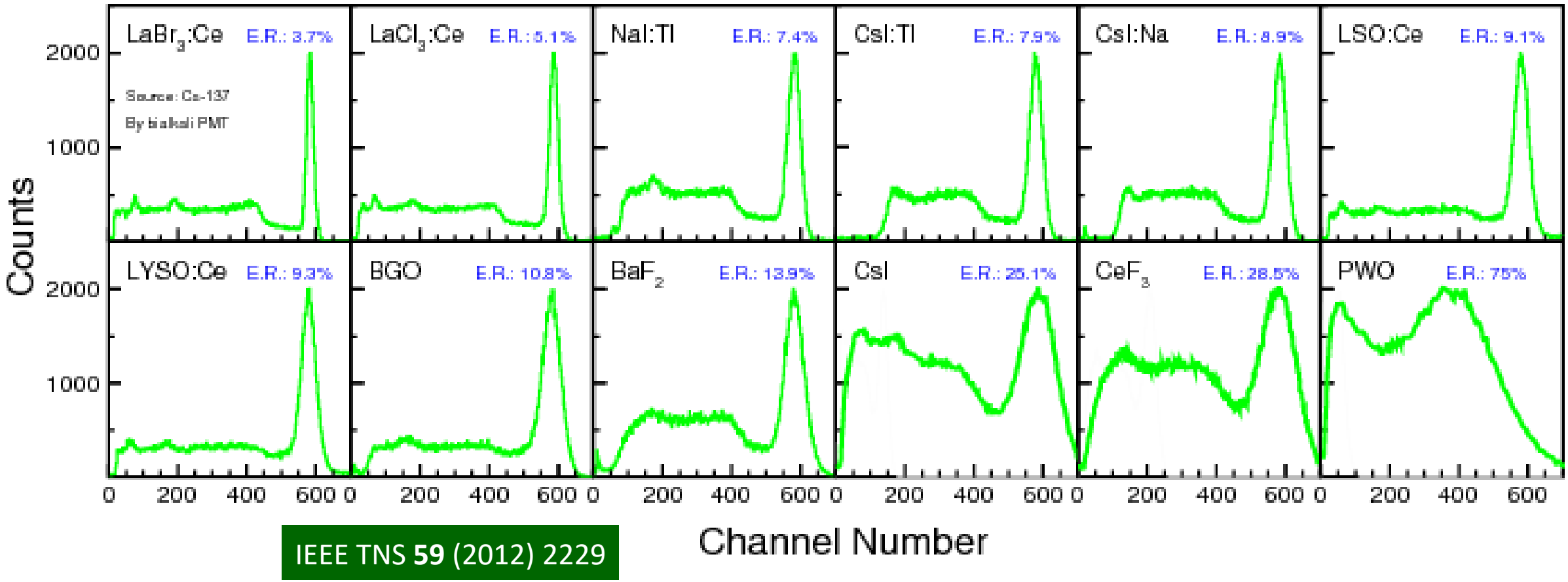

IEEE TNS **59** (2012) 2229

Homeland security application requires 2% for ^{137}Cs γ–rays

Light Output and Decay Kinetics

IEEE TNS **59** (2012) 2229

Measured by a Philips XP2254B PMT (multi-alkali cathode)

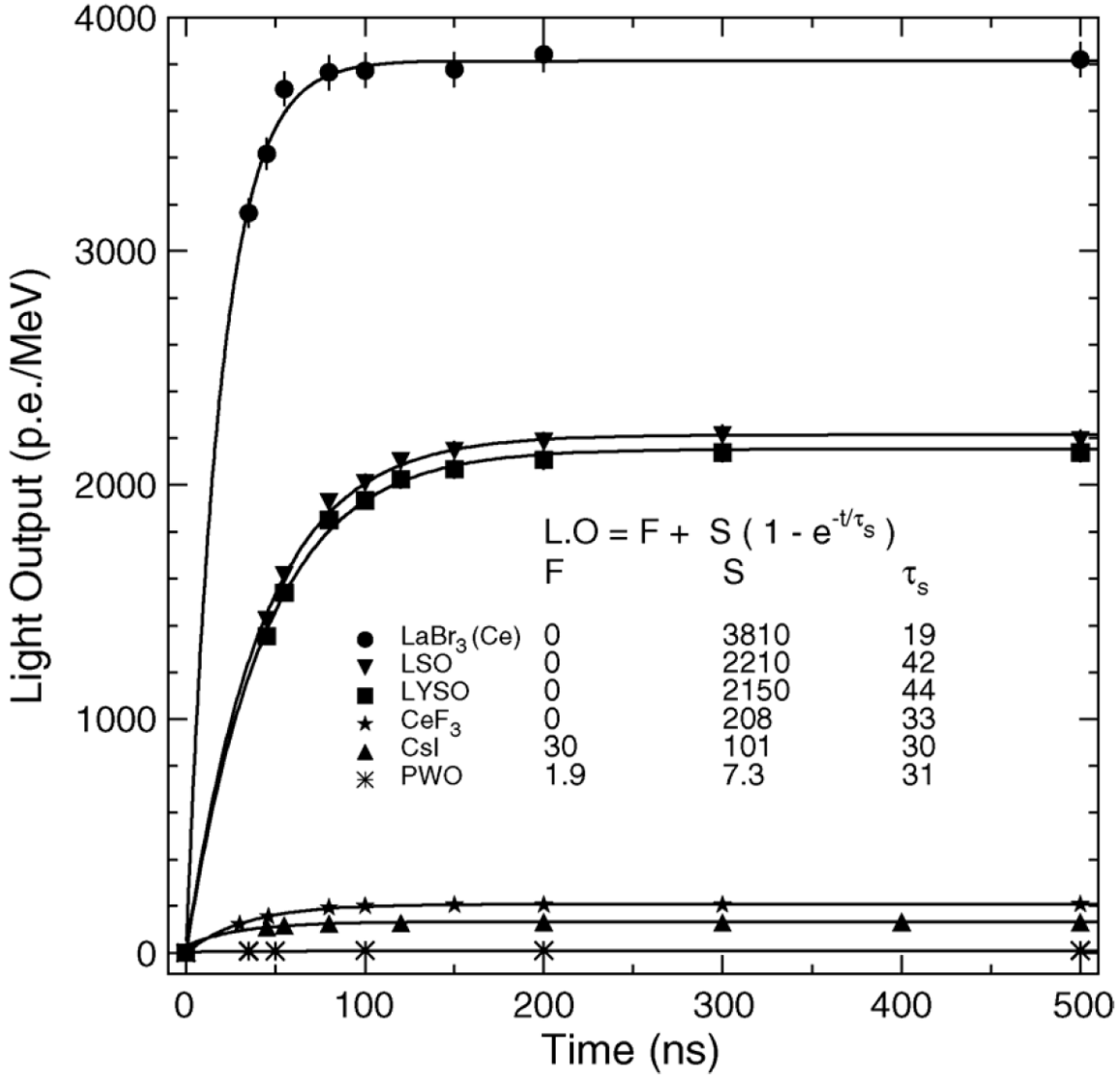

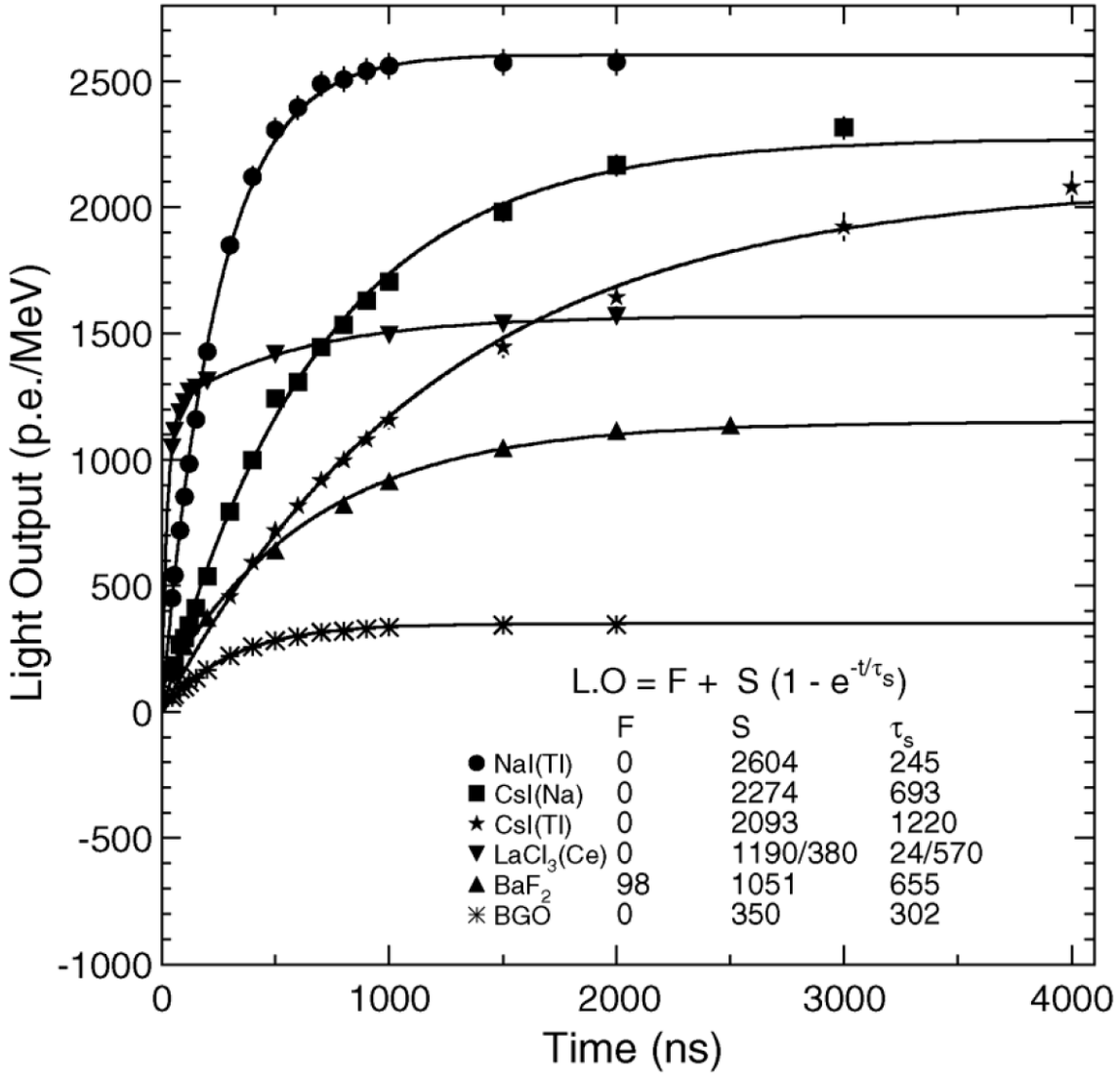

Emission Weighted QE

Taking out QE, LY of LSO/LYSO is 4 and 200 times of BGO and PWO

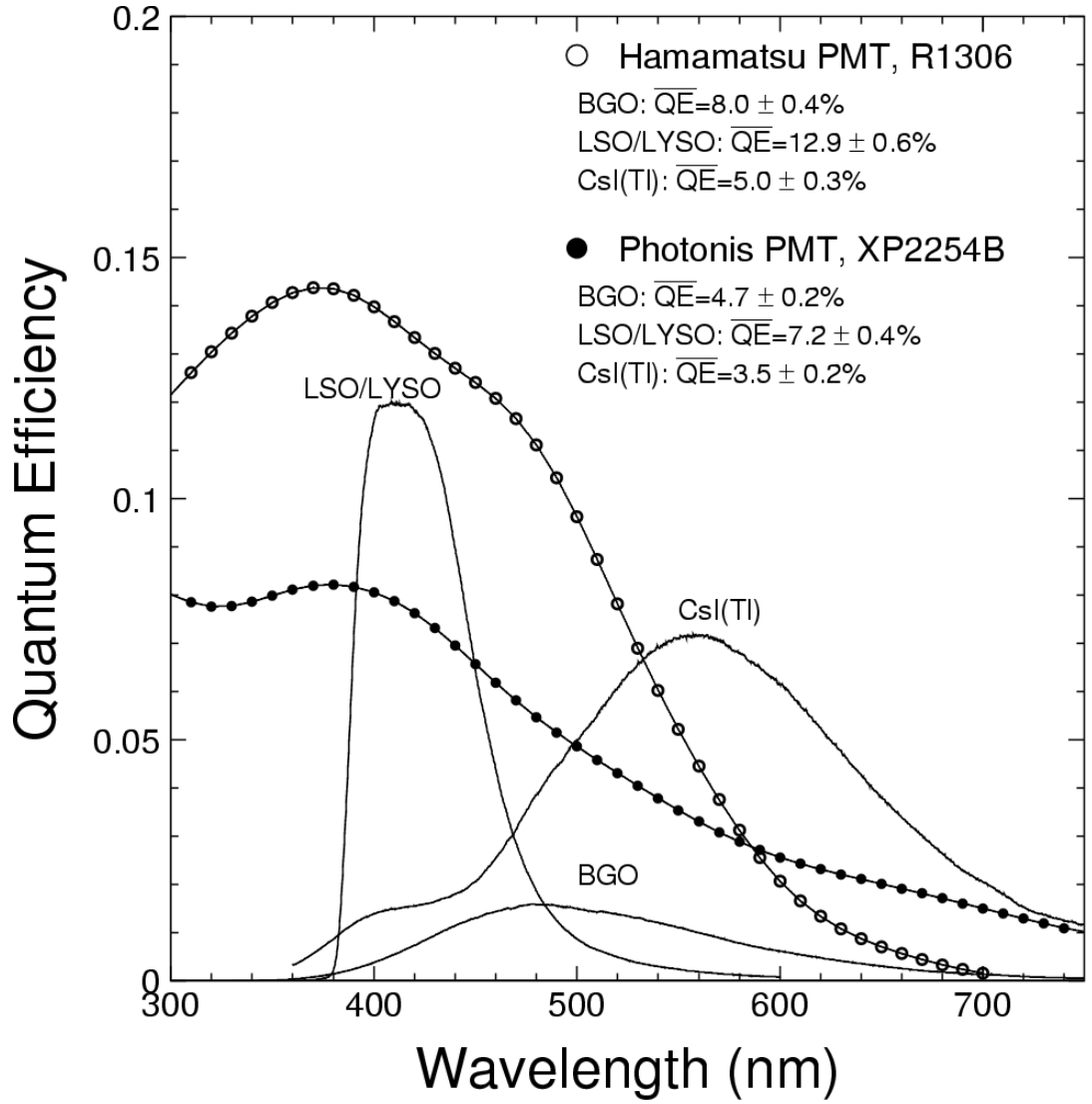

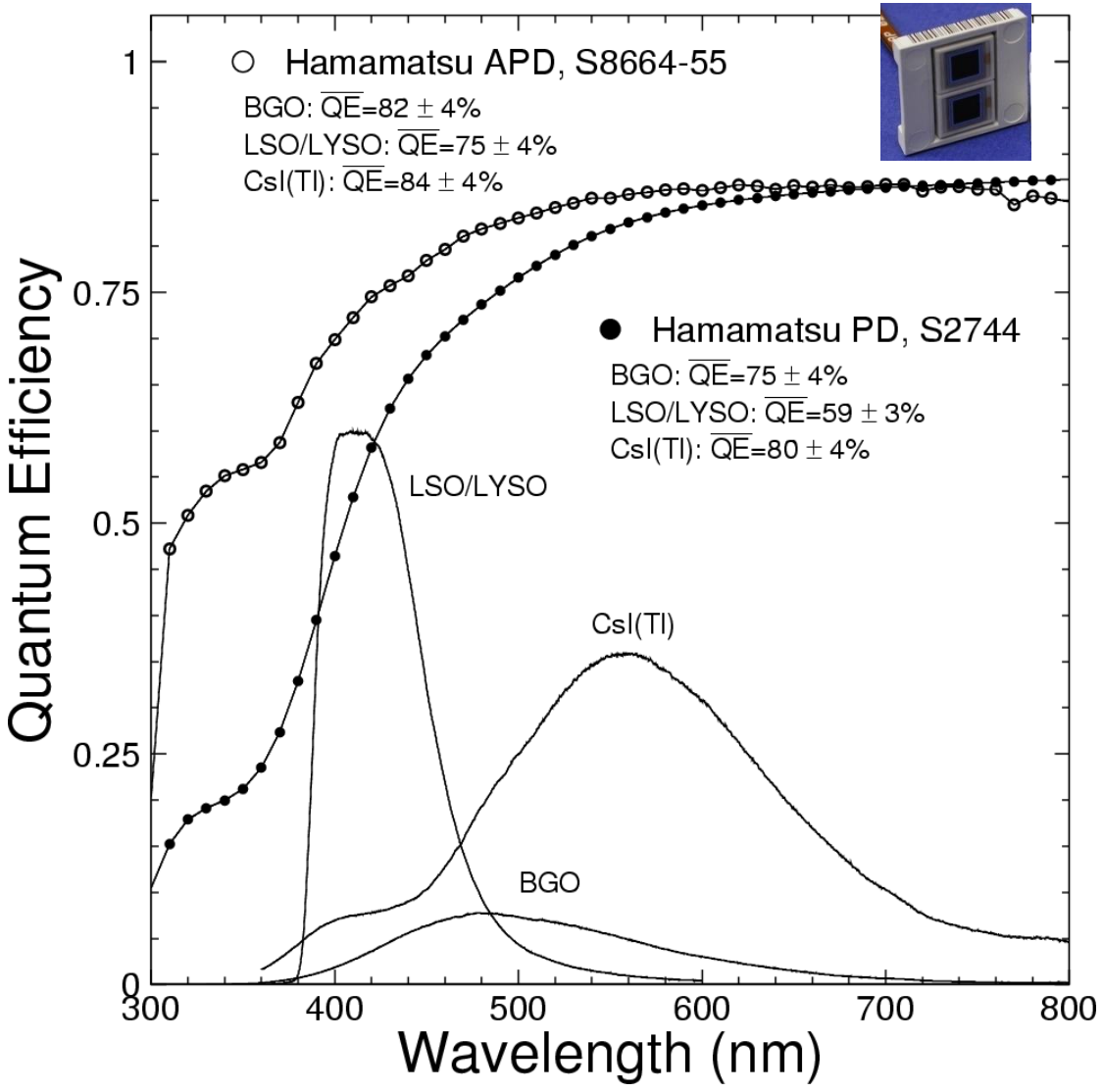

Temperature Coefficient

IEEE TNS **59** (2012) 2229

Temperature Range: 15 - 25ºC

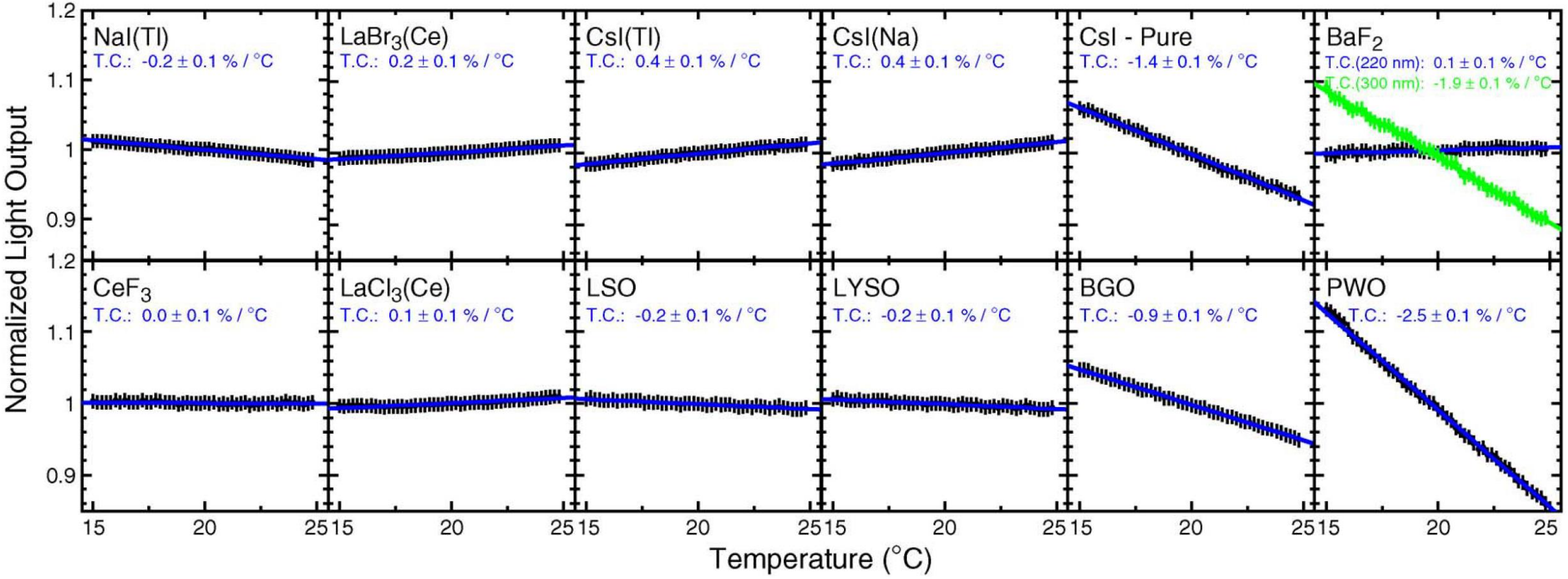

Temperature coefficient > 1%/°C: (BGO), CsI, BaF_2 slow and PWO

Maintain 1% Uncertainty for LO

Require stringent experimental control and temperature corrections

IEEE TNS **48** (2001) 372

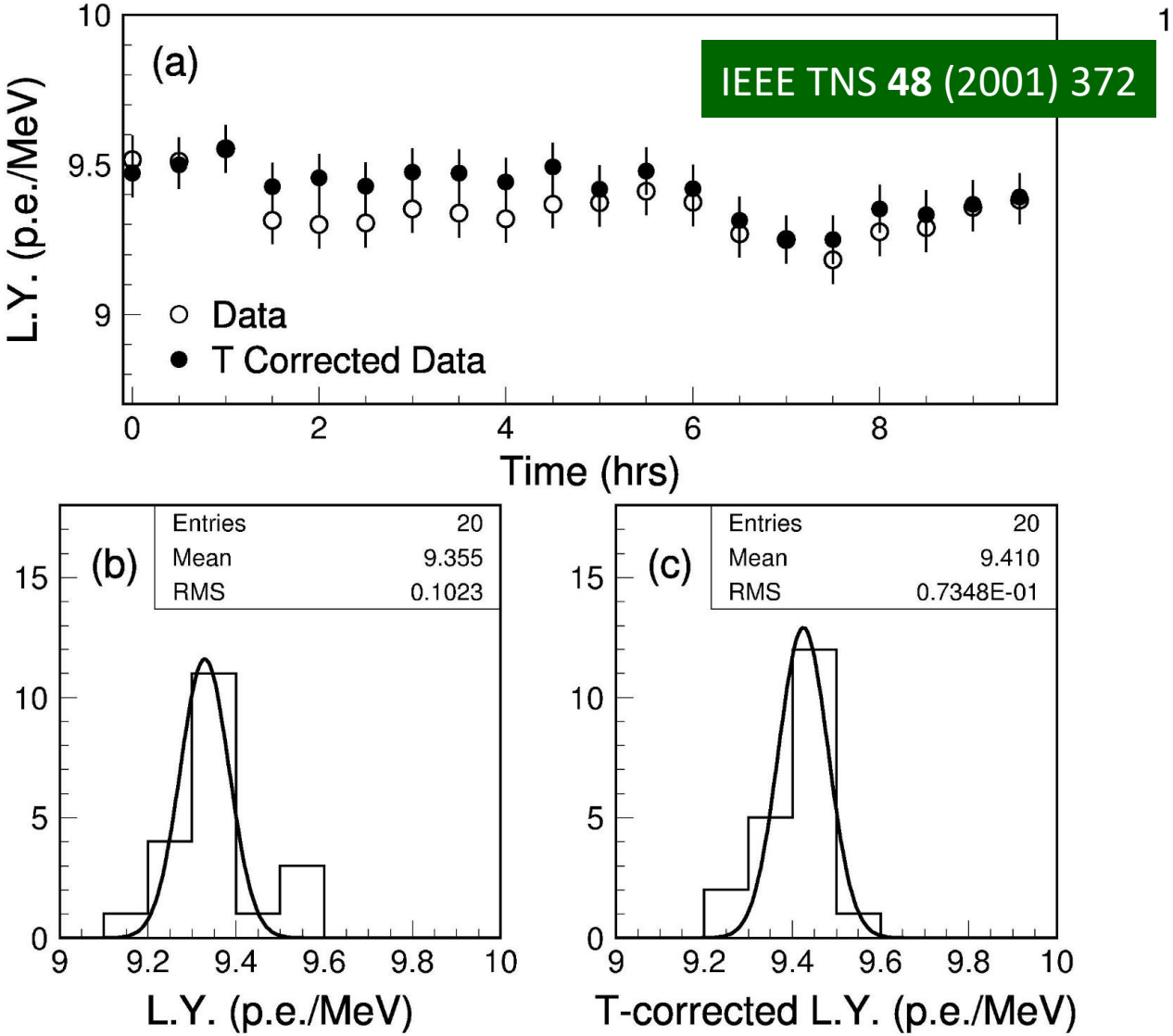

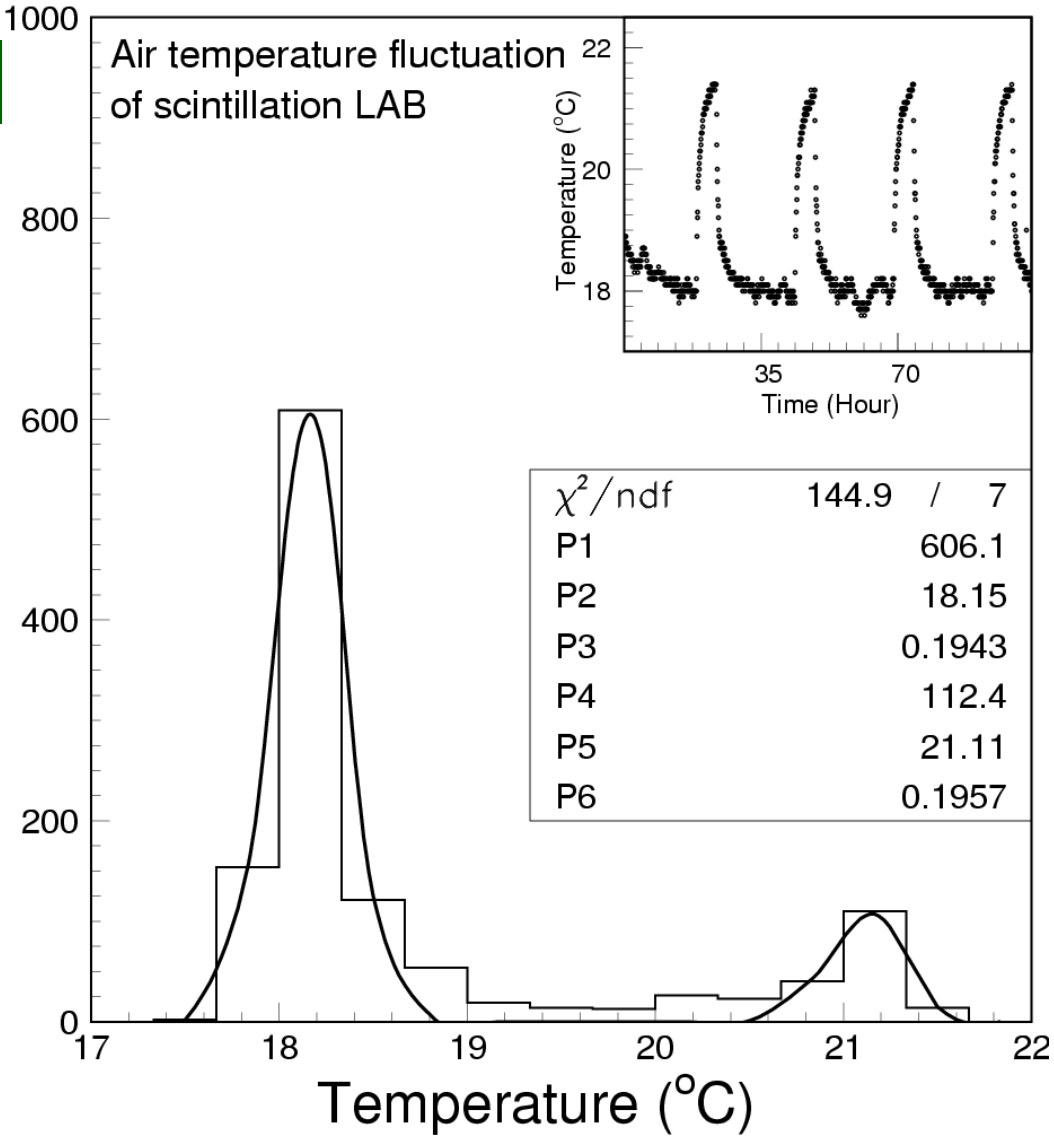

Radiation Damage Effects

NIM A413 (1998) 297, https://doi.org/10.1007/978-3-319-47999-6_22-2

- **Scintillation mechanism damage: reduced LY and LO and maybe also LRU;**
- **Radiation-induced phosphorescence (afterglow): increase dark current, dark counting rate and readout noise;**
- **Radiation-induced absorption (color centers): reduced light attenuation length, LO and maybe also LRU.**

	CsI:Tl	CsI	BaF_2	BGO	PWO	LSO/LYSO
Scintillation mechanism	No	No	No	No	No	No
Phosphorescence (afterglow)	Yes	Yes	Yes	Yes	Yes	Yes
Absorption (color centers)	Yes	Yes	Yes	Yes	Yes	Yes
Recovery	slow	No	No	Yes	Yes	No
Dose rate dependence	No	No	No	No	No	No
Thermal Annealing	No	No	Yes	Yes	Yes	Yes
Optical Bleaching	No	No	Yes	Yes	Yes	Yes

Scintillation Mechanism and Afterglow

https://doi.org/10.1007/978-3-319-47999-6_22-2

Crystal's scintillation mechanism is not damaged by γ -rays, neutrons and charged hadrons, as shown in no variation in the emission spectra measured before and after irradiations. Radiation-induced phosphorescence is measured as the photo-current after radiation, which is at a level of 10^{-5} for BGO and PWO and 3×10^{-4} for LYSO, and 2×10^{-3} for LSO.

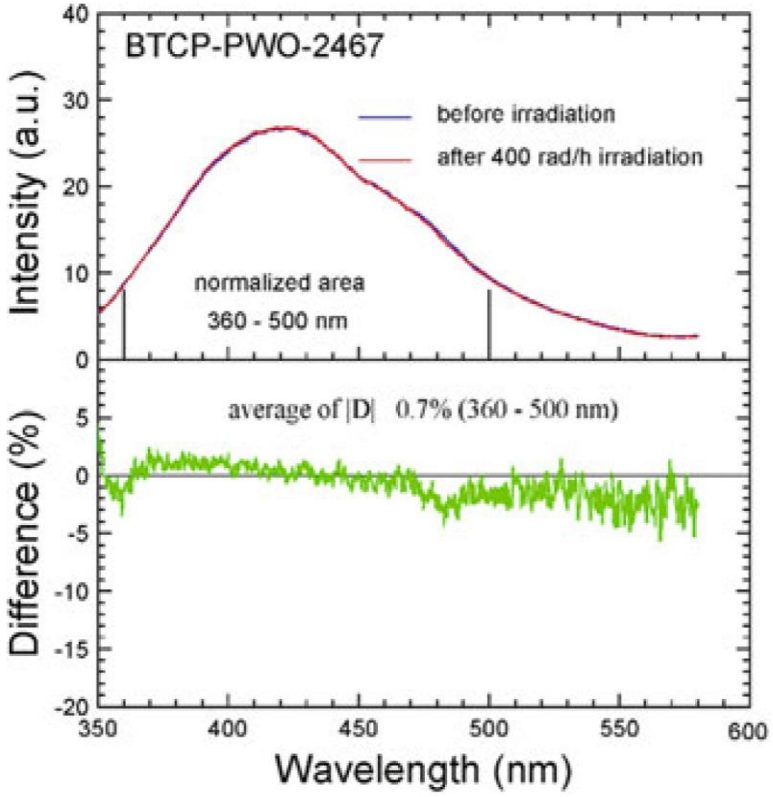

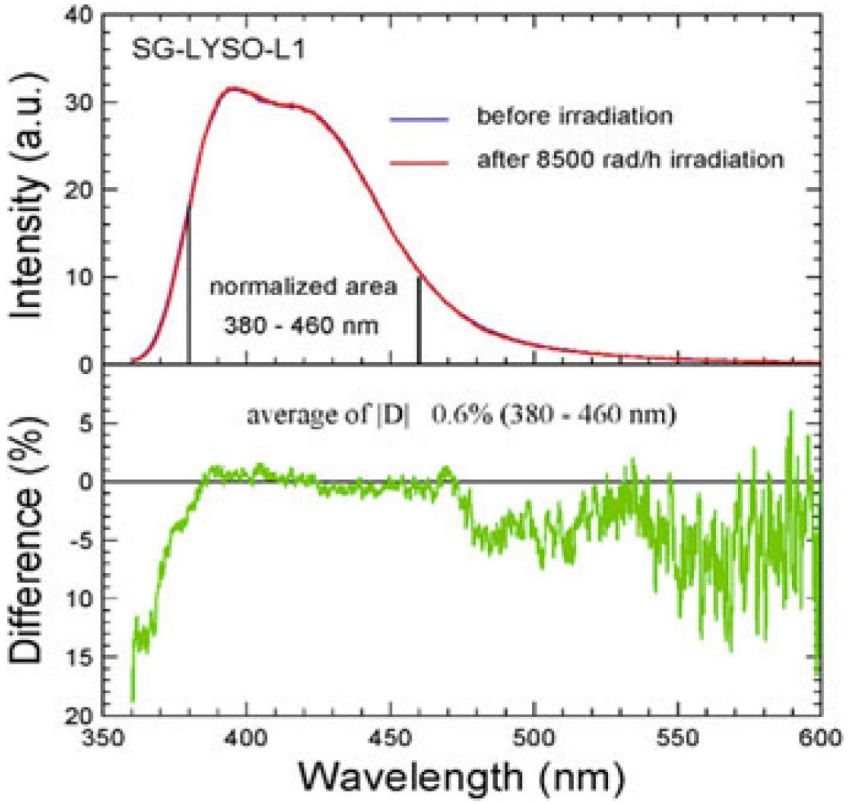

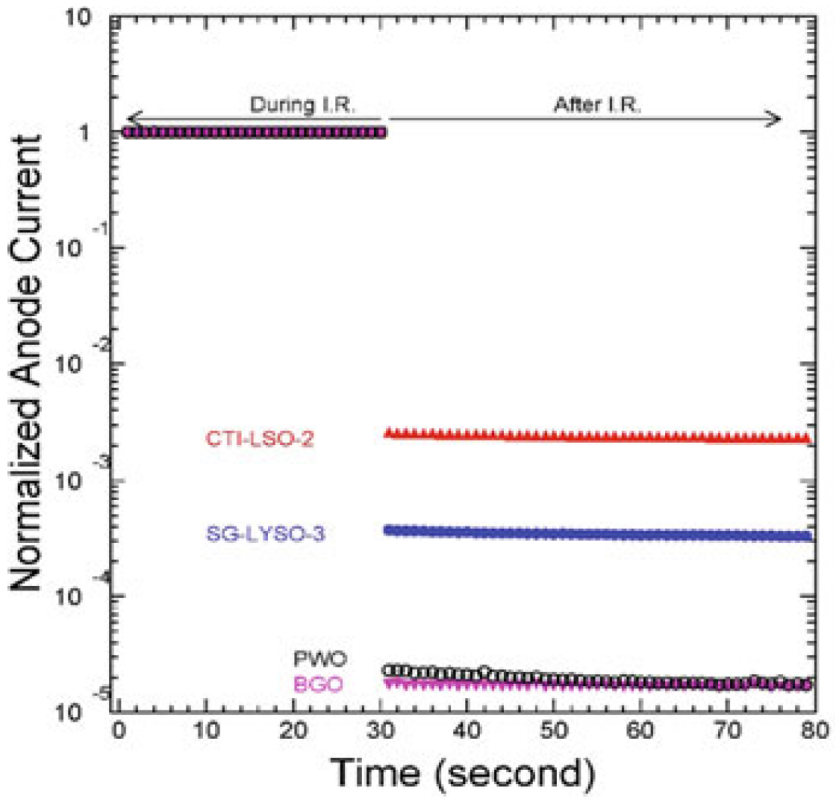

Radiation-Induced Color Centers

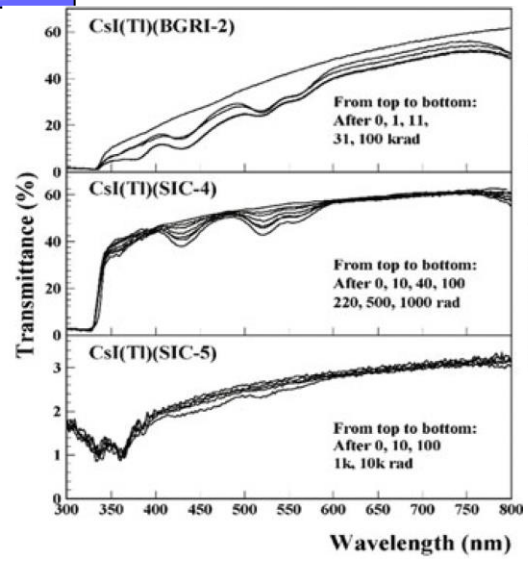

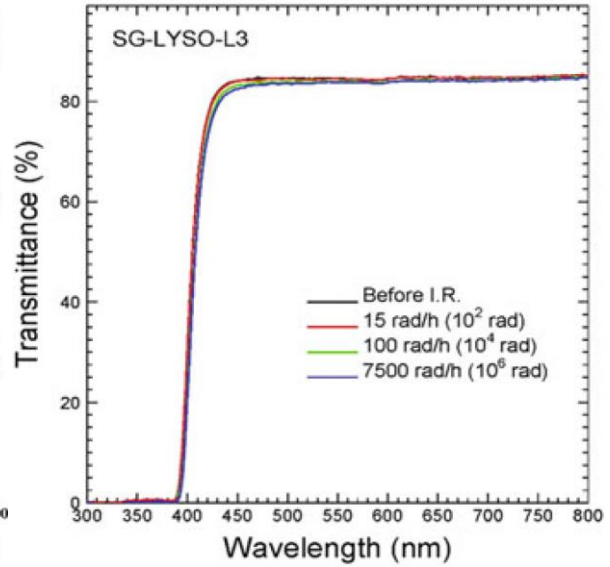

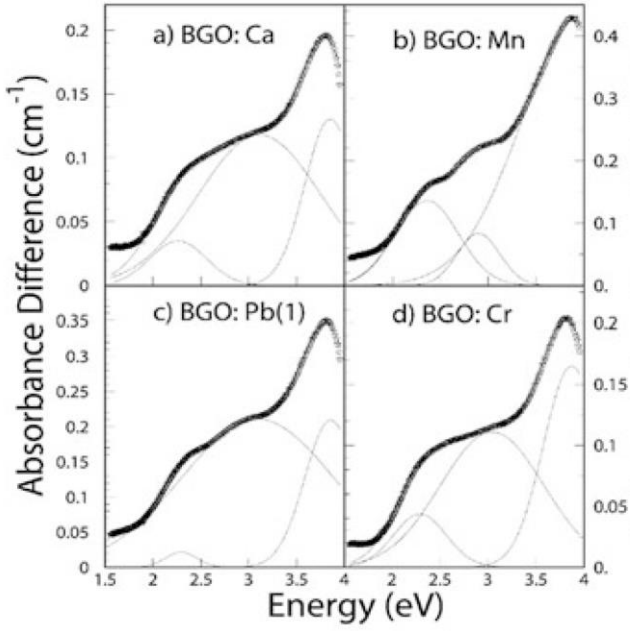

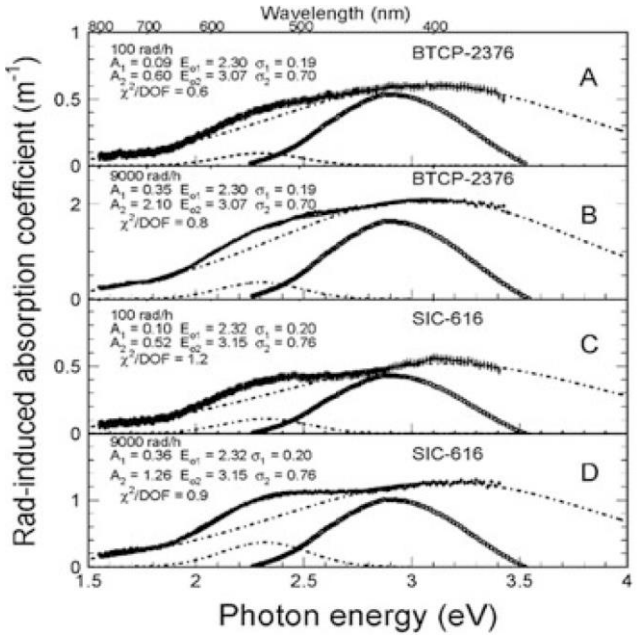

https://doi.org/10.1007/978-3-319-47999-6_22-2

$$EWLT = \frac{\int LT(\lambda)\, Em(\lambda)\, d\lambda}{\int Em(\lambda)\, d\lambda}$$

$$RIAC(\lambda) \text{ or } D(\lambda) = 1/LAL_{\text{after}}(\lambda) - 1/LAL_{\text{before}}(\lambda)$$

$$RIAC(\lambda) = \frac{1}{l}\ln\frac{T_0(\lambda)}{T(\lambda)}$$

$$EWRIAC = \frac{\int RIAC(\lambda)\, Em(\lambda)\, d\lambda}{\int Em(\lambda)\, d\lambda}$$

$$RIAC(\lambda) = \sum_{i=1}^{n} A_i e^{-\frac{(E(\lambda)-E_i)^2}{2\sigma_i^2}}$$

NIM A**302** (1991) 69, NIM A**376** (1996) 319

Dose Rate Dependence & Color Center Kinetics

NIM A413 (1998) 297

Because of the balance between the color center creation (irradiation) and annihilation (recovery) radiation damage in inorganic scintillators may be dose rate dependent. Assuming the annihilation speed of the color center *i* is proportional to a_i and its creation speed is proportional to the product of b_i and the dose rate R, color center density reaches an equilibrium when both processes coexist.

$$dD(\lambda) = \sum_{i=1}^{n} \left\{ -a_i D_i(\lambda)\, dt + \left(D_i^{all}(\lambda) - D_i(\lambda) \right) b_i R dt \right\}$$

$$D(\lambda) = \sum_{i=1}^{n} \left\{ \frac{b_i R D_i^{\text{all}}(\lambda)}{a_i + b_i R} \left[1 - e^{-(a_i + b_i R)t} \right] + D_i^0(\lambda)\, e^{-(a_i + b_i R)t} \right\}$$

$$D_{\text{eq}}(\lambda) = \sum_{i=1}^{n} \frac{b_i R D_i^{\text{all}}(\lambda)}{a_i + b_i R}$$

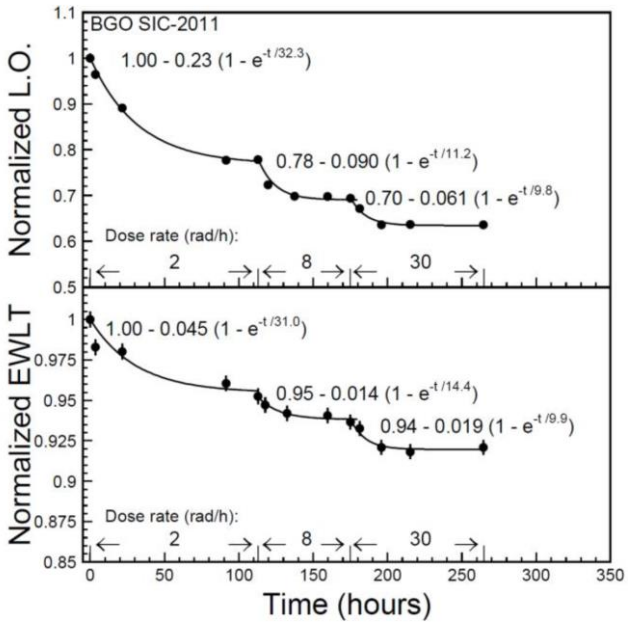

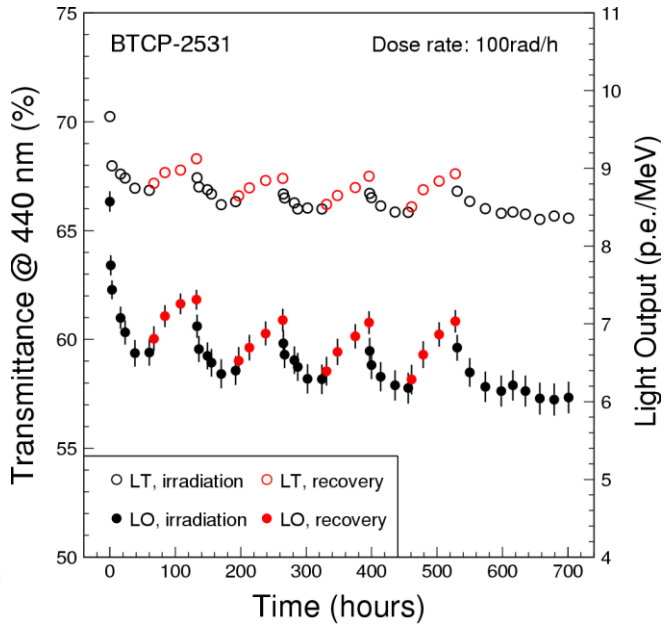

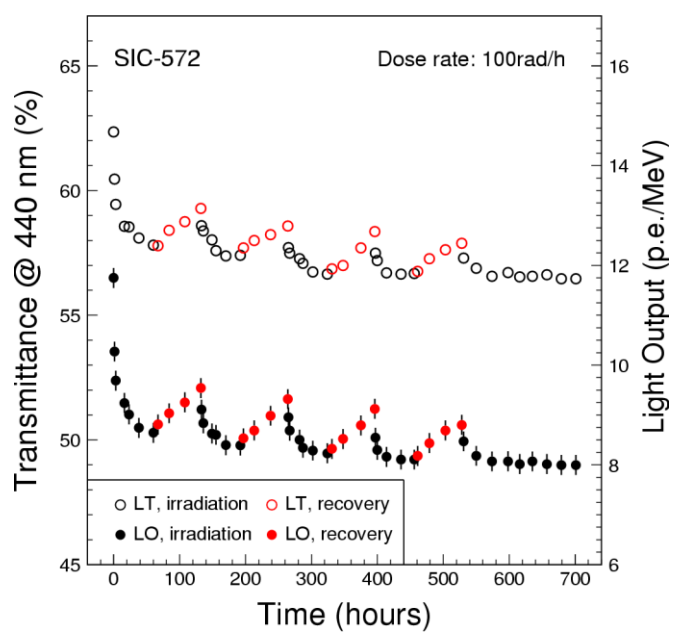

JoP **404** (2012) 012025

Radiation Damage Mechanism

SIMS analysis revealed that damage in alkali halides was caused by the oxygen and/or hydroxyl contamination. Localized stoichiometry analysis by TEM/EDS revealed that damage in oxides was caused by stoichiometry-related defects, e.g. oxygen vacancies.

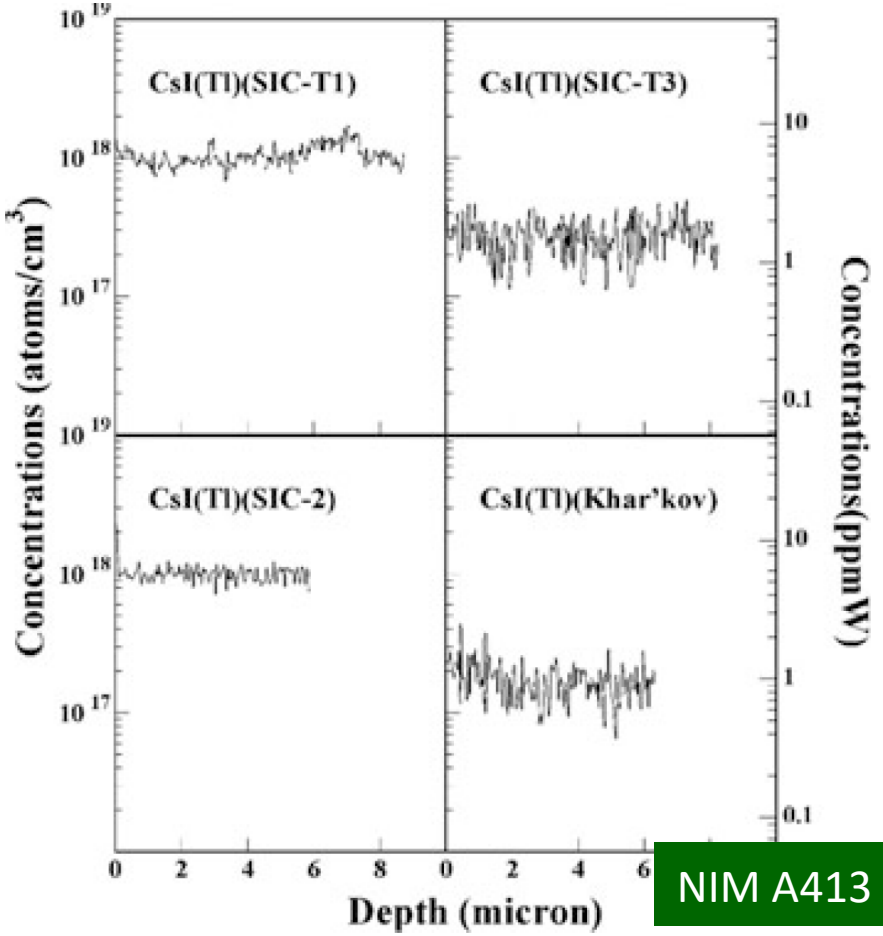

As grown sample

Element	Black spot	Peripheral	$Matrix_1$	$Matrix_2$
O	1.5	15.8	60.8	63.2
W	50.8	44.3	19.6	18.4
Pb	47.7	39.9	19.6	18.4

The same sample after oxygen compensation

Element	$Point_1$	$Point_2$	$Point_3$	$Point_4$
O	59.0	66.4	57.4	66.7
W	21.0	16.5	21.3	16.8
Pb	20.0	17.1	21.3	16.5

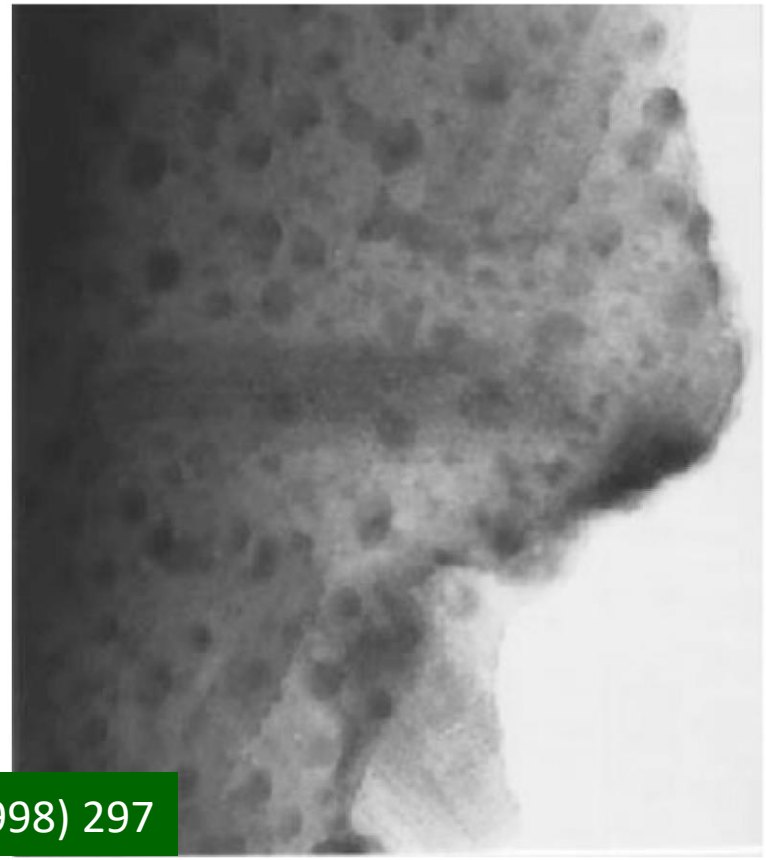

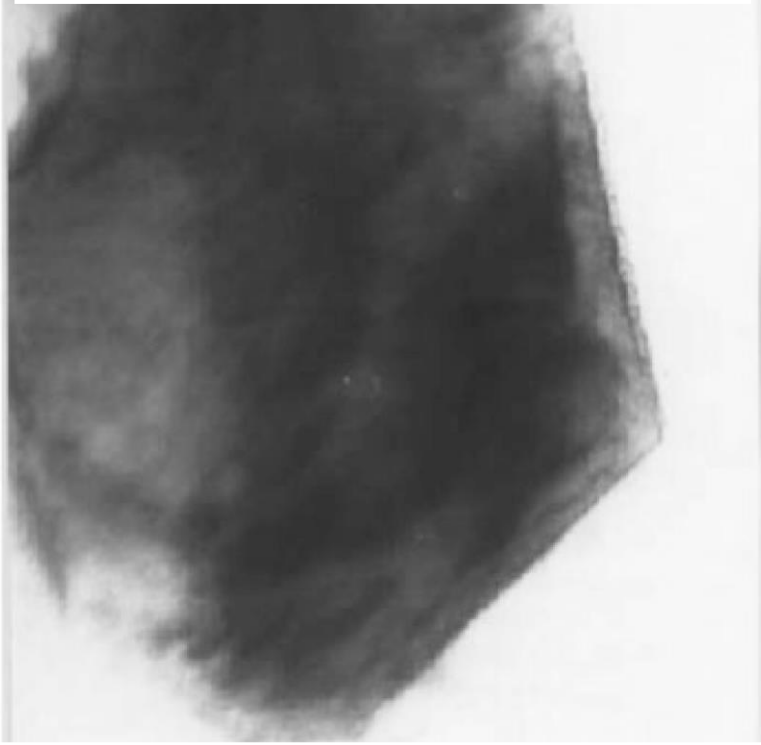

NIM A413 (1998) 297

2019 DOE Basic Research Needs Study
Priority Research Directions for Calorimetry

- Enhance calorimetry energy resolution for precision electroweak mass and missing-energy measurements;
- Advance calorimetry with spatial and timing resolution and radiation hardness to master high-rate environments;
- Develop ultrafast media to improve background rejection in calorimeters and particle identication detectors.

DOE 2019: https://www.osti.gov/servlets/purl/1659761
ECFA 2021: https://cds.cern.ch/record/2784893
Snowmass 2021: https://arxiv.org/abs/2209.14111
Fast/ultrafast, radiation hard and cost-effective inorganic scintillators

Challenge: Radiation Damage at the LHC

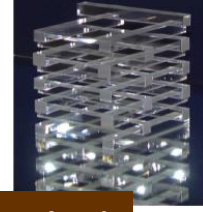

F. Ferri, Calor 2022, https://indico.cern.ch/event/847884/timetable/#20220515

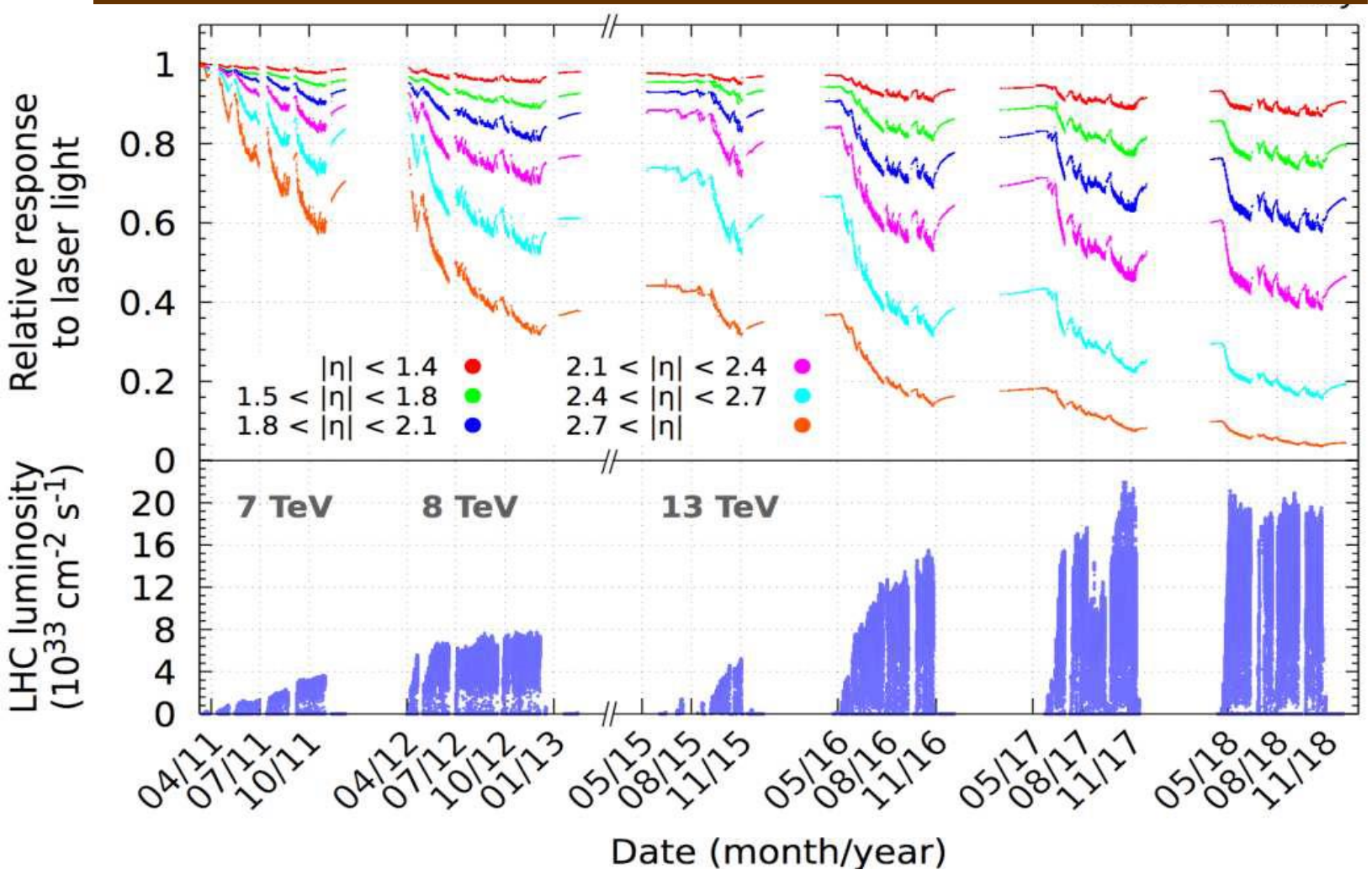

http://www.its.caltech.edu/~rzhu/talks/ryz_161028_PWO_mon.pdf

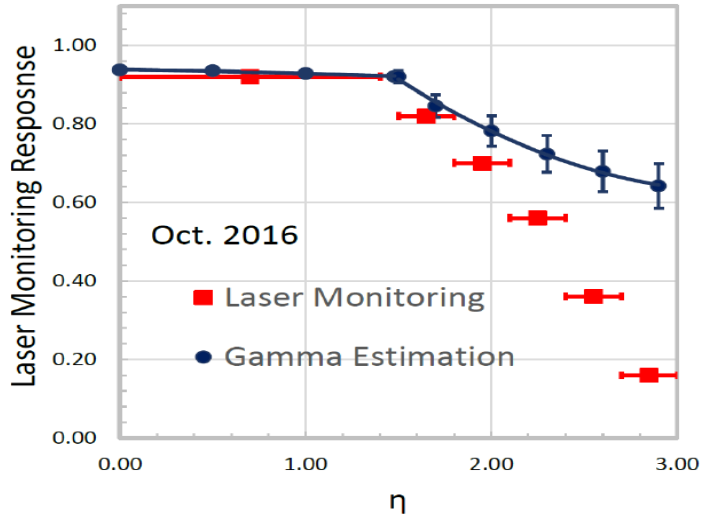

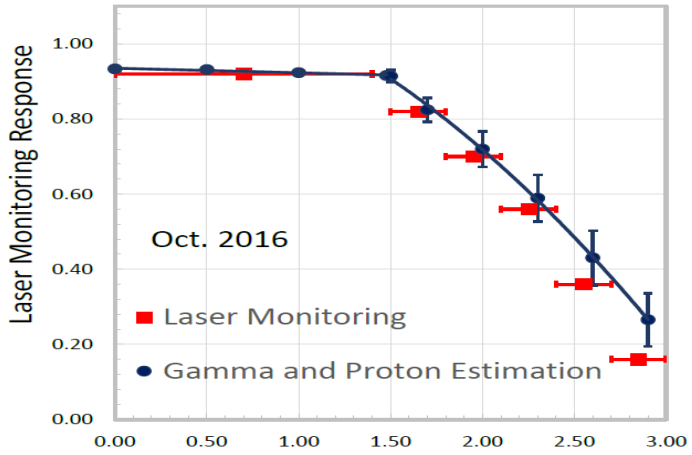

Use materials with monotonic damage: BaF_2, CsI, LYSO:Ce, LuAG:Ce

Neutron damage?

CMS Barrel Timing Detector for HL-LHC

To face challenge of pileup at HL-LHC by using 4D tracking in space and time

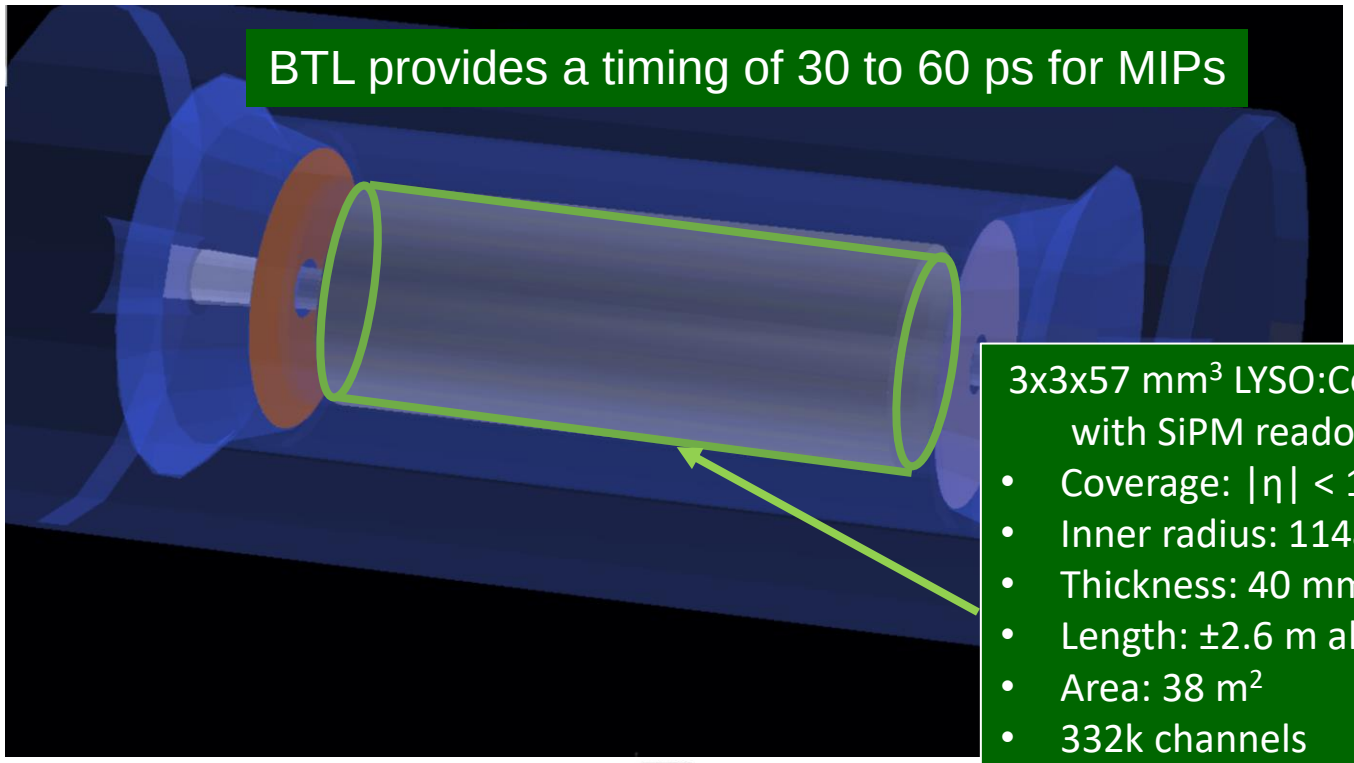

3x3x57 mm^3 LYSO:Ce bars with SiPM readout

- Coverage: $|\eta| < 1.45$
- Inner radius: 1148 mm
- Thickness: 40 mm
- Length: ±2.6 m along z
- Area: 38 m^2
- 332k channels

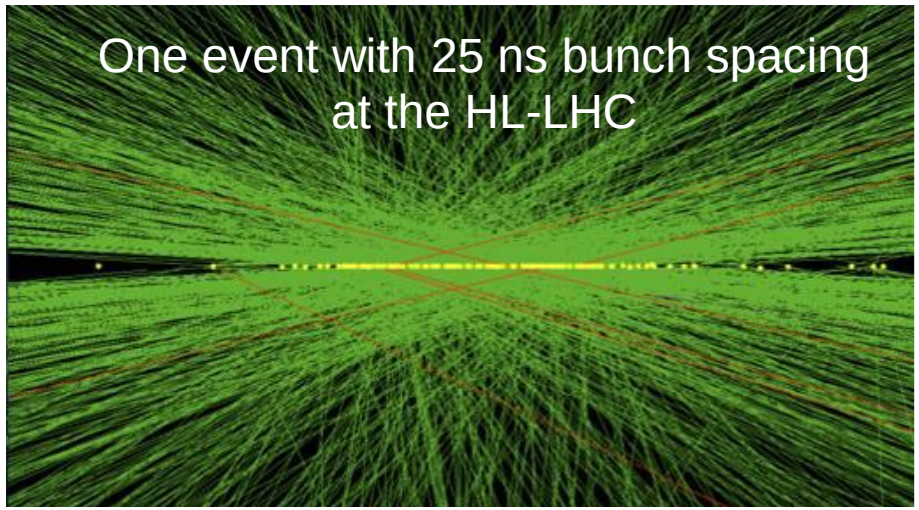

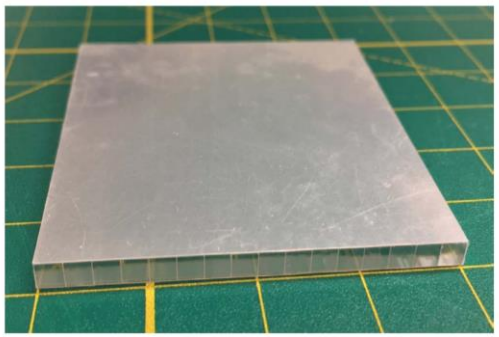

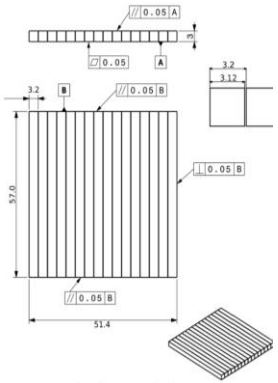

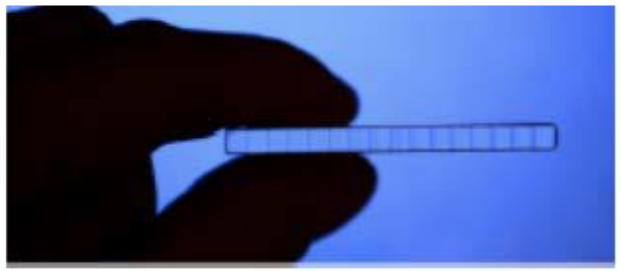

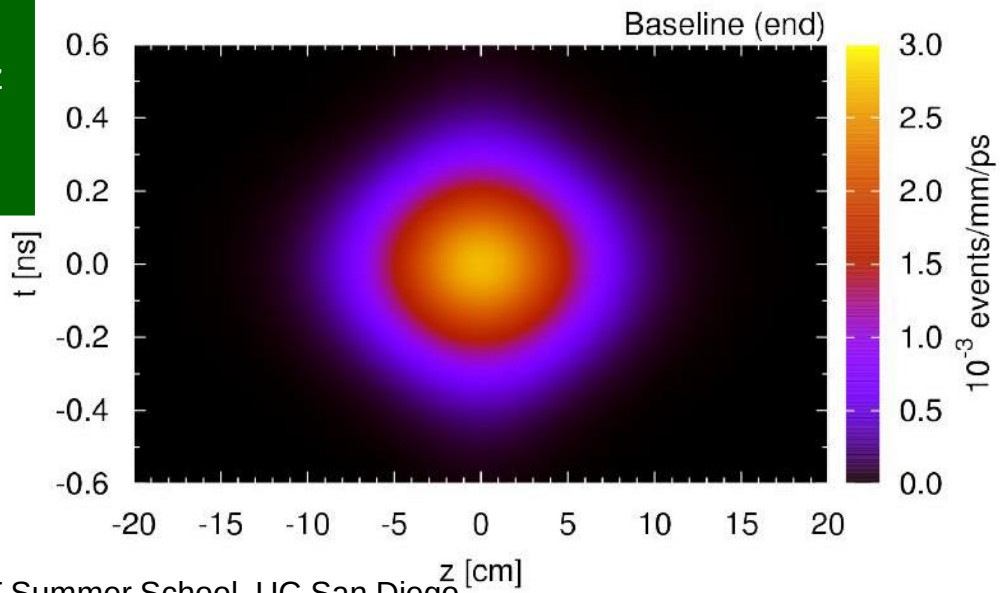

Expected Radiation for CMS ECAL

CMS Barrel/Endcaps: 4.8/68 Mrad, 2.5/21 × 10^{13} p/cm^2 & 3.2/24 × 10^{14} n_{eq}/cm^2

CMS MTD	η	n_{eq} (cm^{-2})	n_{eq} Flux ($cm^{-2}s^{-1}$)	Proton (cm^{-2})	p Flux ($cm^{-2}s^{-1}$)	Dose (Mrad)	Dose rate (rad/h)
Barrel	0.00	2.5E+14	2.8E+06	2.2E+13	2.4E+05	2.7	108
Barrel	1.15	2.7E+14	3.0E+06	2.4E+13	2.6E+05	3.8	150
Barrel	**1.45**	**2.9E+14**	**3.2E+06**	**2.5E+13**	**2.8E+05**	**4.8**	**192**
Endcap	1.60	2.3E+14	2.5E+06	2.0E+13	2.2E+05	2.9	114
Endcap	2.00	4.5E+14	5.0E+06	3.9E+13	4.4E+05	7.5	300
Endcap	2.50	1.1E+15	1.3E+07	9.9E+13	1.1E+06	26	1020
Endcap	**3.00**	**2.4E+15**	**2.7E+07**	**2.1E+14**	**2.3E+06**	**68**	**2700**

Much higher at FCC-hh: up to 0.1/500 Grad and 3/500 x10^{16} n_{eq}/cm^2 at EMEC/EMF

Aleksa *et al.*, Calorimeters for the FCC-hh CERN-FCCPHYS-2019-0003, Dec 23, 2019

LYSO:Ce Radiation Hardness

IEEE TNS 63 (2016) 612-619

CMS BTL LYSO spec: RIAC < 3 m^{-1} after 4.8 Mrad, 2.5 x 10^{13} p/cm^2 and 3.2 x 10^{14} n_{eq}/cm^2

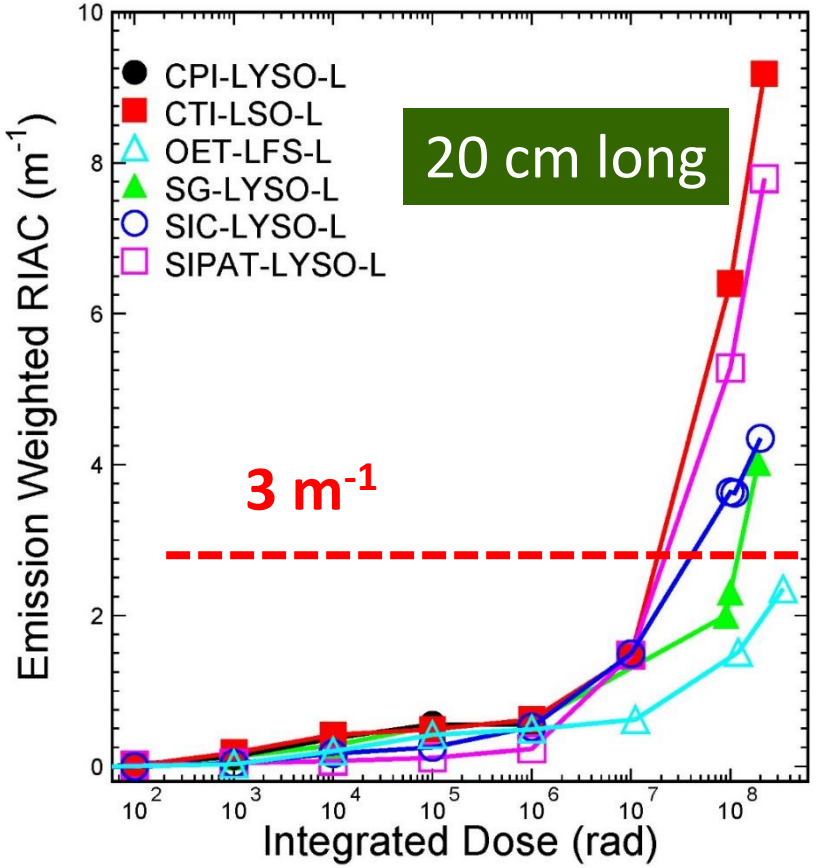

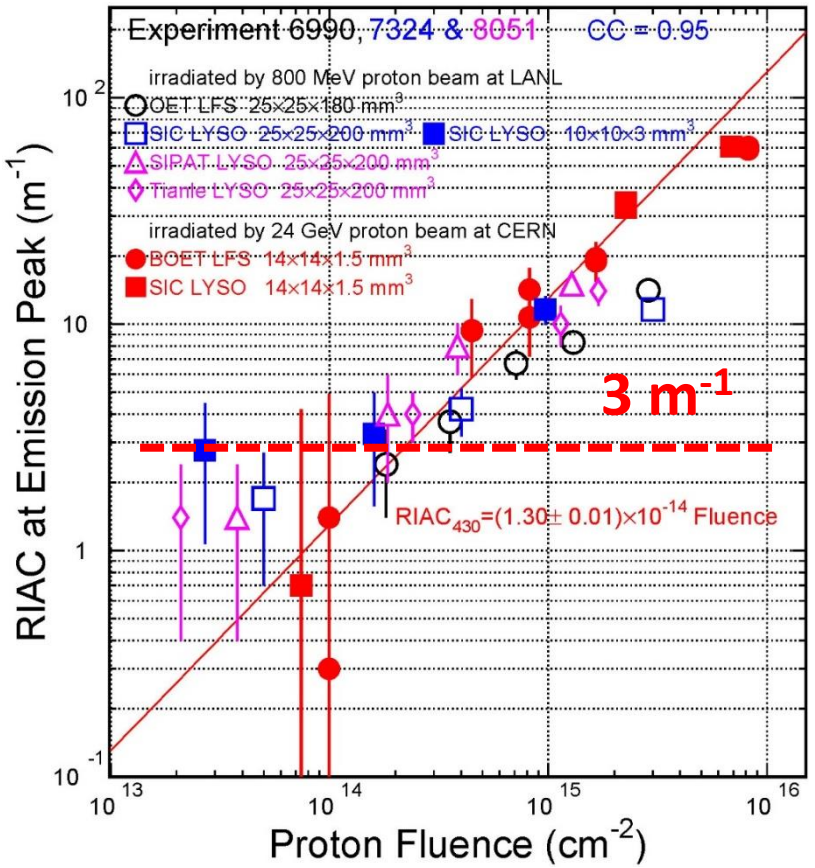

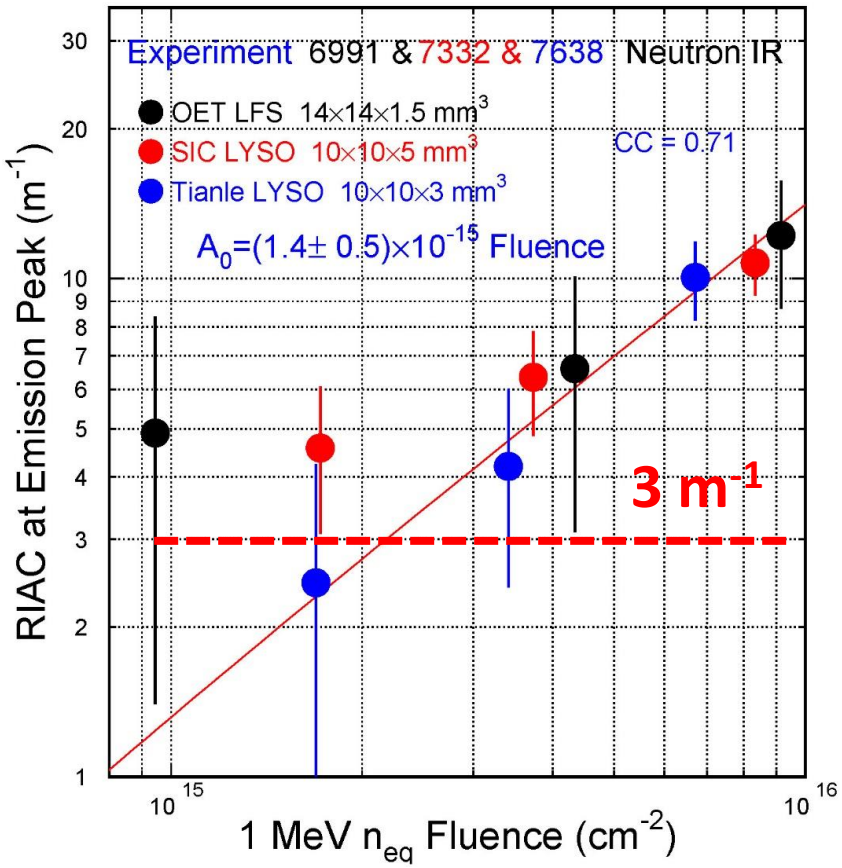

Damage induced by protons is larger than that from neutrons
Due to ionization energy loss in addition to displacement and nuclear breakup

RADiCAL: LYSO/LuAG Shashlik ECAL

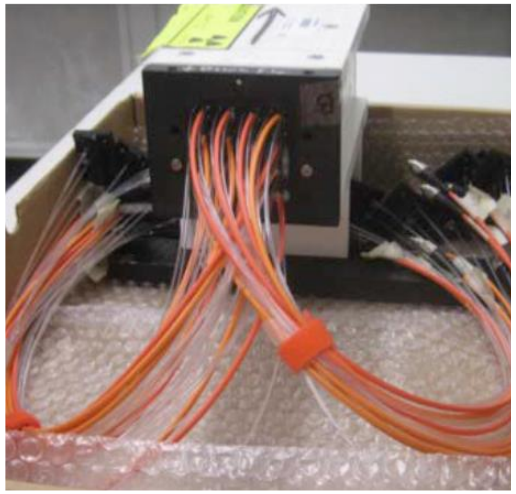

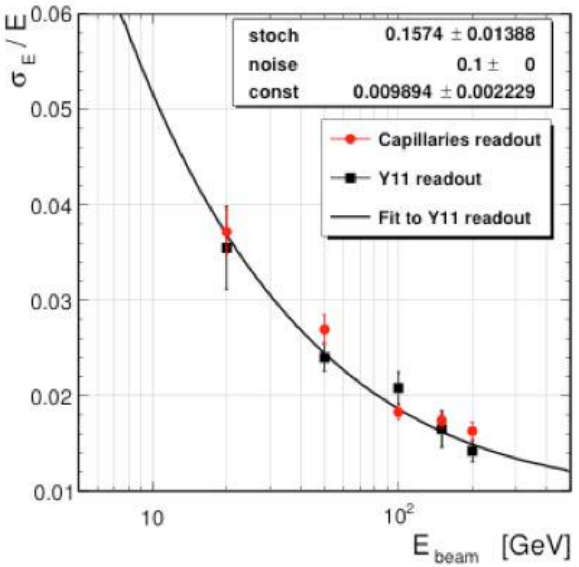

arXiv: 2203.12806 (N35-6)

RADiation hard **CAL**orimetry
Reducing light path length to mitigate radiation damage effect
Using radiation hard materials: LuAG:Ce ceramics excitation matches LYSO:Ce emission

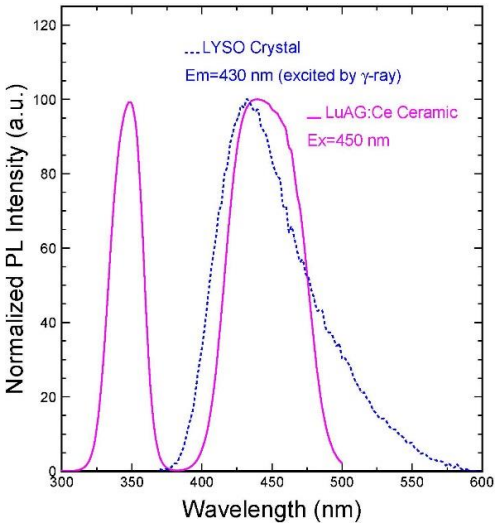

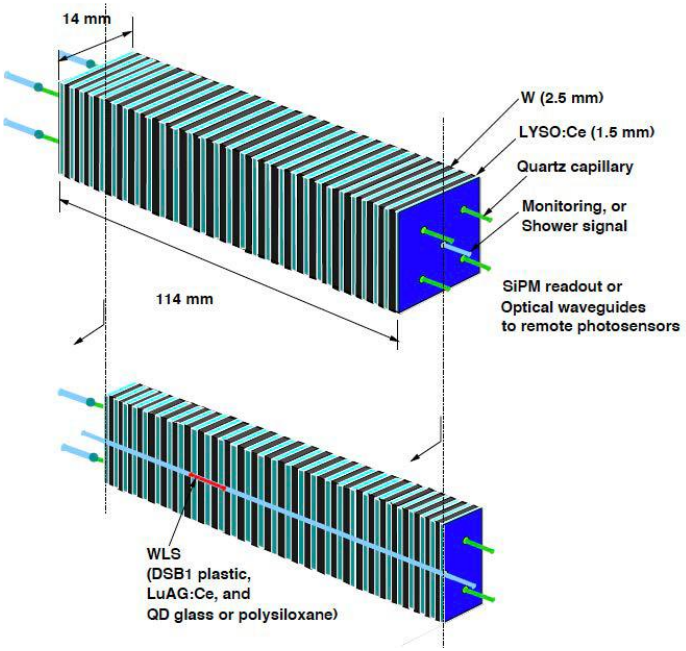

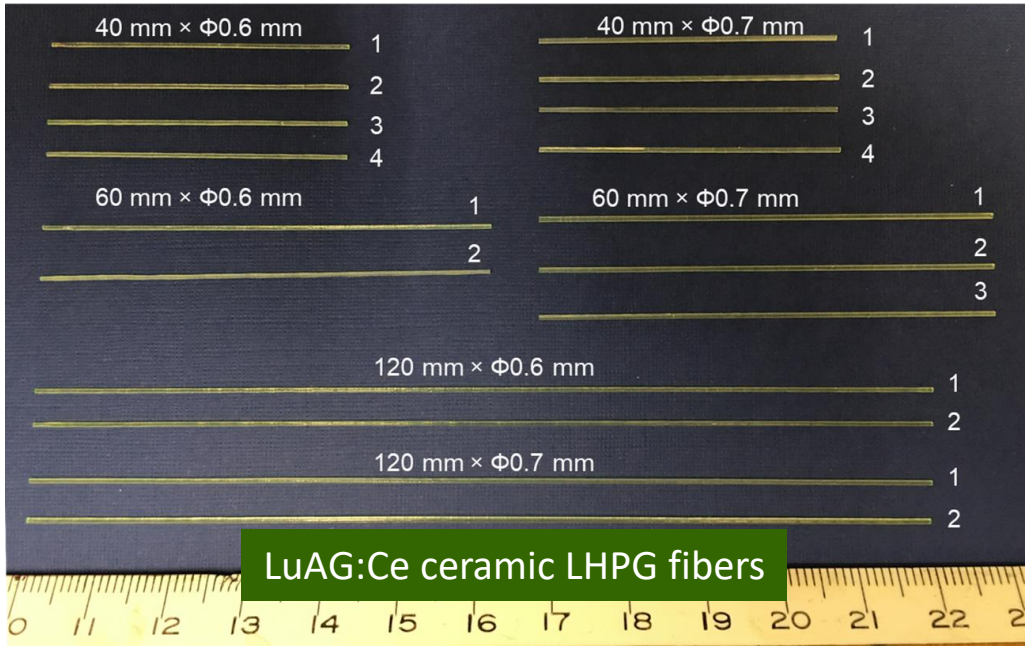

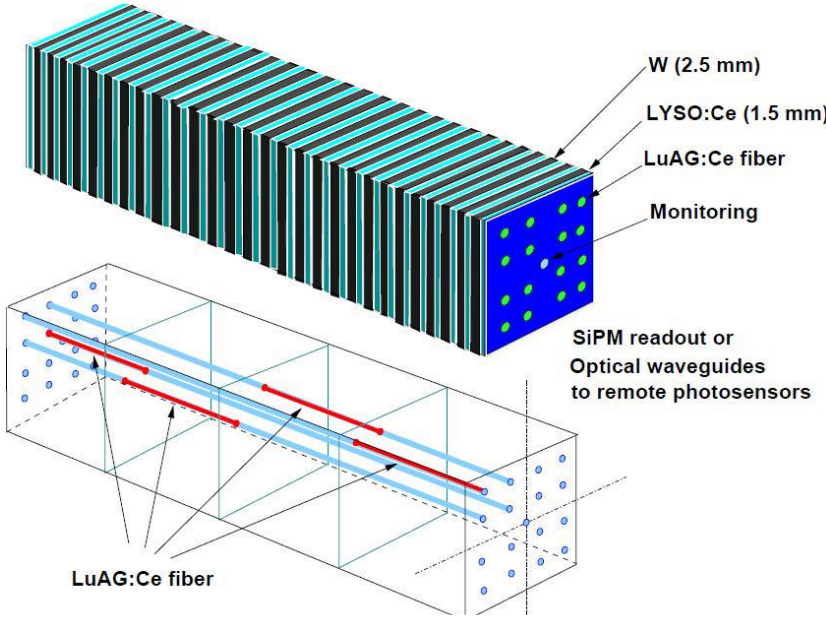

LuAG:Ce Ceramics Radiation Hardness

IEEE TNS 69 (2022) 181-186

LuAG:Ce ceramics show a factor of two smaller RIAC values than LYSO:Ce up to 6.7×10^{15} n_{eq}/cm^2 and 1.2×10^{15} p/cm^2, promising for FCC-hh

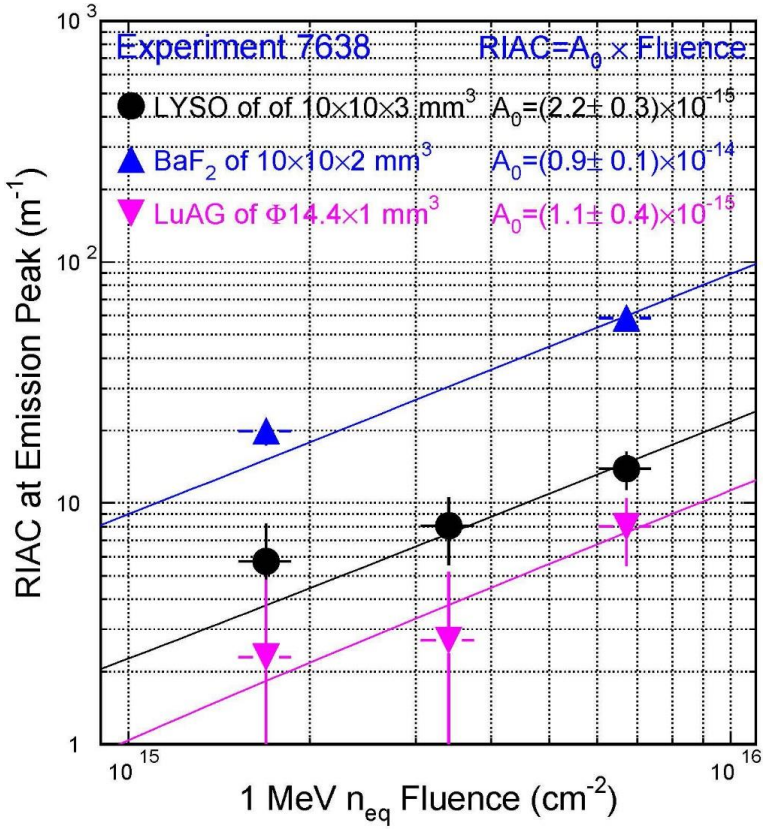

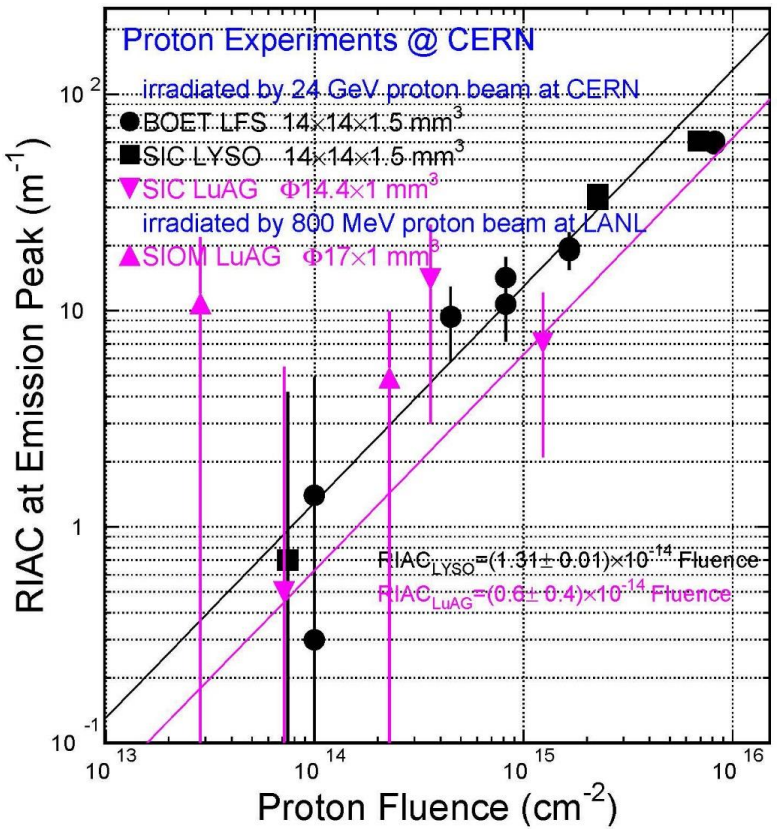

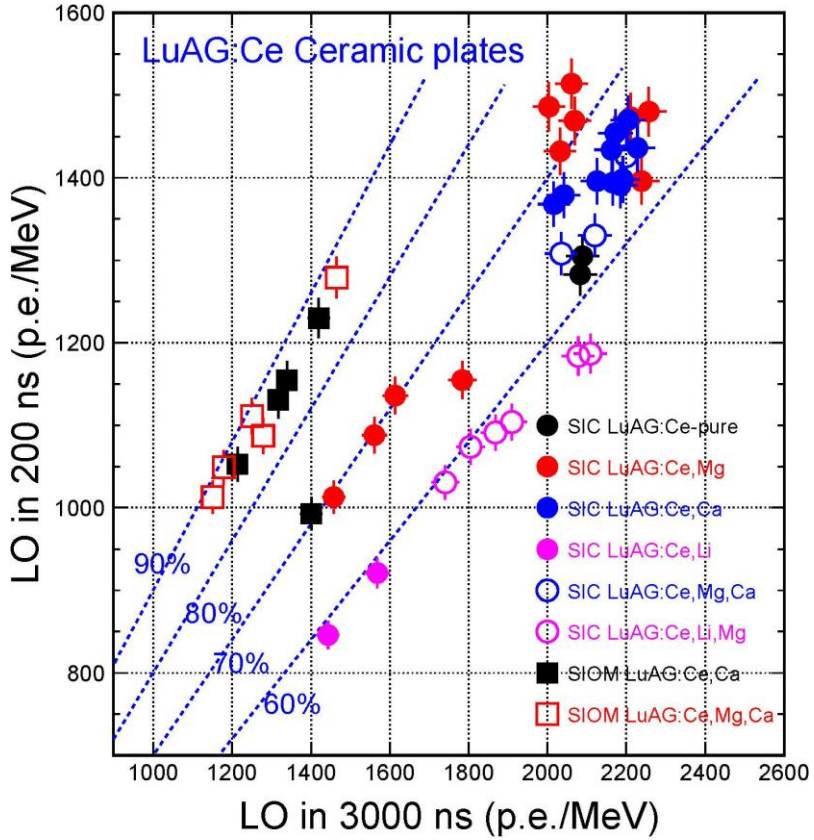

R&D on slow component suppression by Ca co-doping, and radiation hardness by ɣ/p/n

LuAG:Ce Fiber Light Output and Uniformity

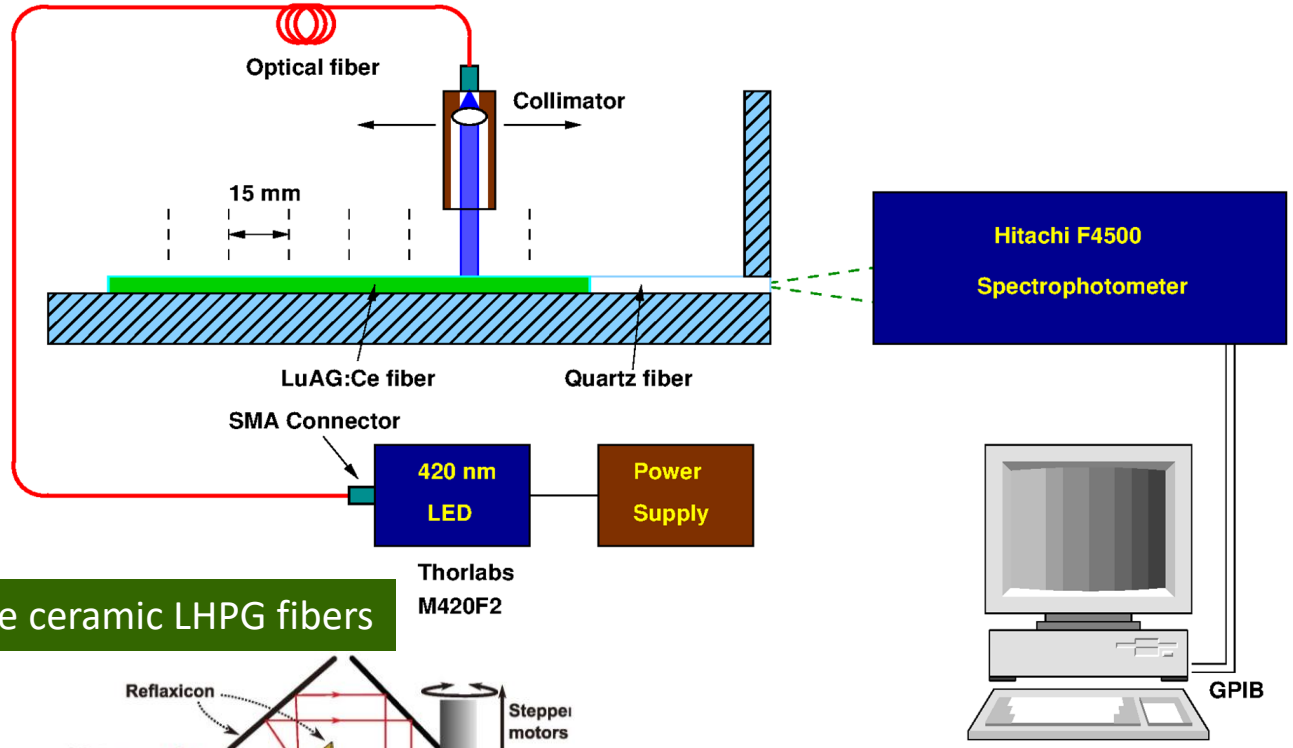

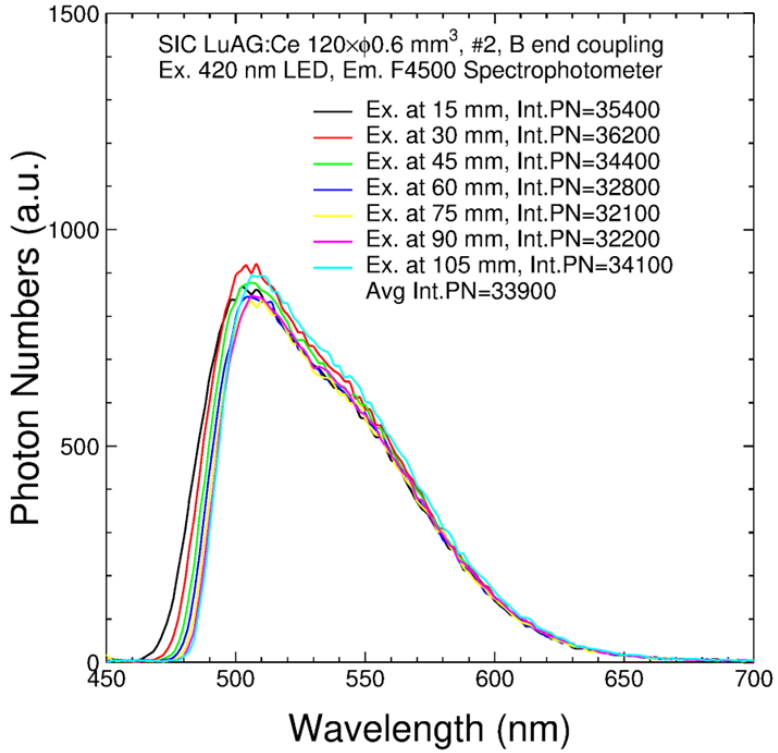

LuAG:Ce ceramic LHPG fibers

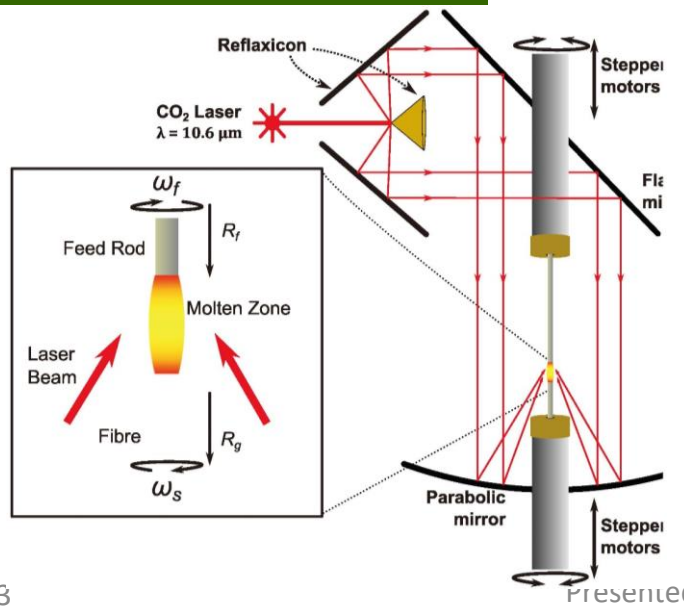

Excellent uniformity observed for Φ0.6 ×120 mm³ LuAG:Ce ceramic fibers excited by a 420 nm LED at different longitudinal location, with a solid coupling to a quartz fiber, mimicking its application in RADiCAL Calorimetry

Ultrafast and Radiation Hard BaF_2

IEEE TNS NS 67, NO. 6 (2020) 1014-1019

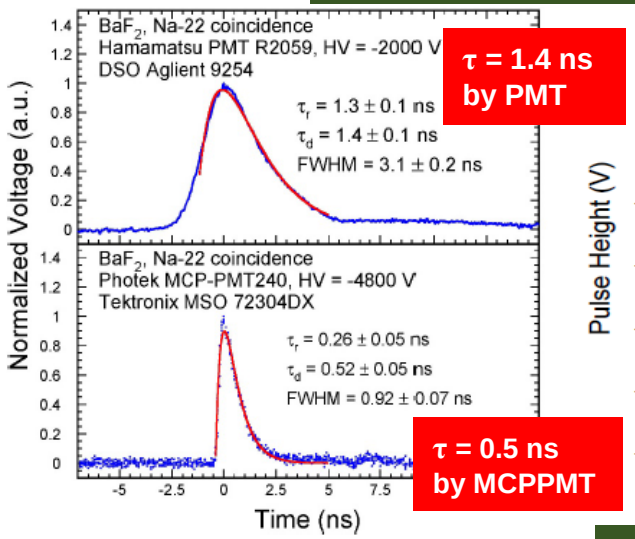

τ = 1.4 ns by PMT

τ = 0.5 ns by MCPPMT

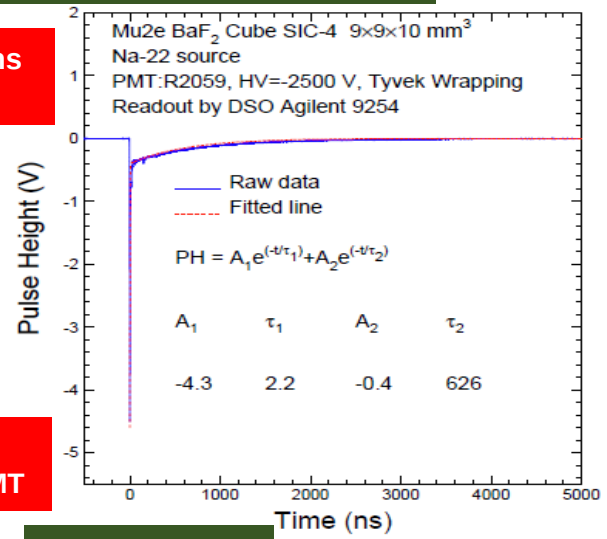

NIMA 340 (1994) 442-457

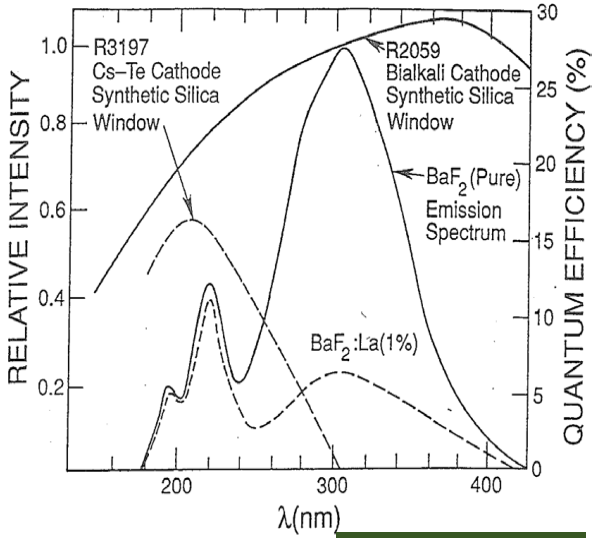

BaF_2 has an ultrafast scintillation component @ 220 nm with **0.5 ns** decay time and a much larger slow component @ 300 nm with 600 ns decay time.

Slow suppression may be achieved by rare earth doping, and/or solar-blind photo-detectors

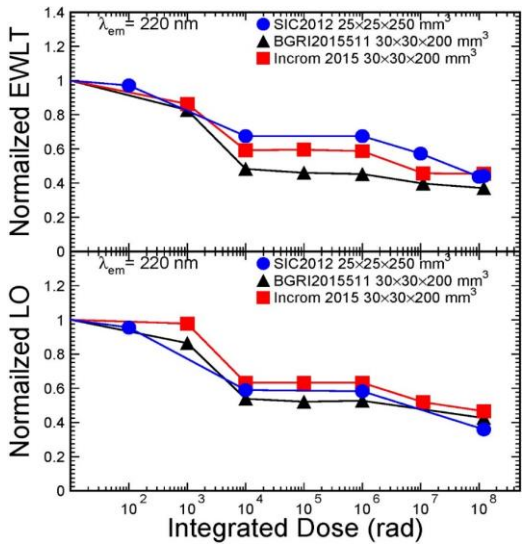

IEEE TNS **63** (2016) 612-619

Blue Room

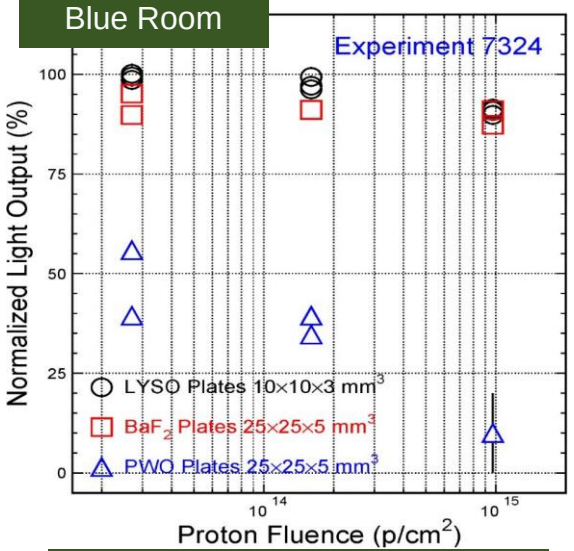

IEEE TNS **65** (2018) 1086-1092

East Port

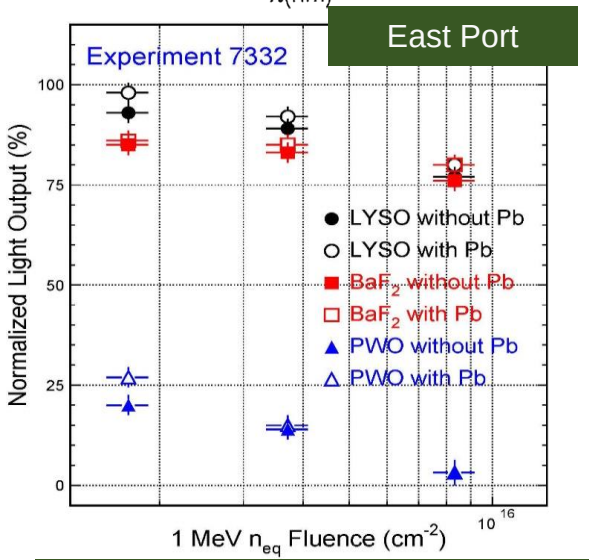

IEEE TNS **67** (2020) 1018-1024

Long BaF_2 shows saturated damage from 10 krad to 1 Mrad, indicating limited color center density against γ-rays

Thin BaF_2 plates tested up to 9.7×10^{14} p/cm^2 and 8.3×10^{15} n_{eq}/cm^2

γ-Ray Induced Damage in Long Crystals

IEEE TNS **63** (2016) 612-619

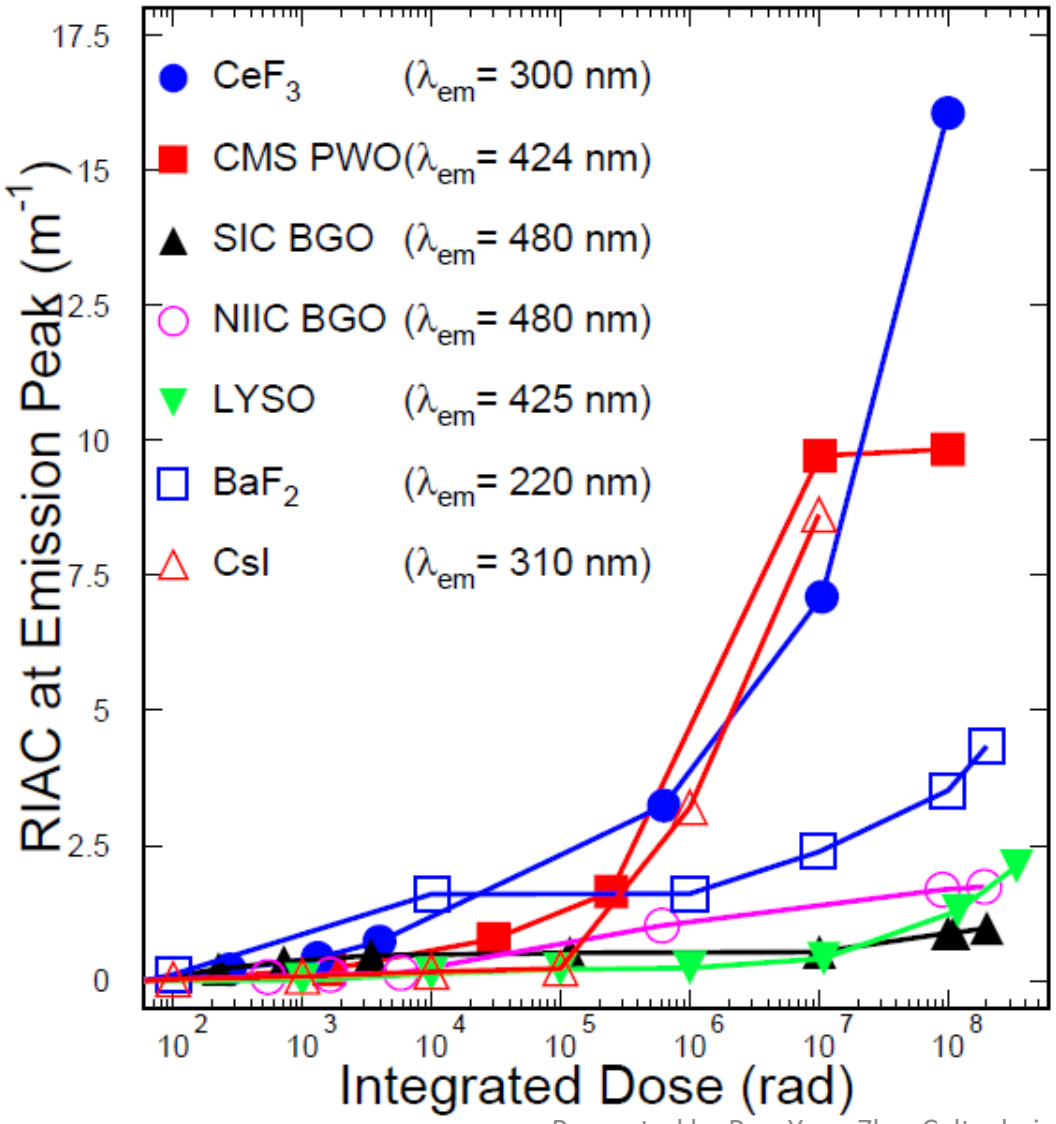

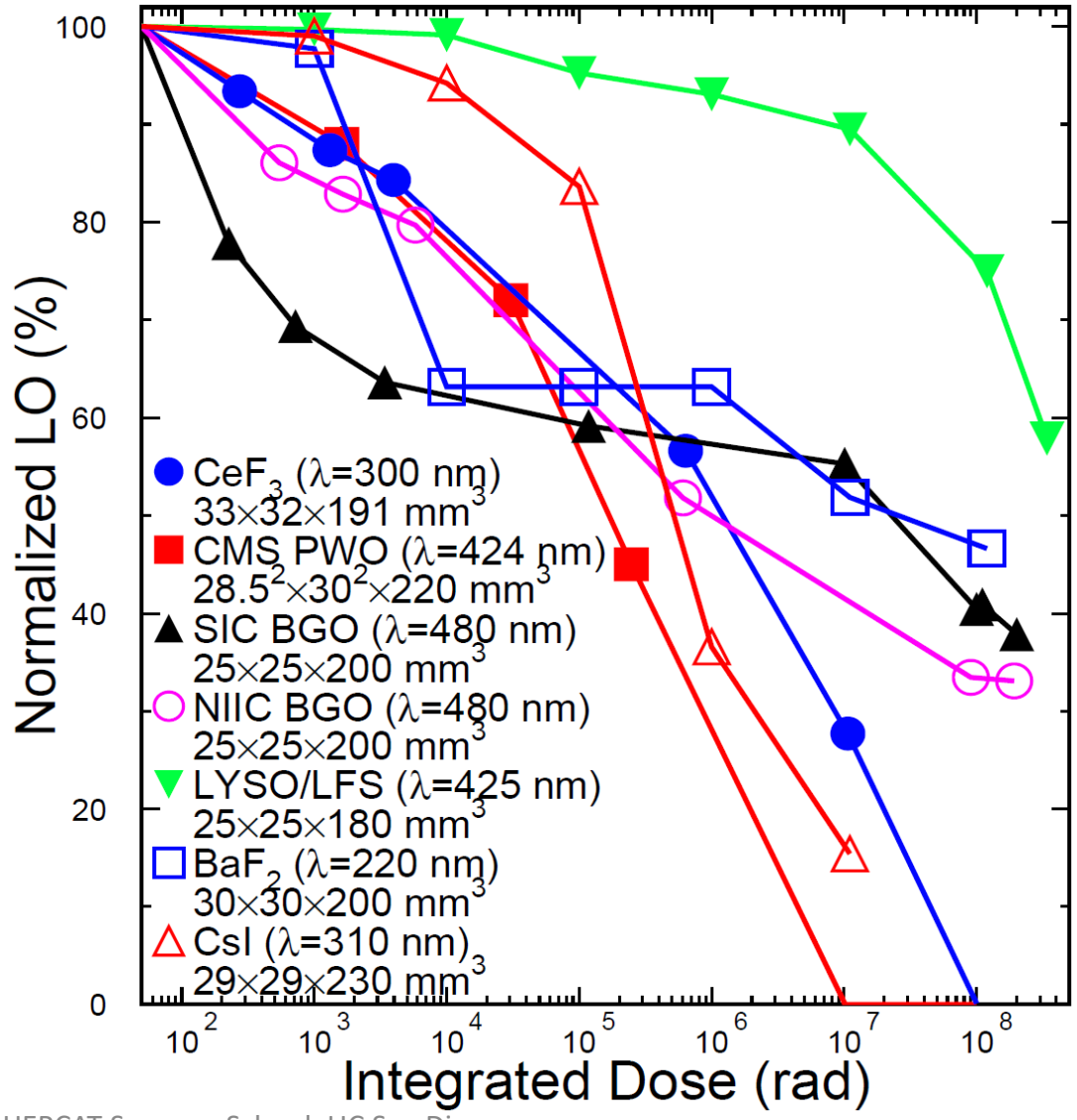

BaF_2:Y for Ultrafast Calorimetry

Increased F/S ratio observed in BGRI BaF_2:Y crystals: Proc. SPIE 10392 (2017)

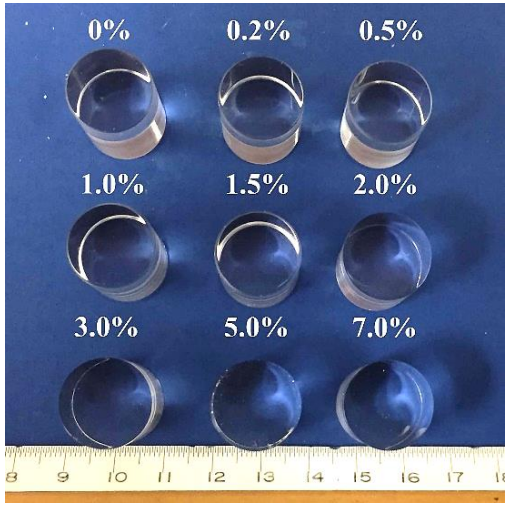

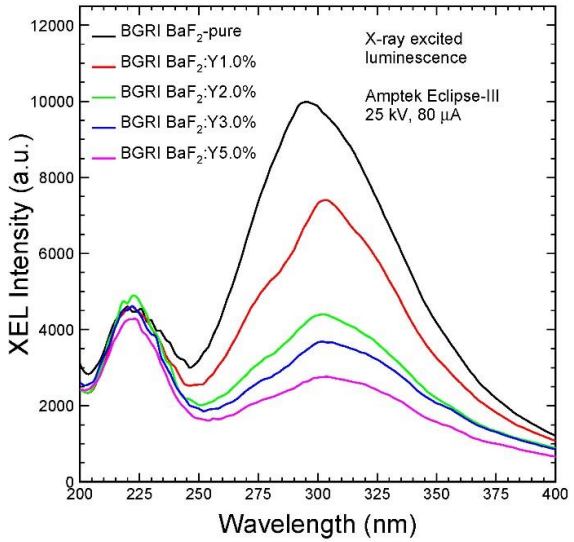

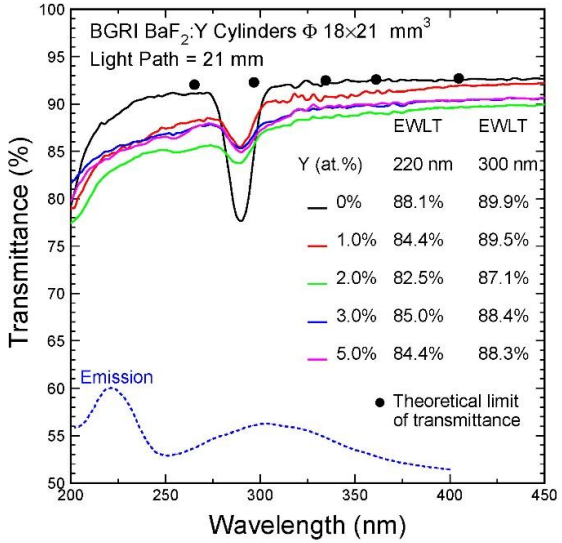

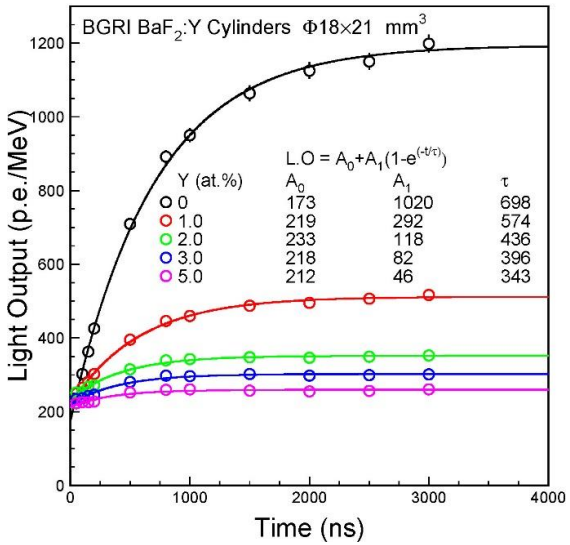

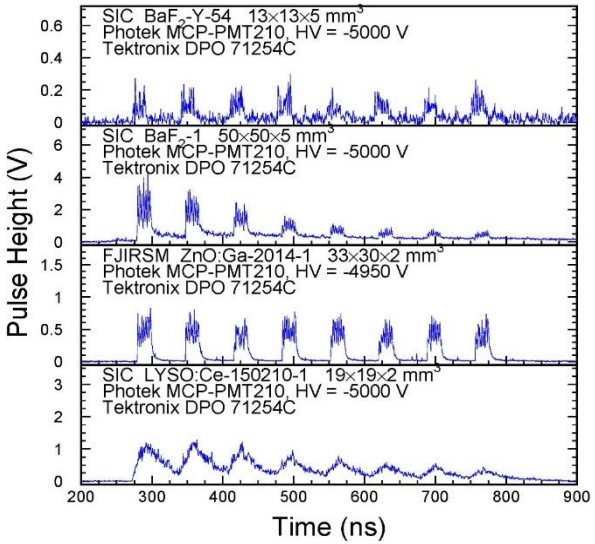

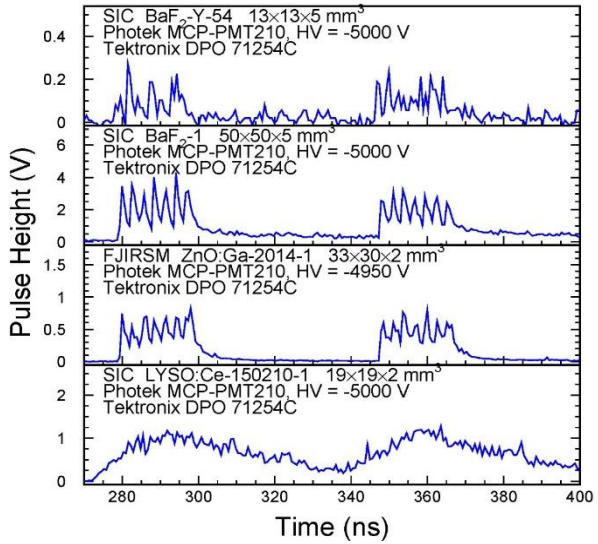

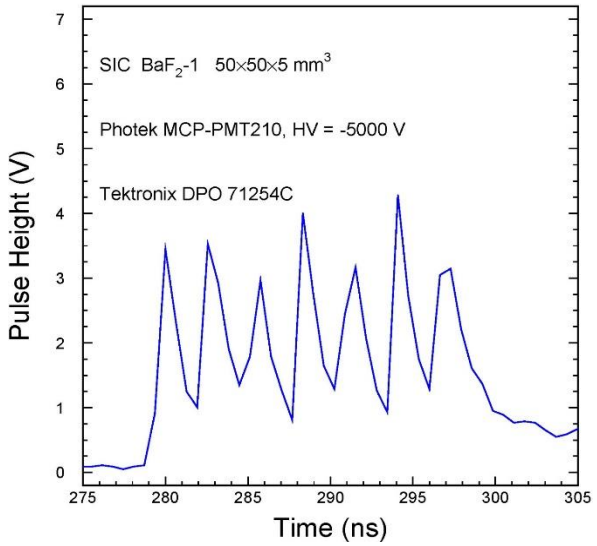

X-ray bunches with 2.83 ns spacing in septuplet are clearly resolved by ultrafast BaF_2:Y and BaF_2 crystals: for GHz Hard X-ray Imaging NIMA 240 (2019) 223-239

RIN:γ and Photodetector QE/PDE

QE/PDE of four VUV photodetectors for BaF_2 and BaF_2:Y

IEEE TNS **69** (2022) 958-964

Photodetector	$EWQE/PDE_{fast}$ (%)	$EWQE/PDE_{slow}$ (%)	$EWQE/PDE_{BaF}$ (%)	$EWQE/PDE_{BaF:Y}$ (%)	Relative LO (50 ns)	Relative F_{BaF}	Relative $F_{BaF:Y}$
Hamamatsu R2059	15.2	20.9	20.0	18.7	1.00	1.00	1.00
Photek Solar-Blind	25.6	10.6	13.0	16.1	1.68	0.65	0.86
FBK SiPM w/UV Filter-I	17.8	12.7	13.5	14.7	1.17	0.68	0.79
Hamamatsu MPPC	10.5	9.8	9.9	10.2	0.69	0.50	0.55

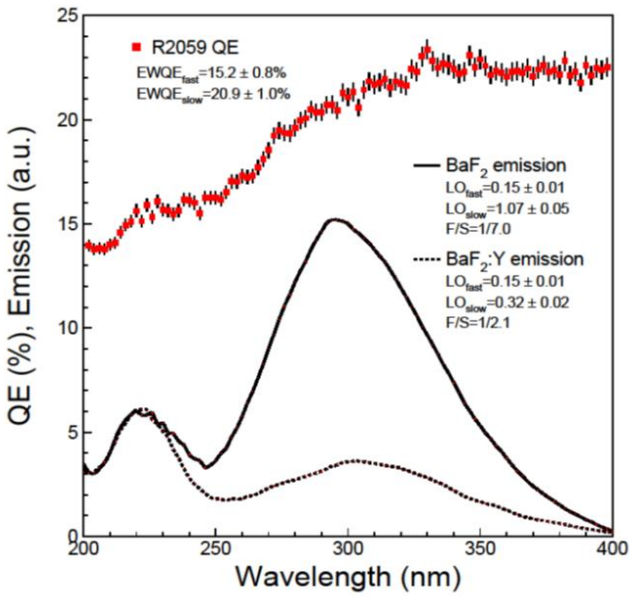

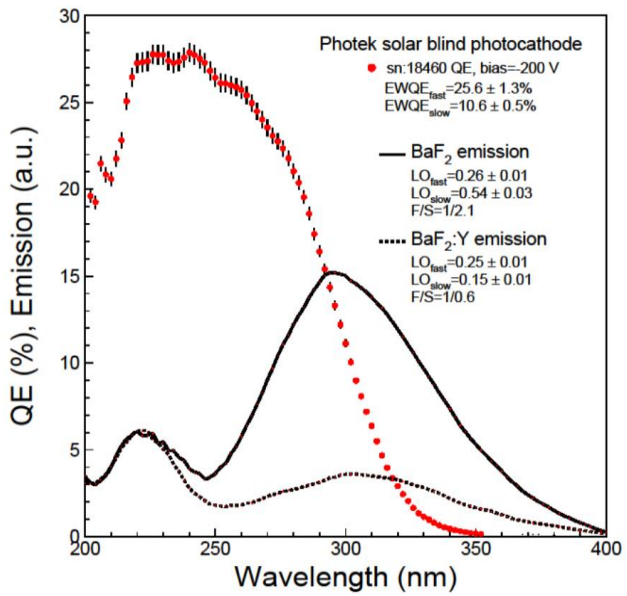

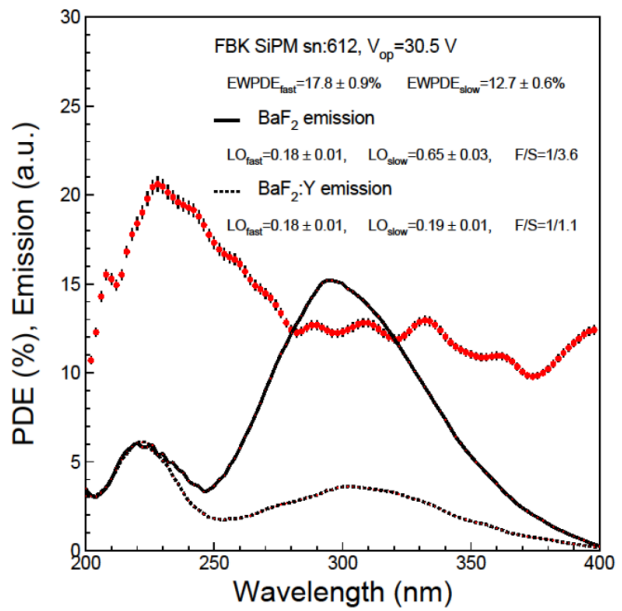

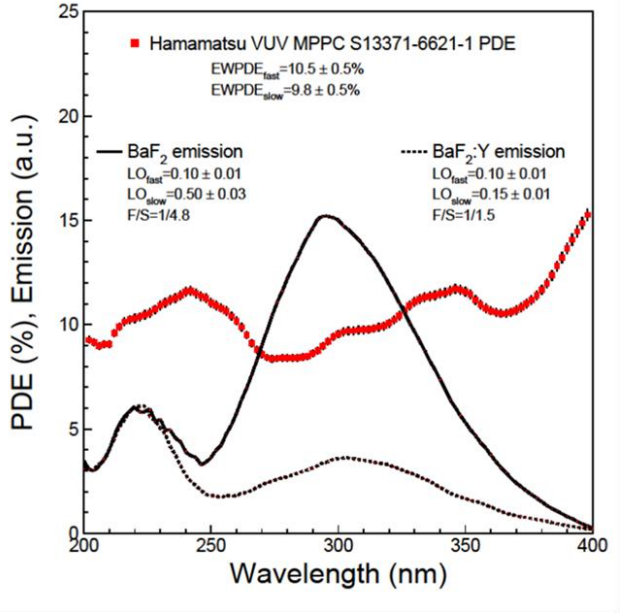

Fast/Ultrafast for HEP TOF & X-ray Imaging

arXiv: 2203.06788

	BaF_2	BaF_2:Y	Lu_2O_3:Yb	YAP:Yb	YAG:Yb	ZnO:Ga	β-Ga_2O_3	LYSO:Ce	LuAG:Ce	YAP:Ce	GAGG:Ce	LuYAP:Ce	YSO:Ce
Density (g/cm^3)	4.89	4.89	9.42	5.35	4.56	5.67	5.94	7.4	6.76	5.35	6.5	7.2[f]	4.44
Melting points (^{o}C)	1280	1280	2490	1870	1940	1975	1725	2050	2060	1870	1850	1930	2070
X_0 (cm)	2.03	2.03	0.81	2.59	3.53	2.51	2.51	1.14	1.45	2.59	1.63	1.37	3.10
R_M (cm)	3.1	3.1	1.72	2.45	2.76	2.28	2.20	2.07	2.15	2.45	2.20	2.01	2.93
λ_I (cm)	30.7	30.7	18.1	23.1	25.2	22.2	20.9	20.9	20.6	23.1	21.5	19.5	27.8
Z_{eff}	51.0	51.0	67.3	32.8	29.3	27.7	27.8	63.7	58.7	32.8	50.6	57.1	32.8
dE/dX (MeV/cm)	6.52	6.52	11.6	7.91	7.01	8.34	8.82	9.55	9.22	7.91	8.96	9.82	6.57
λ_{peak} [a] (nm)	300 220	300 220	370	350	350	380	380	420	520	370	540	385	420
Refractive Index[b]	1.50	1.50	2.0	1.96	1.87	2.1	1.97	1.82	1.84	1.96	1.92	1.94	1.78
Normalized Light Yield[a,c]	42 4.8	1.7 4.8	0.95	0.19[d]	0.36[d]	2.6[d] 4.0[d]	6.5 0.5	100	35[e] 48[e]	9 32	190	16 15	80
Total Light yield (ph/MeV)	13,000	2,000	280	57[d]	110[d]	2,000[d]	2,100	30,000	25,000[e]	12,000	58,000	10,000	24,000
Decay time[a] (ns)	600 0.5	600 0.5	1.1[d]	1.1[d]	1.8[d]	3.0[d] 1.0[d]	110 5.3	40	820 50	191 25	570 130	1485 36	75
LY in 1st ns (photons/MeV)	1200	1200	170	34[d]	46[d]	980[d]	43	740	240	391	400	125	318
LY in 1st ns /Total LY (%)	9.0	64	60	60	43	49	2.0	2.5	1.2	3.3	0.7	1.4	1.3
40 keV Att. Leng. (1/e, mm)	0.106	0.106	0.127	0.314	0.439	0.407	0.394	0.185	0.251	0.314	0.319	0.214	0.334

[a] top/bottom row: slow/fast component; [b] at the emission peak; [c] normalized to LYSO:Ce; [d] excited by Alpha particles; [e] 0.3 Mg at% co-doping; [f] $Lu_{0.7}Y_{0.3}AlO_3$:Ce.

Cost-Effective Inorganic Scintillators for FCC-ee

CalVision Crystal Calorimetry

- A longitudinally segmented **CalVision** crystal ECAL with dual readout combined with the IDEA HCAL promises excellent EM and Hadronic resolution.

- Dense, UV-transparent and cost-effective inorganic scintillators are crucial for the homogeneous hadron calorimeter (**HHCAL**) concept, promising a jet mass resolution at a level of 20%/√E by dual readout for either Cerenkov and scintillation light or dual integration gate.

- Doped PbF_2, PbFCl, BSO, titanium doped sapphire (Al_2O_3:Ti) crystals and AFO glass investigated. Cost-effective inorganic glasses from US industry are under investigation for Higgs factory.

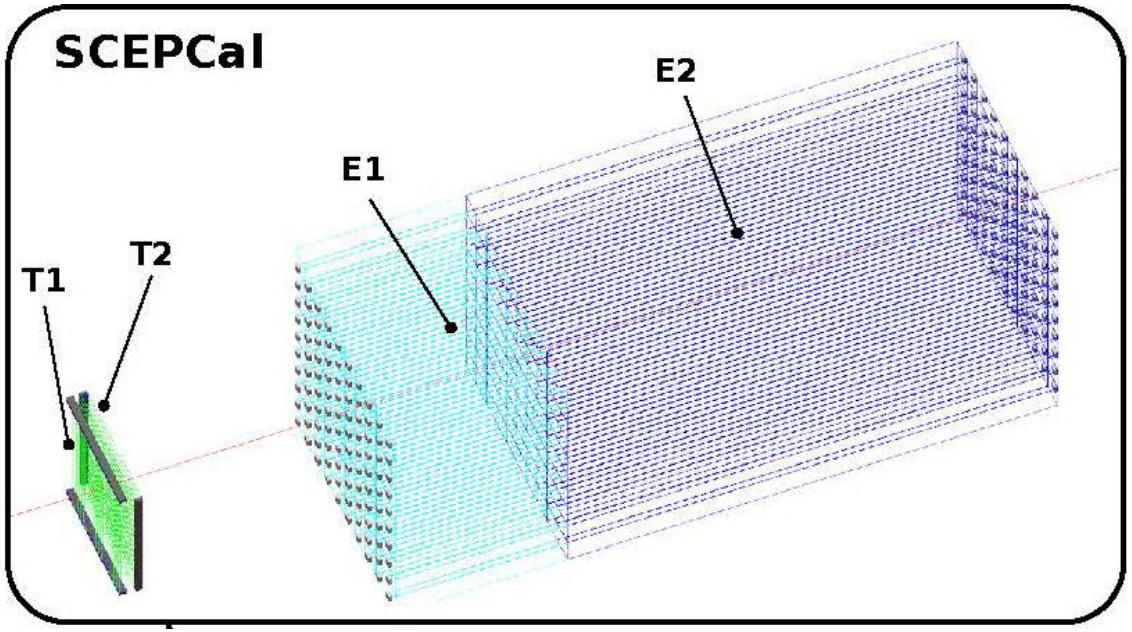

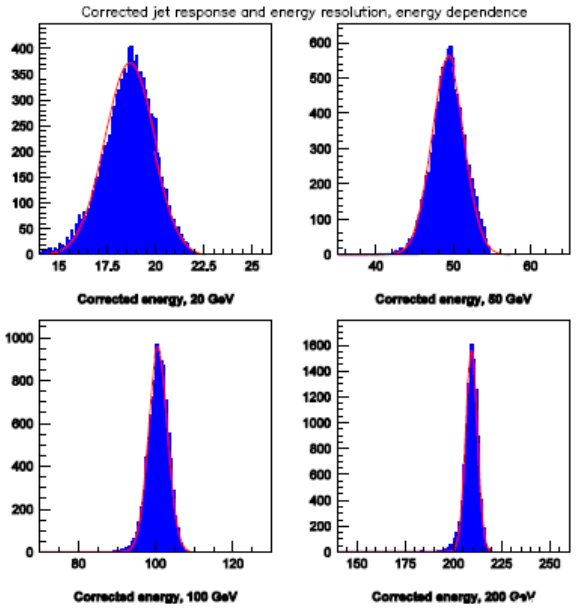

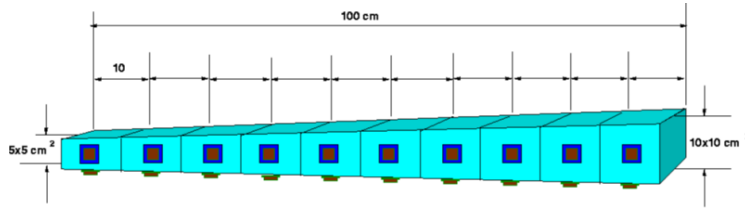

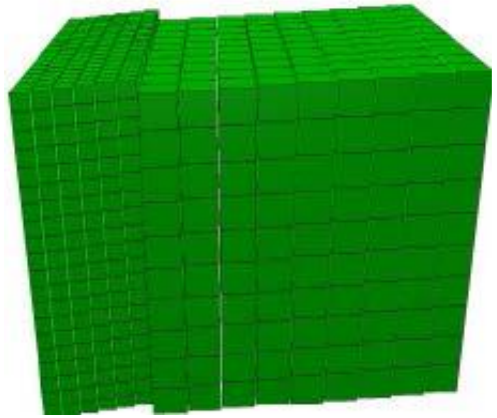

Cost: Mass-Produced Crystals (Mar 2019)

Scaling to X_0, order of crystal cost: PWO, BGO, CsI, BSO, BaF_2:Y, LYSO

Item	Size	1 m^3	10 m^3	100 m^3	Scaled to X_0
BGO	22.3×22.3×280 mm	$8/cc	$7/cc	$6/cc	1.23
BaF_2:Y	31.0×31.0×507.5 cm	$12/cc	$11/cc	$10/cc	2.28
LYSO:Ce	20.7x20.7x285 mm	$36/cc	$34/cc	$32/cc	1.28
PWO	20x20x223 mm	$9/cc	$8/cc	$7.5/cc	1.00
BSO	22x22x274 mm	$8.5/cc	$7.5/cc	$7.0/cc	1.29
CsI	35.7x35.7x465 mm	$4.6/cc	$4.3/cc	$4.0/cc	2.09

Inorganic Scintillators for HHCAL

Snowmass 2022 White Paper: https://doi.org/10.48550/arXiv.2203.06788

	BGO	BSO	PWO	PbF_2	PbFCl	Sapphire :Ti	AFO Glass	DSB:Ce Glass[1]	BGS Glass[2]	ABS Glass[3]	DSB:Ce,Gd Glass[4,5]	HFG Glass[6]
Density (g/cm^3)	7.13	6.8	8.3	7.77	7.11	3.98	4.6	3.8	4.2	4.53	4.7 - 5.4[d]	5.95
Melting point (℃)	1050	1030	1123	824	608	2040	980[7]	1420[8]	1550	?	1420[8]	570
X_0 (cm)	1.12	1.15	0.89	0.94	1.05	7.02	2.96	3.36	2.62	2.41	2.14	1.74
R_M (cm)	2.23	2.33	2.00	2.18	2.33	2.88	2.90	3.52	3.33	3.09	2.56	2.45
λ_I (cm)	22.7	23.4	20.7	22.4	24.3	24.2	26.4	32.8	31.8	28.8	24.2	23.2
Z_{eff} value	71.5	73.8	73.6	76.7	74.7	11.1	41.4	42.9	49.6	51.9	47.2	55.7
dE/dX (MeV/cm)	8.99	8.59	10.1	9.42	8.68	6.75	6.84	5.56	5.90	6.42	7.68	8.24
Emission Peak[a] (nm)	480	470	425 420	\	420	300 750	365	440	430	396	440 460	325
Refractive Index[b]	2.15	2.68	2.20	1.82	2.15	1.76	\	\	\	\	\	1.50
LY (ph/MeV)[c]	7,500	1,500	130	\	150	7,900	450	~500	2,500	800	1,300	150
Decay Time[a] (ns)	300	100	30 10	\	3	300 3200	40	180 30	400 90	1200 260	120, 400 50	25 8
d(LY)/dT (%/°C)[c]	-0.9	?	-2.5	\	?	?	?	-0.04	0.3	?	?	-0.37
Cost ($/cc)	6.0	7.0	7.5	6.0	?	0.6	?	2.0	2.0	?	2.0	?

a. Top line: slow component, bottom line: fast component.
b. At the wavelength of the emission maximum.
c. At room temperature (20°C) with PMT QE taken out.
d. Gd loaded.

1. E. Auffray, et al., J. Phys. Conf. Ser. 587, 2015
2. V. Dormenev, et al., NIMA 1015, 2021
3. G. Tang, et al., Opt. Mater. 130, 2022
4. R. W. Novotny, et al., J. Phys. Conf. Ser. 928, 2017
5. V. Dormenev , et al., the ATTRACT Final Conference
6. E. Auffray, et al., CERN-PPE/96-35, 1996
7. R. A. McCauley et al., Trans. Br. Ceram. Soc., 67. 1968
8. I. G. Oehlschlegel, Glastech. Ber. 44, 1971

Sapphire:Ti Emission and Transmittance

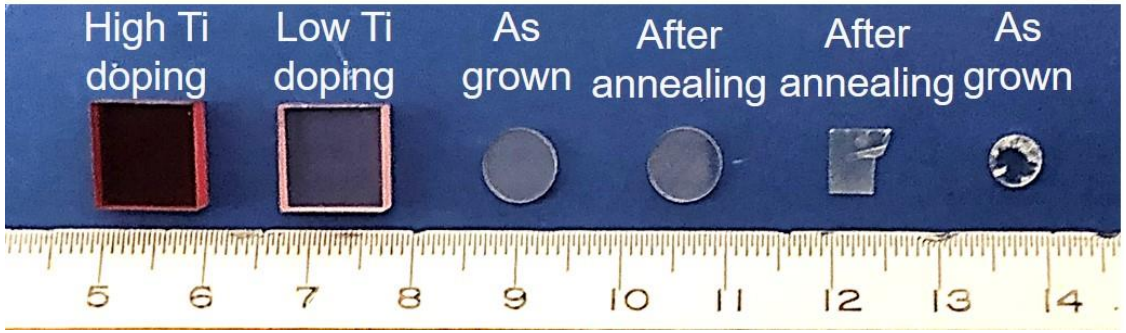

A weak emission at 325 nm with 150 ns decay time
A strong emission at 755 nm with 3 μs decay time

ID	Dimension (mm^3)	#	Polishing
Tongji Al_2O_3:Ti-1,2	**10×10×4**	**2**	**Two faces**
Tongji Al_2O_3:C-1,2	Φ7×1	2	Two faces
Tongji Lu_2O_3:Yb	6.4×4.8×0.4	1	Two faces
Tongji $LuScO_3$:Yb	Φ4.8×1.3	1	Two faces

Fast @325 nm

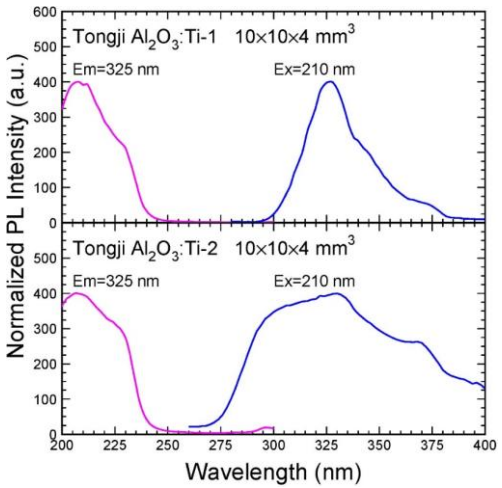

Slow @755 nm

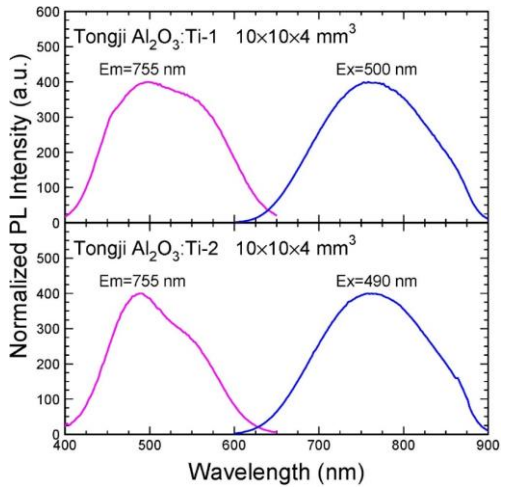

EWLT for Fast & Slow

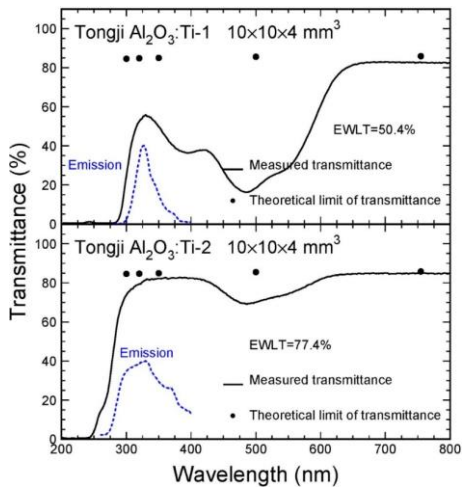

Fast = 162 ns

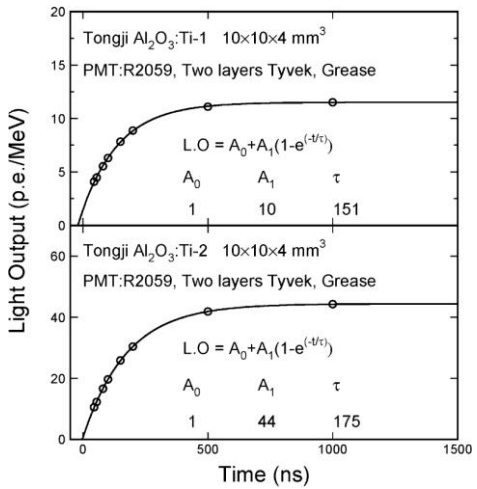

Slow = 3.2 μs

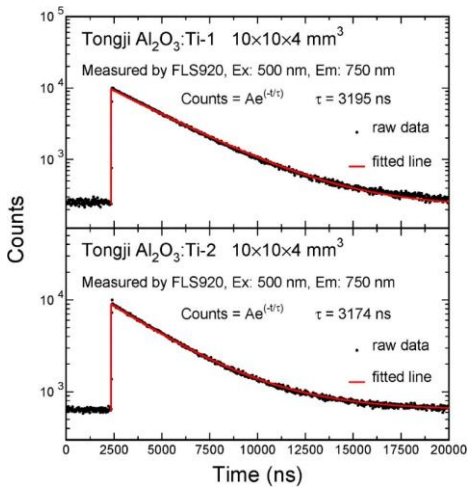

Summary

- Inorganic scintillator-based total absorption electromagnetic calorimeter has played important role in HEP experiments. Novel inorganic scintillators are discovered and developed by academia and industry for physics experiments, homeland security and medical and scientific imaging.
- The Caltech HEP crystal lab has been actively leading R&D on inorganic scintillators for several decades. The lab is now developing rad-hard, fast/ultrafast and cost-effective inorganic scintillators for several novel calorimeter concepts for future HEP calorimetry and TOF system at the energy and intensity frontiers.
- Young physicists are encouraged to join the Caltech crystal lab for this exciting mission.

Acknowledgements: DOE HEP Award DE-SC0011925